Australian Government
Geoscience Australia

Combined marine and land potential-field datasets for the southwest margin of Australia

Ron Hackney

Record
2012/37
GeoCat # 73254

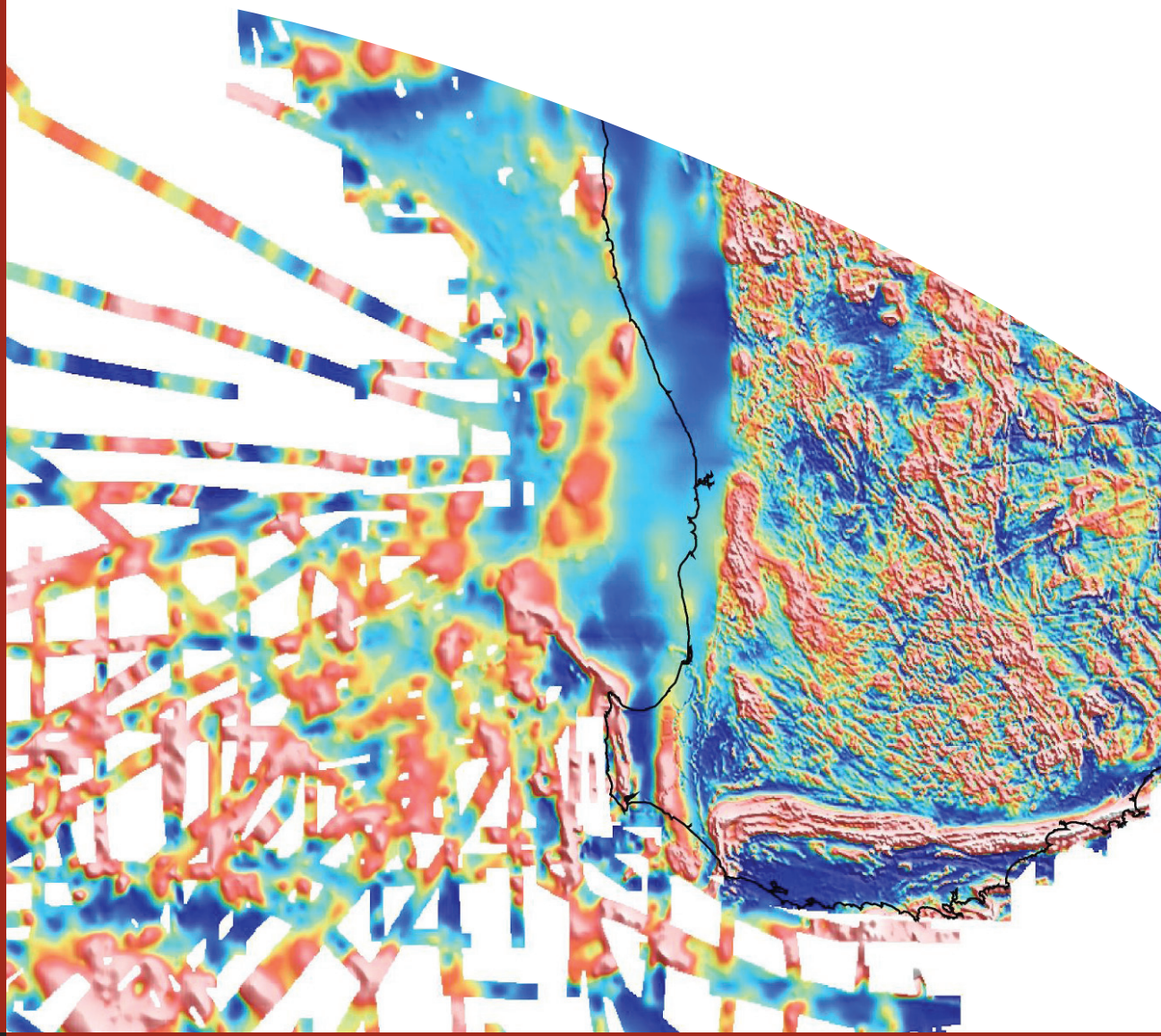

Combined marine and land potential-field datasets for the southwest margin of Australia

GEOSCIENCE AUSTRALIA
RECORD 2012/37

by

Ron Hackney[1]

Australian Government
Geoscience Australia

1. Energy Division, Geoscience Australia, GPO Box 378, Canberra ACT 2601, Australia

Department of Resources, Energy and Tourism
Minister for Resources and Energy: The Hon. Martin Ferguson, AM MP
Secretary: Mr Drew Clarke

Geoscience Australia
Chief Executive Officer: Dr Chris Pigram

ISSN 1448-2177
ISBN 978-1-922103-18-5 (web)
ISBN 978-1-922103-19-2 (CD)
ISBN 978-1-922103-20-8 (Hardcopy)

GeoCat # 73254 (this document) / 72700 (associated dataset)
GeoMet # 14975
ANZLIC ID # ANZCW0703014975

Bibliographic reference: Hackney, R., 2012. Combined marine and land potential-field datasets for the southwest margin of Australia. Geoscience Australia Record 2012/37, 62pp.

Contents

Executive Summary

In 2010 and 2011, the Australian Government released offshore petroleum exploration acreage in the Perth, Mentelle and Southern Carnarvon basins on the southwest margin of Australia. This release was underpinned by two new marine geophysical surveys (GA-310 and GA-2476) that were conducted by Geoscience Australia in late 2008 and early 2009 as part of the Australian Government's Offshore Energy Security Program. These surveys acquired a range of pre-competitive geological and geophysical data that included seismic reflection, gravity, magnetic and swath bathymetry measurements, as well as seafloor dredge samples.

The new surveys provided a total of about 26 000 line km of new gravity and magnetic data that add to existing data from around 150 previous marine surveys conducted off the southwest margin since 1960. This record describes the integration and levelling of the new gravity and magnetic data with existing data, both offshore and onshore, to produce a unified gravity and magnetic dataset for use in constraining regional tectonics, basin structure and petroleum prospectivity.

Levelling is a key step in processing ship-borne gravity and magnetic data. This process minimises the mis-tie errors at ship-track cross-overs that arise from factors such as positioning errors, instrument drift and lack of diurnal corrections to magnetic data. Without accounting for these cross-over errors, gridded data can be rendered un-interpretable by artefacts and distortions at line cross-overs.

The new dataset of gravity and magnetic data is available for download from the Geophysical Archive Data Delivery System (http://www.geoscience.gov.au/gadds). The data available include:

- line-based magnetic and gravity data;
- grids of total field and variable-latitude pole-reduced magnetic anomalies; and
- grids of free-air, Bouguer and residual gravity anomalies.

These data provide comprehensive coverage of the southwest margin of Australia, both offshore and onshore, in the region bound by 106–120°E and 19–37°S.

1 Introduction

The major geological components of the southwest margin of Australia include the Perth, Mentelle, Southern Carnarvon and Northern Carnarvon basins and the Naturaliste and Wallaby plateaus (Figure 1.1). The under-explored frontier basins on this margin formed within an obliquely-oriented extensional rift system during the Paleozoic to Mesozoic break-up of Australia and Greater India (Quaife et al., 1994; Mory and Iasky, 1996; Norvick, 2004). Only the onshore and inboard parts of the Perth Basin have proven hydrocarbon resources (e.g. Buswell et al., 2004), but in 2010 and 2011, offshore petroleum exploration acreage was released by the Australian Government in the Perth (Nicholson et al., 2008; Jones et al., 2011b), Mentelle (Borissova et al., 2010) and Southern Carnarvon (Borissova and Nelson, 2011) basins.

Given the interest in the hydrocarbon potential of Australia's southwest margin and the need to map and understand seabed environments, two marine geophysical surveys (GA-310 and GA-2476) were conducted by Geoscience Australia in late 2008 and early 2009 as part of the Australian Government's Offshore Energy Security Program (Geoscience Australia, 2011). These surveys acquired a range of pre-competitive geological and geophysical data that included seismic reflection, gravity, magnetic, swath bathymetry and seafloor dredge samples (Daniell et al., 2009; Foster et al., 2009; Nelson et al., 2009; Payne et al., 2009). The new surveys provided a total of about 26 000 km of new gravity and magnetic data (Hackney et al., 2012). These data add to existing data from around 150 previous marine surveys conducted since 1960 in the region 106–118°E and 19–37°S. The new data partly fill gaps in existing coverage, but also provide higher resolution coverage for much of the continental shelf and slope of the southwest margin.

This record describes the integration and levelling of new gravity and magnetic data with existing data, both offshore and onshore, to produce unified gravity and magnetic datasets for use in constraining regional tectonics, basin structure and petroleum prospectivity (Jones et al., 2011a; Hackney et al., 2012; Hall et al., 2012; Johnston and Petkovic, 2012; Hall, in prep.; Johnston and Petkovic, in prep.; Petkovic, in prep.). Levelling is a key step in processing ship-borne magnetic and gravity data. This process minimises the mis-tie errors at ship-track cross-overs that arise from factors such as positioning errors, instrument drift and lack of diurnal corrections to magnetic data (e.g. Prince and Forsyth, 1984; Wessel and Watts, 1988). Without accounting for these cross-over errors, gridded data can be rendered un-interpretable by artefacts and distortions at line cross-overs.

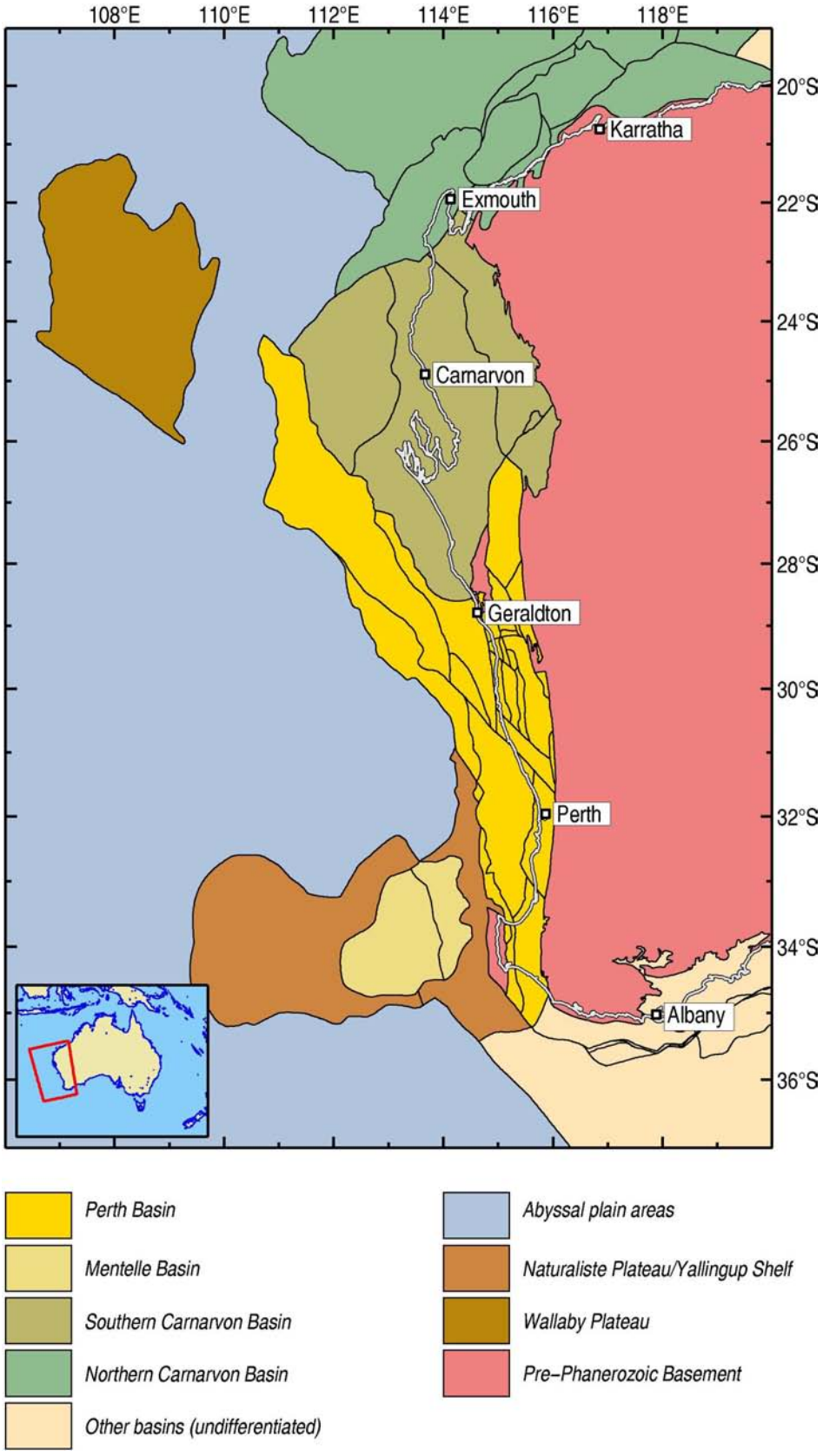

Figure 1.1: *Map showing major geological elements of the southwest margin of Australia from the Geoscience Australia Provinces Database (http://www.ga.gov.au/provexplorer/).*

2 Existing Data

This section describes existing gravity and magnetic data that covered the southwest margin of Australia (i.e. between longitudes 106–120°E and latitudes 19–37°S) prior to the most recent surveys conducted by Geoscience Australia in late 2008/early 2009. Earlier data are available from a range of marine surveys conducted by industry, government and academia.

2.1 MARINE POTENTIAL-FIELD DATA

2.1.1 Existing levelled dataset

Geoscience Australia holds ship-track gravity and magnetic data from about 680 marine surveys covering the period 1960–2009. The data were last combined and levelled in the late 1990s using methods developed by Desmond Fitzgerald and Associates Pty Ltd (now Intrepid Geophysics) under contract to the Australian Geological Survey Organisation (now Geoscience Australia) (DFA, 1999; Petkovic et al., 2001). The portions of this levelled gravity and magnetic dataset covering the southwest margin of Australia are shown in Figure 2.1. The area of interest includes data from 136 marine surveys.

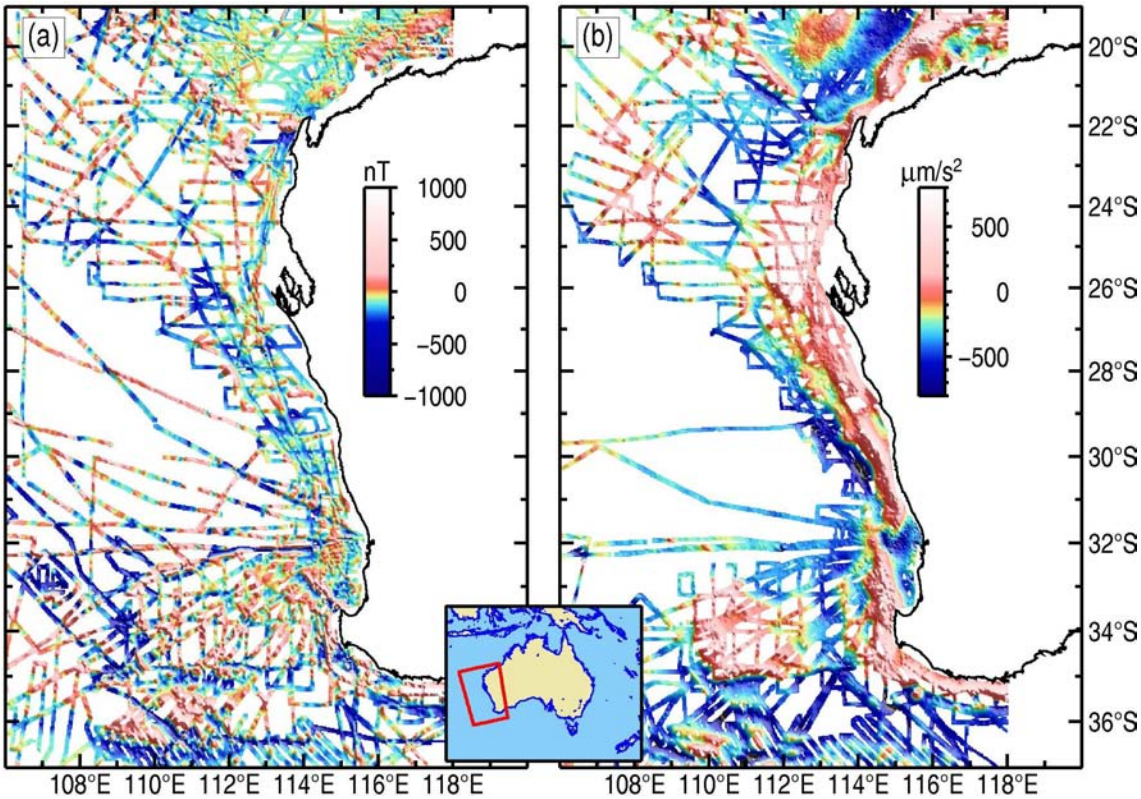

Figure 2.1: *Levelled marine* ***(a)*** *total magnetic intensity and* ***(b)*** *free-air gravity data for the southwest margin of Australia from the compilation described by Petkovic et al. (2001).*

The magnetic data were levelled using standard loop adjustment techniques to minimise misfits around closed loops of crossing ship tracks (cf. Prince and Forsyth, 1984; Mishra and Tiwari, 2011). The gravity data were levelled using a polynomial misfit function computed from crossover mis-ties between the ship-track data and satellite-altimetry derived data. In coastal regions, continental shelves and shallow seas, the quality of gravity data derived from satellite altimetry is reduced by the difficulty in applying altimeter range corrections for tidal and atmospheric effects (Andersen and

Knudsen, 2000; Deng and Featherstone, 2006; Hwang et al., 2006). Therefore, marine gravity data for some parts of the Australia margin (e.g. Bass Strait) were not levelled against the satellite-based reference surface. A satellite reference surface was used for the new levelling described here (see Section 4.4).

2.1.2 Additional offshore data

Data from twenty marine surveys off the southwest margin of Australia were not included in the 2001 compilation of levelled marine gravity and magnetic data (Table 1, Figure 2.2). Some data were not included because they were acquired after the levelling was conducted. The reasons for not including other data are unclear, but it is possible they were excluded during quality control.

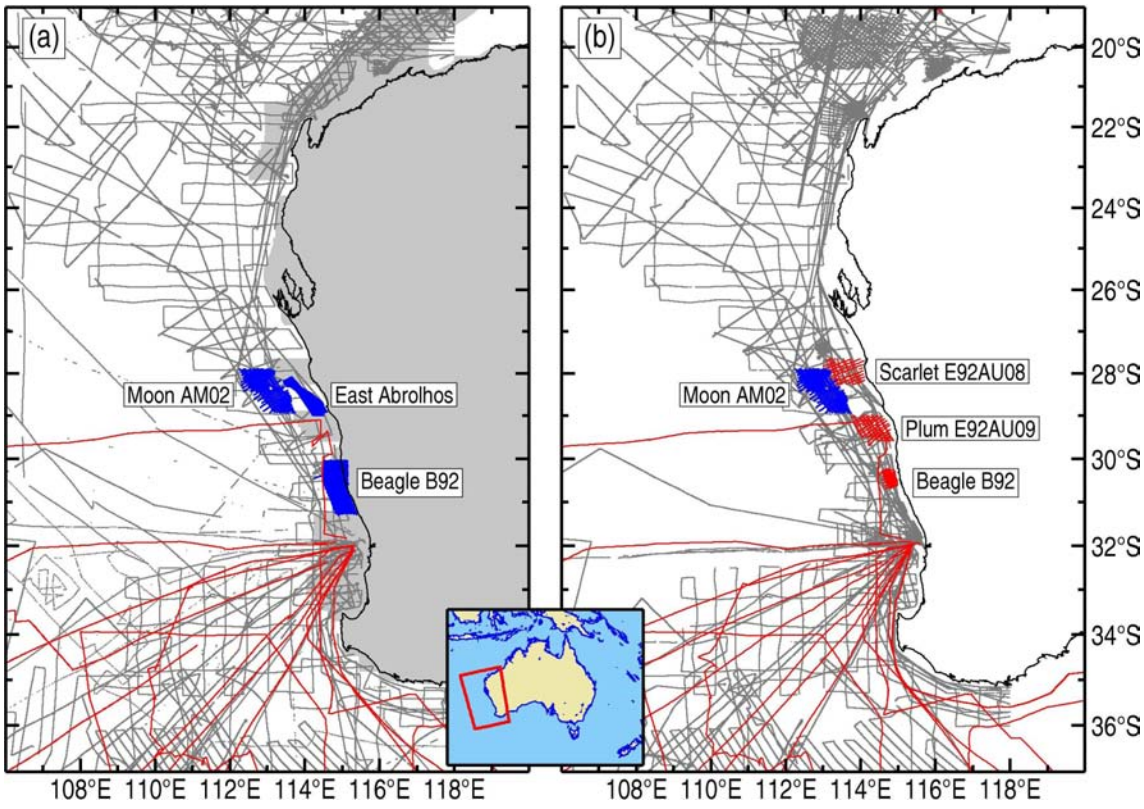

Figure 2.2: *Map showing location of* ***(a)*** *magnetic and* ***(b)*** *gravity data not included in the Petkovic et al. (2001) compilation (grey lines). Blue lines show data that were included in the new compilation described here, while red lines were not included for the reasons outlined in Table 1. The grey shading in (a) highlights the area covered by the 5th Edition Magnetic Anomaly Map of Australia (Milligan et al., 2010).*

Of the data not included in the 2001 compilation, only marine gravity and magnetic data from the "Moon AM02" survey (Austin Exploration, 2003; Intrepid Geophysics, 2004) were incorporated into the new levelling described here. Data from two offshore aeromagnetic surveys ("East Abrolhos" and "Beagle B92") were also included, neither of which were used in the compilation of aeromagnetic data that makes up the 5th Edition of the Magnetic Anomaly Map of Australia (see Section 2.2.1).

Data from a number of other marine surveys were not included in the new compilation of southwest margin data (Table 1, Figure 2.2). Closely-spaced ship tracks on frequently-traversed transit routes tend to cause problems when levelling data, so data from nine transit lines were not included.

Gravity data from three industry marine gravity surveys (Plum 2D E92AU09, Scarlet 2D E92AU08 and Beagle B92) were not included because the data were only available as raw instrument readings (densely-spaced red lines in Figure 2.2b). Processing these data from scratch was not feasible, but the data are available from Geoscience Australia's Petroleum Data Repository[1] and may be included in future compilations.

Table 1: Surveys with gravity and/or magnetic data that were not included in the Petkovic et al. (2001) compilation with an indication of whether or not they were included in the new levelling described in this record.

DATASET/GA SURVEY (LEASE AREA)	YEAR	GRAVITY	MAGNETIC	INCLUDED IN NEW COMPILATION
GA-1894	1968	Marine	Marine	No: Southern Ocean data only; old survey
GA-1861, 1862, 1863, 1864, 1865, 1866, 1867, 1868, 1905	1970–1972	Marine	Marine	No: single tracks along transit routes out of Fremantle Harbour; old surveys
"South Turtle Dove 82" (WA-165-P)	1982	Marine	Marine	No: data could not be located
"Beagle B92" (WA-228-P)	1992	Marine	Airborne	*Gravity data*, No: only raw instrument data were located *Airborne magnetic data*, Yes: added because *not* included in the 5th Edition Magnetic Map of Australia
"Plum 2D E92AU09" (WA-230-P)	1992	Marine	Airborne	*Gravity data*, No: only raw instrument data were located *Airborne magnetic data*, Yes: already included in the 5th Edition Magnetic Map of Australia
"Scarlet 2D E92AU08" (WA-231-P)	1992	Marine	Airborne	*Gravity data*, No: only raw instrument data were located *Airborne magnetic data*, Yes: already included in the 5th Edition Magnetic Map of Australia
GA-1844	1997	Marine	--	No: only one short line segment within the area of interest
"Moon AM02" (WA-326-P/328-P)	2002/03	Marine	Marine	Yes
"East Abrolhos" (WA-325-P)	2003	--	Airborne	*Airborne magnetic data*, Yes: added because *not* included in the 5th Edition Magnetic Map of Australia
GA-236, 245	2003	Marine	--	No: single tracks along transit routes out of Fremantle Harbour
GA-265	2004	--	Marine	No: magnetic data only, predominantly outside area of interest

[1] http://www.ga.gov.au/energy/projects/petroleum-data-repository.html (last visited 26 March 2012)

2.2 ONSHORE POTENTIAL-FIELD DATA

2.2.1 Magnetics

Geoscience Australia maintains a database of airborne magnetic data covering the Australian continent and some parts of near-shore marine areas (Milligan et al., 2010; Percival, 2010). The data used for this compilation (Figure 2.3a) were downloaded in grid form from the Geophysical Archive Data Delivery System (GADDS[2]) on 18 April 2011.

The line spacing for the aeromagnetic data used in this grid compilation varies from 1500–1600 m over coastal areas, to 500 m or less over cratonic areas to the east (Percival, 2010). At the time of writing, new airborne surveys were being flown over large parts of the onshore Perth Basin (Preview, 2011). These data will be included in future releases of the Magnetic Anomaly Map of Australia.

2.2.2 Gravity

Onshore gravity data are available as point data from the Australian National Gravity Database (e.g. Tracey and Nakamura, 2010). The data used for this compilation (Figure 2.3b) were downloaded from GADDS on 18 April 2011. Station spacing in this dataset is about 1–11 km (Wynne and Bacchin, 2009).

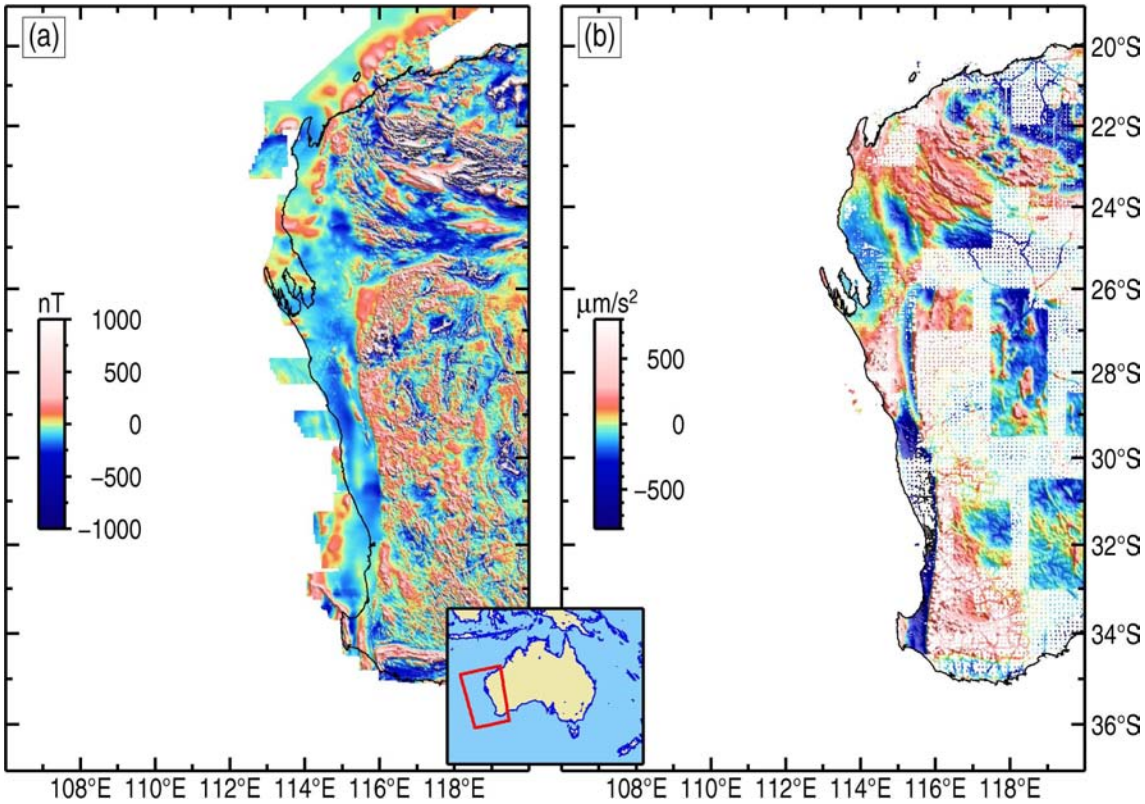

Figure 2.3: *Map of the southwestern parts of Western Australia showing* ***(a)*** *aeromagnetic data (TMI) from the 5th Edition of the Magnetic Map of Australia (Milligan et al., 2010), and* ***(b)*** *free-air anomalies from the 2010 release of the Australian National Gravity Database (grid cell size 0.01°, two-cell extrapolation limit).*

[2] http://www.geoscience.gov.au/gadds/ (last visited 26 March 2012)

2.3 GLOBAL GRAVITY AND MAGNETIC DATASETS

Regional coverage of Australia's southwest margin is available at lower resolution from global datasets. Figure 2.4 shows the EMAG2 global compilation of magnetic anomalies (Maus et al., 2009) and free-air gravity anomalies from the DNSC08GRA satellite altimetry dataset (Andersen et al., 2010a).

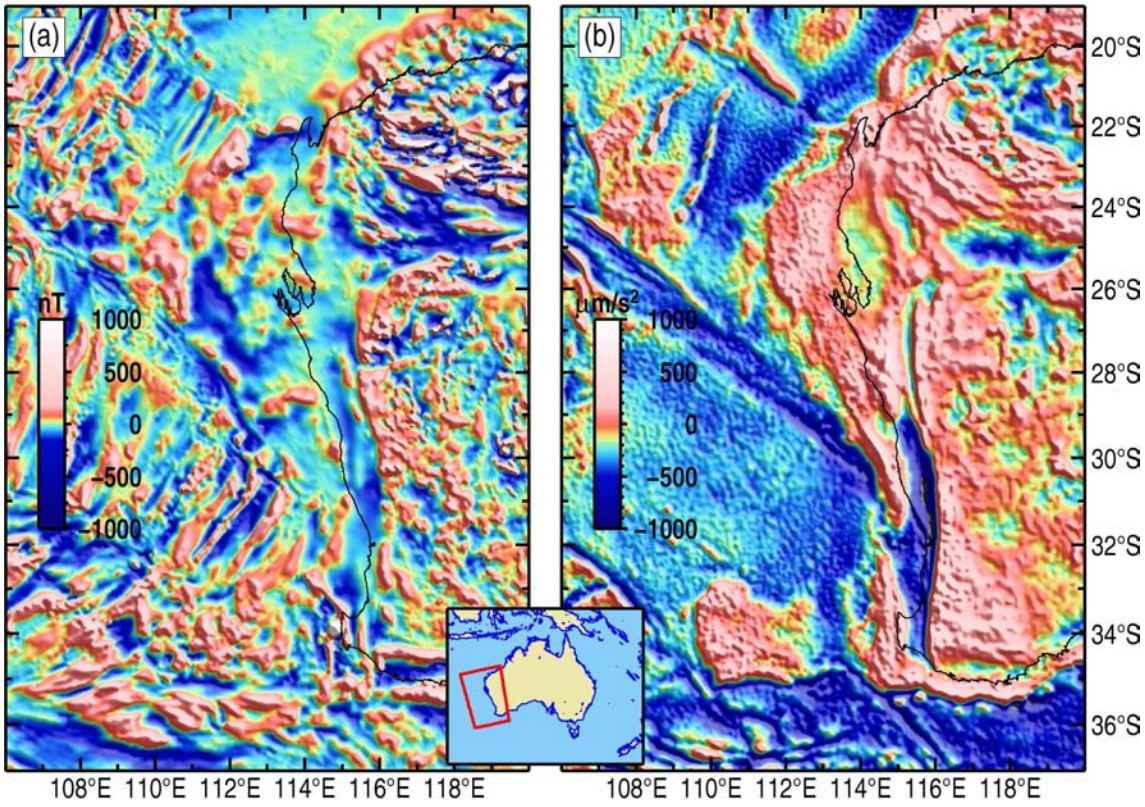

Figure 2.4: *Maps of Australia's southwest margin showing* ***(a)*** *the EMAG2 global compilation of magnetic data (Maus et al., 2009) and* ***(b)*** *free-air gravity anomalies from the DNSC08GRA dataset (Andersen et al., 2010a).*

The EMAG2 dataset (Maus et al., 2009) is a global two arc minute compilation of aeromagnetic and ship-borne magnetic data that incorporates the CHAMP 'MF6' lithospheric magnetic field model (Maus et al., 2008) for wavelengths greater than 330 km (Figure 2.4a). By using directional gridding methods guided by ocean-floor age grids, this model resolves ocean floor magnetic lineations related to seafloor spreading. The EMAG2 anomaly data are provided at an elevation of 4 km above mean sea level (geoid).

The DNSC08GRA free-air gravity data shown in Figure 2.4b are derived from satellite radar altimetry measurements of ocean surface slope. These slope measurements are related to the geoid, the equipotential surface that best fits mean sea level. Gravity anomalies can be computed from the derivative of potential, so the ocean surface slope measurements can be used to infer gravity anomalies for the world's oceans at wavelengths less than about 400 km (e.g. Sandwell and Smith, 1997; Andersen et al., 2010b). Current waveform tracking methods for determining ocean surface slope lead to gravity anomalies with an accuracy of 20–30 μm/s^2 (Sandwell and Smith, 2009). However, the spatial resolution of altimetry-derived gravity anomalies is limited to 16–25 km (e.g. Louis et al., 2010) by the spacing between satellite tracks and the filtering required to reduce noise associated with factors such as wave-induced roughness of the ocean surface.

2.4 BATHYMETRY DATA

Computations of Bouguer and terrain corrections (Section 4.5.1) were made using the 2009 version of the Bathymetry and Topography Grid of Australia (Whiteway, 2009), here referred to as AUSBATH09 (Figure 2.5). In areas where shipboard swath bathymetry data have been obtained, this dataset has a resolution of about 250 m (9 arc seconds). In other areas, the dataset incorporates data from the ETOPO1 global bathymetry dataset (Amante and Eakins, 2009). Onshore data included in AUSBATH09 are from Geoscience Australia's 4th Edition 9-arc-second digital elevation model of Australia.

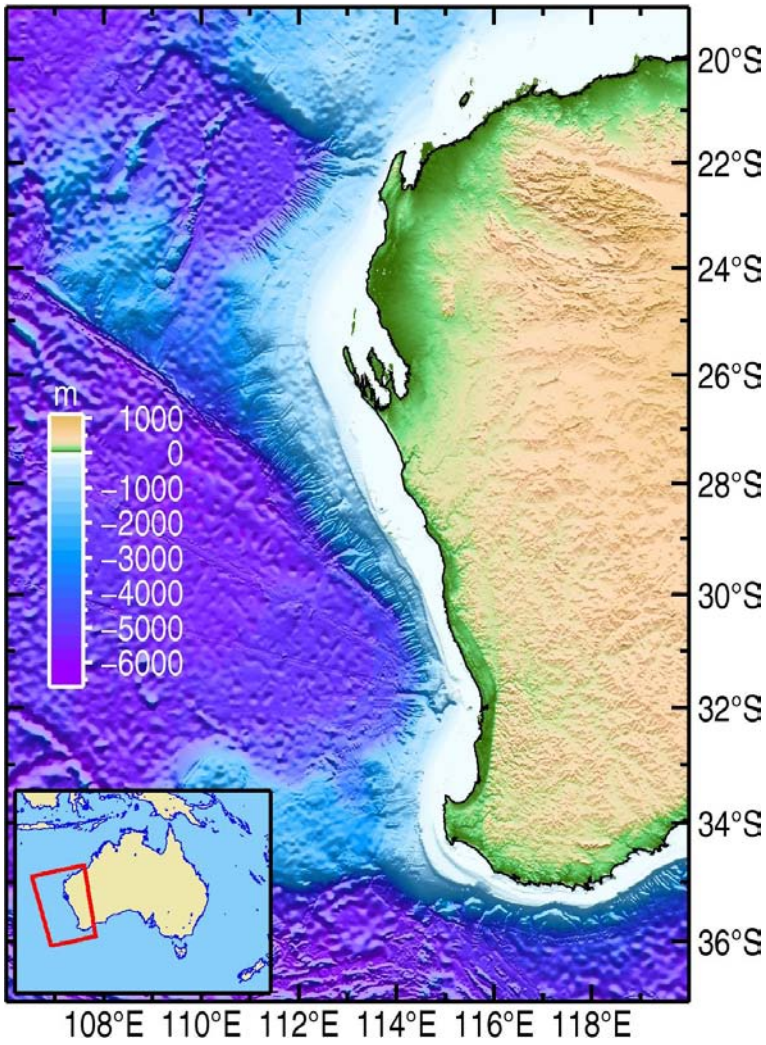

Figure 2.5: *Bathymetry of the southwest margin of Australia from the AUSBATH09 dataset (Whiteway, 2009).*

3 New Marine Surveys

In late 2008 and early 2009, two marine surveys (GA-310 and GA-2476) acquired geophysical data over the Mentelle, Perth and Southern Carnarvon basins, as well as the Wallaby Plateau (Foster et al., 2009). The acquisition and initial contractor processing of the gravity and magnetic data from these surveys is summarised below.

3.1 SURVEY GA-310

Survey GA-310 acquired about 7 300 km of seismic reflection, gravity and magnetic data. The ship-tracks for this survey are shown by the red lines in Figure 3.1. Acquisition and processing of gravity and magnetic data are summarised below, but acquisition details are described in Austin Exploration (2009) and initial data processing steps are outlined in ARK (2009).

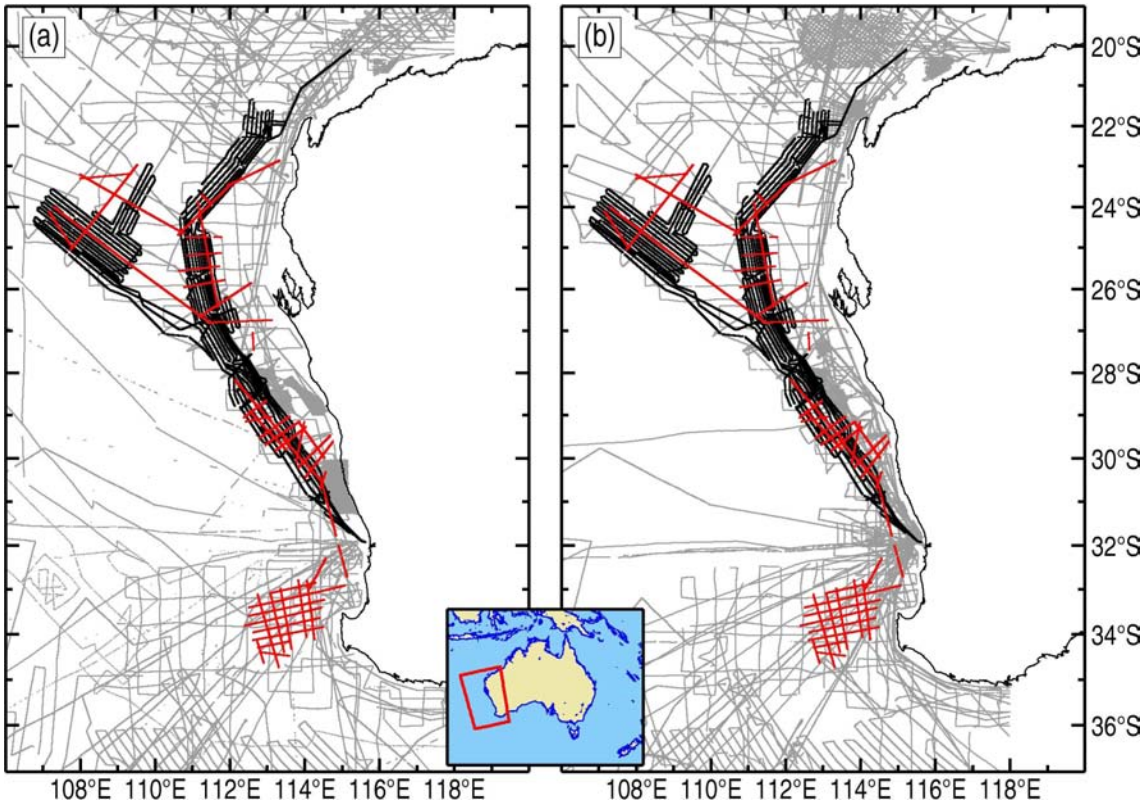

Figure 3.1: *Maps showing ship-tracks for new marine surveys conducted as part of the Energy Security Program: GA-310 (red lines) and GA-2476 (black lines).* ***(a)*** *Tracks with magnetic data,* ***(b)*** *tracks with gravity data. Grey lines show other ship tracks and airborne surveys included in the new levelling (cf. Figure 2.2).*

3.1.1 Acquisition

Gravity data were acquired by Austin Exploration Inc. under contract to CGG Veritas (the seismic operator) using a ZLS UltraSys marine gravity system incorporating a gravity sensor with serial number S-108. Magnetic data were recorded from a SeaSPY marine magnetometer system (towfish serial number 13387). The Overhauser sensor was towed 292 m behind and 14.9 m starboard of the ship. Both gravity and magnetic data were recorded at one second intervals.

3.1.2 Processing

Raw data from the gravity meter were processed according to standard procedures involving conversion of meter units to gravity units using the meter calibration constant, application of Eötvös, drift and Earth-tide corrections, and a tie to a land reference station in Broome.

The free-air gravity anomaly, Δg_{FA}, is computed by subtracting a model gravity value from the observed gravity value at each data point according to:

$$\Delta g_{FA} = g_{obs} - \left(\gamma - \delta g_f\right), \tag{1}$$

where g_{obs} is observed gravity after all appropriate corrections have been applied, γ is normal gravity on the reference ellipsoid and δg_f is the free-air correction that adjusts normal gravity to the level of the measurement point (e.g. Hackney, 2011). The free-air correction is not necessary at sea, provided that it is assumed there is a negligible gravity effect associated with the separation between the reference ellipsoid and the geoid (mean sea level). Normal gravity is computed using either a Chebyshev approximate formula or an exact analytical expression referred to as the Somigliana–Pizetti formula (e.g. Götze, 2011):

$$\gamma = \gamma_e \frac{1 + k \sin^2 \phi}{\sqrt{1 - e^2 \sin^2 \phi}} \quad . \tag{2}$$

In this equation, γ is normal gravity at latitude ϕ, γ_e is normal gravity at the equator, and k and e^2 are parameters related to the form of the reference ellipsoid (i.e. normal gravity constant and first numerical eccentricity).

Free-air anomalies for the GA-310 survey were computed by subtracting normal gravity computed from the "1984 WGS ellipsoidal formula" (ARK, 2009), though the exact formula used is not stated (i.e. Chebyshev approximation or Somigliana–Pizetti formula). However, testing showed that the contractor-processed free-air gravity values were identical to those computed using Equation (2) to compute normal gravity, the formula preferred here for anomaly computation.

A small number of spikes were removed from the raw magnetic data and, after corrections for the offset between sensor and navigation reference point, magnetic anomalies were computed by subtracting the 2005 version of the International Geomagnetic Reference Field (IGRF-10, Macmillan and Maus, 2005). Diurnal corrections were applied on the basis of data from the Gnangara and Learmonth observatories.

In order to suppress noise, the processing contractor applied low-pass cosine filters to gravity line data and low-pass Gaussian filters to magnetic line data with cut-off parameters that varied from line to line (ARK, 2009).

3.2 SURVEY GA-2476

Survey GA-2476 was a marine reconnaissance survey that utilised the RV Sonne to collect about 19 000 km of gravity and magnetic data during a swath mapping and seafloor rock sampling survey (Daniell et al., 2009; Foster et al., 2009; Nelson et al., 2009; Payne et al., 2009). Relatively high resolution gravity and magnetic data resulted from the closely-spaced ship-tracks (5–10 km, depending on water depth) that are necessary for swath mapping (black lines in Figure 3.1).

3.2.1 Acquisition

Gravity data were obtained using a CHEKAN-AM gravity meter system. Magnetic data were measured using a Geometrics G-882 caesium marine magnetometer. The sensor was towed 267 m behind the ship. Gravity data were recorded every one second and magnetic data every 0.1 seconds.

3.2.2 Processing

As for the GA-310 survey, standard processing was applied to the raw gravity data. However, Earth-tide corrections were not applied as they are generally negligible (less than ± 3 $\mu m/s^2$) compared to the error in marine gravity measurements. Land ties were made in Singapore, Fremantle and Port Hedland. Gravionic used parameters of the WGS84 ellipsoid to compute normal gravity from Equation (2) and computed free-air anomalies using Equation (1).

Processing of magnetic data included de-spiking, subtraction of the IGRF 2005 reference field and diurnal corrections based on reference stations installed in Carnarvon and Geraldton or magnetic observatory data in Gnangara and Learmonth.

Both the gravity and magnetic data for Survey GA-2476 were internally levelled (i.e. adjusted to minimise mismatches at line cross-overs), but this generally proved difficult owing to the nature of the survey design. Being designed primarily as a swath mapping survey, ship-tracks are generally sub-parallel to the coastline and there are few cross lines and a limited number of cross-over points at which to constrain mis-ties. Gravionic also undertook a preliminary merge of GA-2476 and GA-310 data. However, this only involved a grid-based merge of the individually levelled marine surveys and did not incorporate other existing data in the region.

4 Levelling of marine gravity and magnetic data

Line levelling is a key step in processing ship-borne gravity and magnetic data. The levelling process minimises the mis-tie errors at ship-track cross-overs that arise from factors such as (e.g. Prince and Forsyth, 1984; Wessel and Watts, 1988):

- positioning errors: these can be particularly large (several kilometres) for surveys conducted prior to the advent of GPS;
- poorly constrained instrument drift: constraining the inherent drift in marine gravity meters is made difficult by infrequent ties to land reference stations;
- diurnal corrections to magnetic data: older surveys tend not to have diurnal corrections applied and the large separation (often hundreds of kilometres) between the survey ship and a land-based reference station can mean that the applied diurnal corrections are not representative of those in the survey area.

Without accounting for cross-over errors, gridded ship-track data can be rendered un-interpretable by artefacts and distortions at line cross-overs (Figure 4.1). The levelling methods used here are similar to those used previously to level ship-track data around the Australian margin (DFA, 1999; 2001; Petkovic et al., 2001; Hackney, 2010).

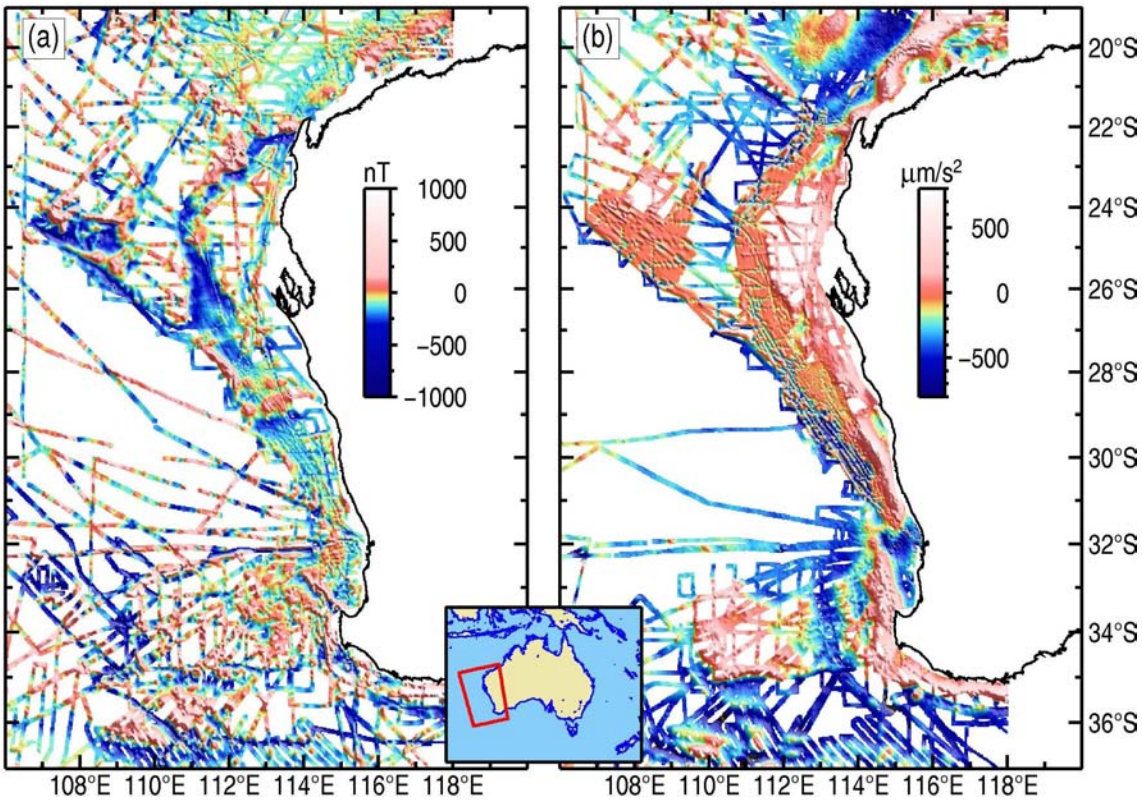

Figure 4.1: *Grids of unlevelled* ***(a)*** *magnetic (TMI) and* ***(b)*** *free-air gravity data from Survey GA-310 (Section 3.1), Survey GA-2476 (Section 3.2) and the previously-levelled dataset described by Petkovic et al. (2001) (Section 2.1.1). Grid cell size is 0.02° (~2 km).*

4.1 OUTLINE OF LEVELLING PROCESS

This section summarises the levelling methodology used to generate the southwest margin dataset (see also DFA, 1999; Hackney, 2010).

4.1.1 Free-air anomaly computation

In the case of gravity data, levelling corrections were applied to free-air anomaly values. For some datasets, free-air anomalies were recomputed according to Equation (1) to ensure all gravity data were computed in a consistent manner using WGS84 ellipsoidal parameters and normal gravity from Equation (2). In some cases this involved back-computing an observed gravity value from the free-air anomaly using the appropriate INTREPID gravity "datum".

An INTREPID gravity "datum" implicitly comprises a coordinate datum tied to a specific reference ellipsoid, specific formulae for computing normal gravity, free-air and Bouguer corrections, and possibly corrections for atmospheric mass and the geoid–ellipsoid separation. The processing described here utilised the INTREPID WGS84 gravity "datum". This datum incorporates the WGS84 ellipsoid (which requires that coordinates also be referenced to WGS84), uses Equation (2) to compute normal gravity and does not incorporate a correction for the gravity effect of the geoid–ellipsoid separation.

4.1.2 Line splitting

To facilitate the levelling process, ship-tracks are split into relatively straight line segments using INTREPID's `splitcruise` tool. This step ensures that each line segment has a roughly constant bearing so as to avoid the generation of multiple cross-over values for the same pair of lines. This allows rapid location of line cross-overs within the dataset. Data recorded during changes in line direction, particularly gravity data, are prone to errors related to the lateral forces induced by the turning ship. The `splitcruise` process also removes potentially error-prone data recorded during changes in direction.

The `splitcruise` tool requires parameters to be set that determine where a line is to be split. These parameters include (Table 2):

- an angle defining the maximum allowable direction change,
- an angle and a distance (number of samples) over which gradual changes in line direction are detected,
- the minimum number of data points required for a line segment; this avoids preserving short line segments that can be difficult to level,
- the maximum allowable distance between data points; this breaks lines where data are missing.

Table 2 shows the parameters used to split lines in the different datasets that were combined and levelled. These parameters vary depending on the data sample interval (10–60 seconds, ~25–150 m). Lines within the GA-310 and Moon AM02 datasets were not split because these datasets already contained well-defined lines with constant bearing and appropriate segregation.

4.1.3 Line filtering

Noisy data degrades the levelling process because noise-related high-frequency variations near line cross-overs make it difficult to determine a truly representative mis-tie value. To avoid this problem, most line data were smoothed by applying a Fuller low-pass spatial filter with different window sizes for each dataset. A window size was chosen for each dataset, but the chosen window size was not necessarily optimal for all lines in a dataset. However, the large number of lines precluded the

application of unique filters on a line-by-line basis (as done in initial processing by contractors, see Section 3). The details of the line filter applied to each of the southwest margin datasets are described in Section 4.2.

Table 2: Parameters used for each survey in the INTREPID `splitcruise` process. Variations in parameters reflect differences in sampling interval. Surveys GA-310 and GA-3597 ("Moon AM02") were not split because the original datasets were already separated into discrete survey lines. The maximum distance parameter is in the same units as the coordinate system of the dataset (degrees in this case, so lines are effectively not split at any gap length).

PARAMETER	2001 LEVELLED	GA-310	GA-2476	GA-3597 "MOON AM02"
Sharp Angle Tolerance (°)	20	--	20	--
Trend Angle Tolerance (°)	20	--	20	--
Trend Distance In Samples	10	--	100	--
Minimum Samples Before Drop	150	--	800	--
Maximum Distance Between Samples (°)	10000	--	10000	--

4.1.4 Line levelling

The INTREPID `marinelevel` tool calculates mis-ties at line cross-overs and then performs a network adjustment to minimise the mis-tie errors throughout the survey area. Several different methods for the network adjustment are available. For the purposes of this work, a loop levelling approach was adopted (`LevelLoop`). This approach involves distributing mis-closures (mis-ties) around closed loops using network adjustment methods (e.g. Prince and Forsyth, 1984; Mishra and Tiwari, 2011). The distributed mis-closure errors are then used to define a correction function.

The loop levelling can also be applied using a reference surface. The reference dataset might be a recent, high-quality dataset to which other datasets can be tied with confidence. In the case of gravity data, the survey lines can be adjusted against a regional, satellite-derived dataset. This approach was used to level the Australia-wide dataset in 2001 (Section 2.1.1) (DFA, 1999; Petkovic et al., 2001).

Once the correction function is computed for each survey (or combined dataset), adjustments are calculated at every observation point by interpolating a value from the correction function. The interpolation is made using an Akima spline, optionally out to a certain distance, beyond which linear interpolation is used.

Several other parameters and options must be considered and set. These are:

- `ByCruise`: determines whether or not lines without any cross-overs are levelled. If yes, then the levelling corrections are applied to the whole of a cruise/survey (identified by the `FlightNumber` alias in the INTREPID database) on the basis of the correction function for that survey. Note that the correction function is defined for the whole of a cruise area, so an adjustment value can be interpolated from the correction function for all lines, even those without cross-overs.
- `DoPseudoFidsAsRecords`: marine levelling requires a fiducial (FID) field, but if this field doesn't exist then a pseudo FID is computed from cumulative distance. In the case of the southwest margin, the different datasets had inconsistent FIDs, so new ones were generated (but not preserved) as part of the levelling process.
- `SaveEmptyGroupsInXover`: allows line segments without cross-overs to be included in the cross-over dataset.
- `DuplicateCrossOver_Fid_Tolerance`: if two cross-overs are within a certain distance of each other, one is rejected. This avoids levelling instabilities caused by extreme gradients between points that are too close (even small differences can induce extreme

gradients). This tolerance is checked as the levelling adjustments are applied because the cross-over dataset includes all cross-overs, regardless of how close they are. Units are as for coordinates.

- `MaximumPointSeparation`: if adjacent data points around a line cross-over are too widely spaced, then the mis-tie value is deemed unreliable and excluded. Units are as for coordinates.
- `MaximumInterpolationGap`: controls the use of spline or linear interpolation when interpolating an adjustment value from the correction function. Units are as for the fiducial field.

The parameters used for levelling the southwest margin dataset are described in Sections 4.3 and 4.4.

4.2 DATASET PREPARATION

4.2.1 2001 levelled dataset

The pre-existing dataset of levelled gravity and magnetic data from 2001 (Section 2.1.1) was used as a starting dataset to which other datasets were added. The benefit of starting with this dataset is that considerable time had already been spent on resolving issues such as poor data quality. These data have a sample interval of 10 seconds and are archived internally at Geoscience Australia.

After importing gravity and magnetic data into a single INTREPID database file, data preparation included line splitting using the parameters shown in Table 2. A map with survey lines before and after splitting is shown in Figure 4.2. Free-air anomalies in the 2001 levelled dataset were computed using normal gravity from an outdated Chebyshev approximate formula. Therefore, free-air anomaly values were recomputed using Equation (2) (with WGS84 ellipsoid parameters) and observed gravity values.

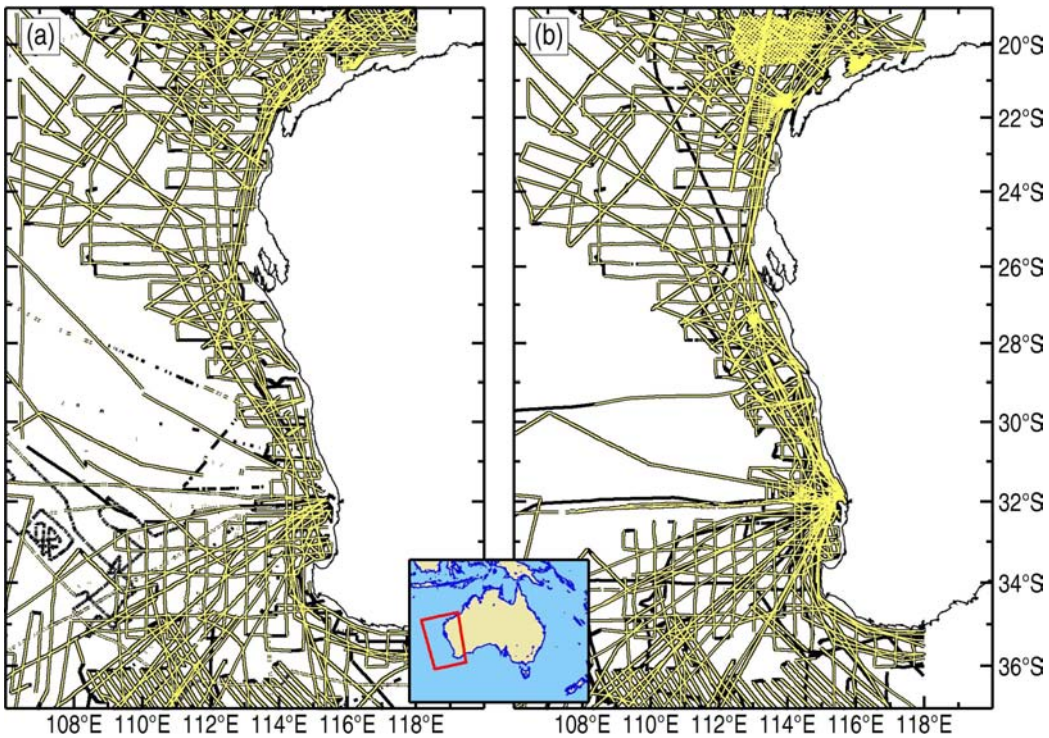

Figure 4.2: *Map showing ship tracks from the 2001 levelled dataset before (black lines) and after (yellow-on-black lines) line splitting and editing.* ***(a)*** *Lines with magnetic data,* ***(b)*** *lines with gravity data.*

Noise levels for the 2001 levelled dataset are of the order of ±1–5 nT for the magnetic data (Figure 4.3a,b) and ±20 μm/s^2 (±50–100 μm/s^2 at worst) for the gravity data (Figure 4.4a,b). For the reasons stated in Section 4.1.3, the data were smoothed by applying a Fuller low-pass filter with a window size as shown in Table 3.

Table 3: Parameters used for low-pass line filtering of the different datasets to smooth out noise.

DATASET/GA SURVEY (LEASE AREA)	FILTER WINDOW SIZE (DATA POINTS)	
	Gravity	Magnetics
2001 Levelled	41	21
GA-310	151	35
GA-2476	151	25
"Moon AM02"/GA-3597 (WA-326-P/328-P)	--	--

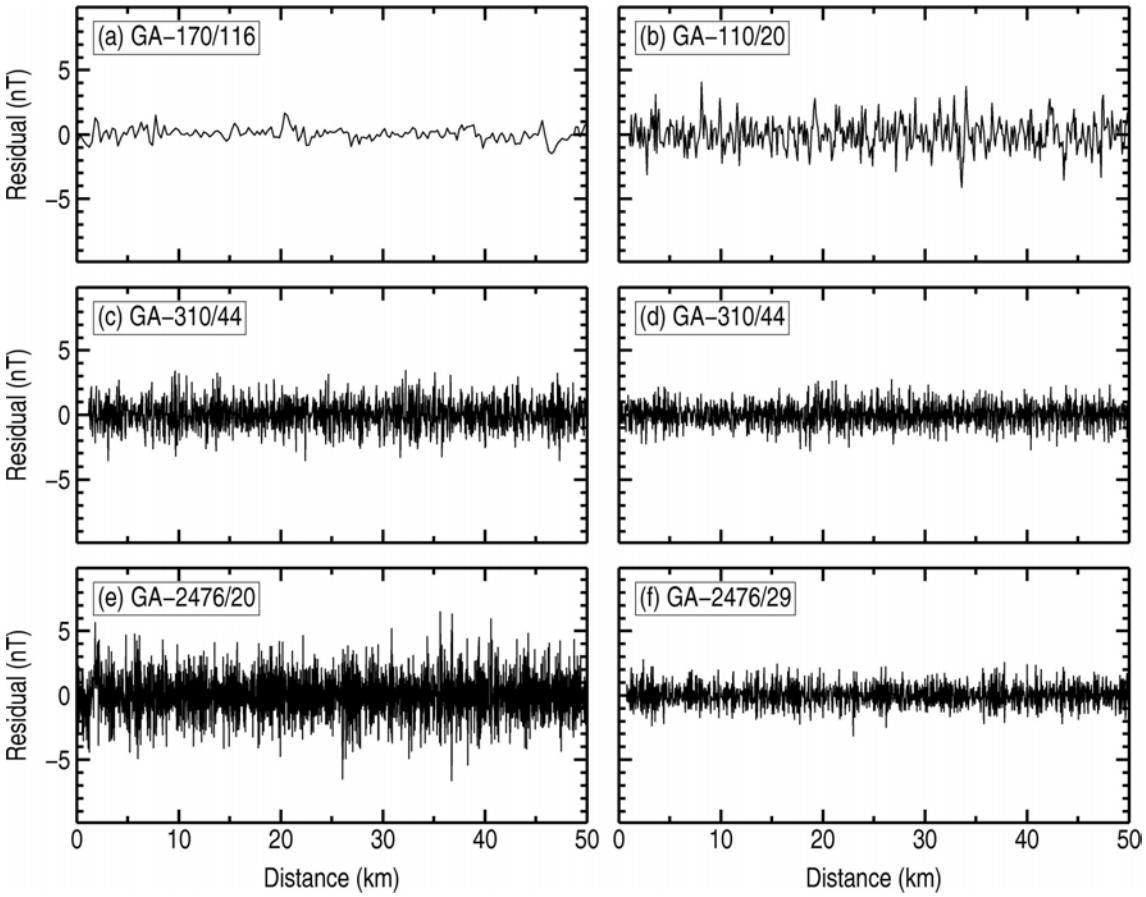

Figure 4.3: *Line segments giving an indication of noise levels in magnetic line data. The profiles show the difference between un-filtered and low-pass filtered data computed using the parameters shown in Table 3. Sample data shown are from the 2001 levelled dataset (**a** and **b**); the GA-310 survey (**c** and **d**); and the GA-2476 survey (**e** and **f**).*

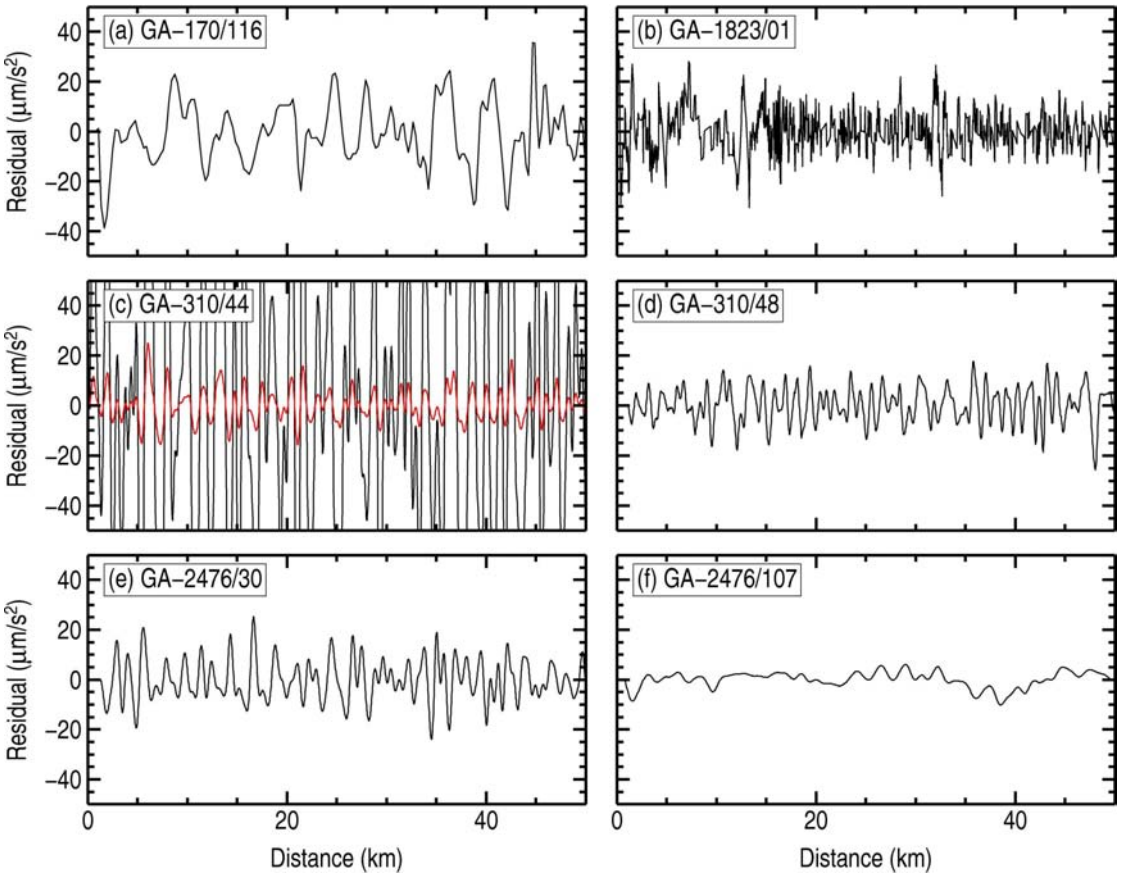

Figure 4.4: *Line segments giving an indication of noise levels in gravity line data. The profiles show the difference between un-filtered and low-pass filtered data computed using the parameters shown in Table 3. Sample data shown are from the 2001 levelled dataset (**a** and **b**); the GA-310 survey (**c** and **d**); and the GA-2476 survey (**e** and **f**). The data for line GA-310/44 shown in (c) appear to be erroneous and have probably been unnecessarily converted from mGal to µm/s² (the red lines shows the residual values divided by 10).*

4.2.2 Survey GA-310

Prior to import into a single INTREPID database file, the Survey GA-310 gravity and magnetic data supplied by the contractor (Section 3.1) were edited as follows:

- data extrapolated into measurement gaps were removed;
- an observed gravity value was back-computed from the free-air data (because no observed gravity value was provided by the contractor);
- some short line segments were merged into longer lines so that the resulting lines were directly compatible with seismic line numbers.

The contractor applied diurnal corrections based on land reference stations (Section 3.1.2), but these corrections induced some substantial offsets in the magnetic data. Diurnally-corrected magnetic data were, therefore, not used. A number of offsets along continuous line segments were adjusted manually. Line splitting was not necessary for this survey because the data were already assigned to discrete lines that coincided with lines containing seismic data.

Noise levels in the GA-310 magnetic data are of the order of ±2–5 nT (Figure 4.3c,d) and ±10–20 µm/s² for the gravity data (Figure 4.4c,d). For the reasons stated in Section 4.1.3, the data were smoothed by applying a Fuller low-pass filter with a window size as shown in Table 3.

4.2.3 Survey GA-2476

Magnetic and gravity data from Survey GA-2476 were treated separately during data preparation because they were supplied by the contractor in separate files without merging data to common coordinates. The magnetic data retained the coordinates of the sensor position (i.e. behind the ship), whereas gravity data were linked to the coordinates of the ship. In addition, magnetic data were supplied in discrete line segments, but gravity data were not. Initial data preparation involved assigning gravity data to the same lines as the magnetic data.

The sample interval was 0.1 s for the magnetic data and 1 s for the gravity data. This high data logging rate tends to oversample anomaly information and results in large file sizes. Therefore, during import into separate INTREPID database files, both datasets were downsampled to a 10 s sample interval. This downsampling did not reduce the ability to resolve anomalies of interest, but made the files more manageable during processing.

The `splitline` procedure was applied to the magnetic and gravity data in order to remove some short line segments and some lines with substantial bearing changes. Free-air anomalies were not recomputed because they were already computed using Equation (2). A Fuller low-pass filter was also applied to both the gravity and magnetic data (Figure 4.3e,f and Figure 4.4e,f) using the parameters shown in Table 3.

4.2.4 Moon AM02 (GA-3597)

Gravity and magnetic data for the "Moon AM02" survey (Austin Exploration, 2003; Intrepid Geophysics, 2004) were obtained via the Geoscience Australia Petroleum Data Repository[3] and assigned a Geoscience Australia survey number GA-3597. The gravity and magnetic data were imported into a single INTREPID database file. No additional pre-processing was required for the magnetic data. Free-air gravity anomalies in the imported database were computed using the 1967 International Gravity Formula (i.e. simplified Chebyshev formula for normal gravity) and GRS67 ellipsoid parameters. The gravity data were therefore transformed to the INTREPID WGS84 gravity "datum", an observed gravity field was back-computed from the free-air anomaly values, converted from mGal to $\mu m/s^2$ and, finally, free-air anomalies were re-computed using Equation (2) and WGS84 ellipsoidal parameters.

The imported gravity and magnetic data were already separated into discrete lines, so the `splitline` procedure was not necessary. No filtering was applied to the gravity and magnetic data prior to levelling, but a 60 s low-pass filter had already been applied by the processing contractor to the data that were imported (Austin Exploration, 2003).

4.3 LEVELLING OF MAGNETIC DATA

For the purposes of line levelling, each of the datasets described in Section 4.2 were merged into a single INTREPID database file. Table 4 lists the different datasets used for levelling the magnetic data and includes the total length of lines with magnetic data.

The magnetic data were levelled using the loop levelling method (Section 4.1.4). The parameters used in the INTREPID `marinelevel` tool are shown in Table 5. Initial levelling tests highlighted some issues with the levelled data related to a small number of closely-spaced lines, short line segments and ends of lines without cross-overs. One complete line and a segment of another were excluded from levelling (Table 6) by nulling their latitude and longitude fields using the INTREPID

[3] http://www.ga.gov.au/energy/projects/petroleum-data-repository.html (last visited 26 March 2012)

Flight Path Editor. A grid of the line-levelled magnetic data is shown in Figure 4.5 and mis-tie statistics at line cross-overs before and after levelling are shown in Table 7.

Table 4: List of the marine datasets used to produce the levelled ship-track magnetic datasets covering the offshore parts of the southwest margin of Australia.

DATASET/GA SURVEY (LEASE AREA)	YEAR	REFER SECTION	LINE KM (PRE SPLIT)	LINE KM (POST SPLIT)
Petkovic et al. (2001)	1960 – 2001	2.1.1	299309*	212816
GA-310	2008/09	3.1	6884	6884
GA-2476	2008/09	3.2	19590	16564
"Moon AM02"/GA-3597 (WA-326-P/328-P)	2002/03	2.1.2	5207	5207
Total line km			330990*	241471

*line length includes lines or line segments that do not have magnetic data

Table 5: Parameters used for loop levelling of gravity and magnetic data.

PARAMETER	VALUE	COMMENT
RunType	LevelLoop	
ByCruise	Yes	
PopulationAnalysis	No	
DoPseudoFidsAsRecords	Yes	
SaveEmptyGroupsInXover	Yes	
DuplicateCrossOver_Fid_Tolerance	0.02	Same units as database coordinates (°, ~2.2 km)
MaximumPointSeparation	10000	i.e. assume no gap is too large
MaximumInterpolationGap	10000	i.e. spline interpolation used everywhere

Table 6: List of surveys and lines that were excluded from magnetic levelling due to their short length or proximity to other lines. The numbers in brackets denote the range of data points excluded.

SURVEY	YEAR	LINE NUMBER (AS DEFINED DURING `splitline` PROCESS)
GA-235	2001	01 (1429–1533), 03 (all)

Table 7: Magnetic anomaly data range and mis-tie statistics before and after levelling (values in nT).

	MINIMUM	MAXIMUM	MEAN	MEDIAN	SD
Before levelling	-3107	2338	50.6	147.8	55.3
After levelling	-3110	2390	0.4	0.0	1.7

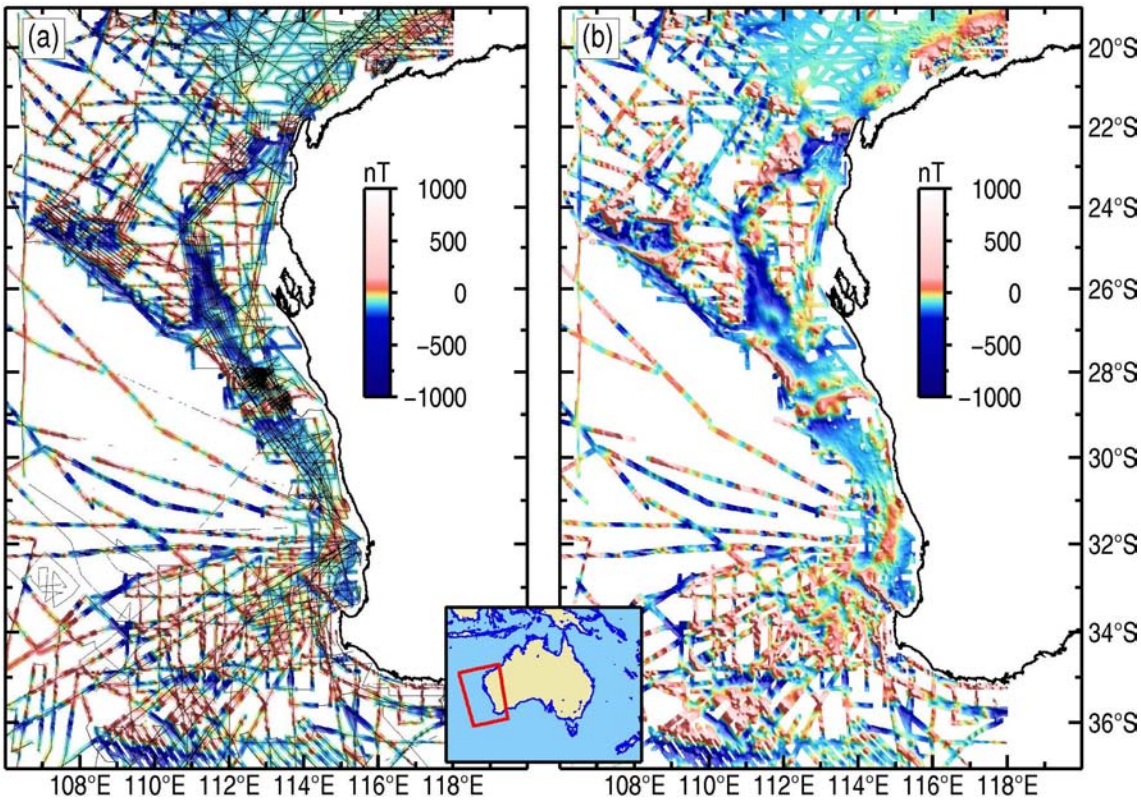

Figure 4.5: *Maps showing levelled magnetic data (TMI, nT) with* ***(a)*** *and without* ***(b)*** *ship-tracks. Grid cell size is 0.01°. The ship-tracks in (a) without colour either do not contain magnetic data or were excluded from the levelling process due to their proximity to other tracks or due to spurious data.*

4.4 LEVELLING OF GRAVITY DATA

For the purposes of line levelling the gravity data, each of the datasets described in Section 4.2 were merged into a single INTREPID database file (separate to the database used for levelling magnetic data). Table 8 summarises the different datasets used for levelling the gravity data and the total length of lines with gravity data.

Table 8: List of the marine datasets used to produce the levelled ship-track gravity dataset covering the offshore parts of the southwest margin of Australia.

DATASET/GA SURVEY (LEASE AREA)	YEAR	REFER SECTION	LINE KM (PRE SPLIT)	LINE KM (POST SPLIT)
Petkovic et al. (2001)	1960 – 2001	2.1.1	299309*	212816
GA-310	2008/09	3.1	6884	6884
GA-2476	2008/09	3.2	19344	16862
“Moon AM02”/GA-3597 (WA-326-P/328-P)	2002/03	2.1.2	5207	5207
Total line km			330744*	241769

*line length includes lines or line segments that may not have gravity data

Several of the INTREPID levelling methods were trialled, including loop and polynomial levelling, both with and without a reference surface. The best results were achieved using loop levelling and a reference surface defined by the DNSC08GRA satellite altimetry dataset (cf. Section 2.3). For levelling purposes, gridded DNSC08GRA free-air data were converted to a line dataset comprising

both north–south and east–west lines with a separation equivalent to the cell size in the original DNSC08GRA grid (1').

The parameters used in the INTREPID `marinelevel` tool for levelling the gravity data are shown in Table 5. As for the magnetic data, initial levelling highlighted some issues with the levelled data related to closely-spaced lines, short line segments and ends of lines without cross-overs. Table 9 shows the lines or line segments that were excluded from levelling by nulling their latitude and longitude fields. A grid of the line-levelled gravity data is shown in Figure 4.6 and mis-tie statistics at line cross-overs before and after levelling are shown in Table 10.

Table 9: List of surveys and lines that were excluded from gravity levelling due to their short length or proximity to other lines. The numbers in brackets denote the range of data points excluded, 'e' denoting the nearest end of line.

SURVEY	YEAR	LINE NUMBER (AS DEFINED DURING `splitline` PROCESS)
GA-17	1972	37 (e231)
GA-53	1986	204 (e1174), 205 (e10)
GA-55	1986	41 (all), 44 (e60)
GA-127	1994	34 (all), 36 (all)
GA-170	1996	101 (e10)
GA-208	1998	14 (e178)
GA-310	2008/09	02 (e6565), 09 (e4122), 27 (e1165), 28 (e31), 43 (e5549), 44 (e2890)
GA-1038	1976	03 (e29)
GA-1153	1994	04 (e4)

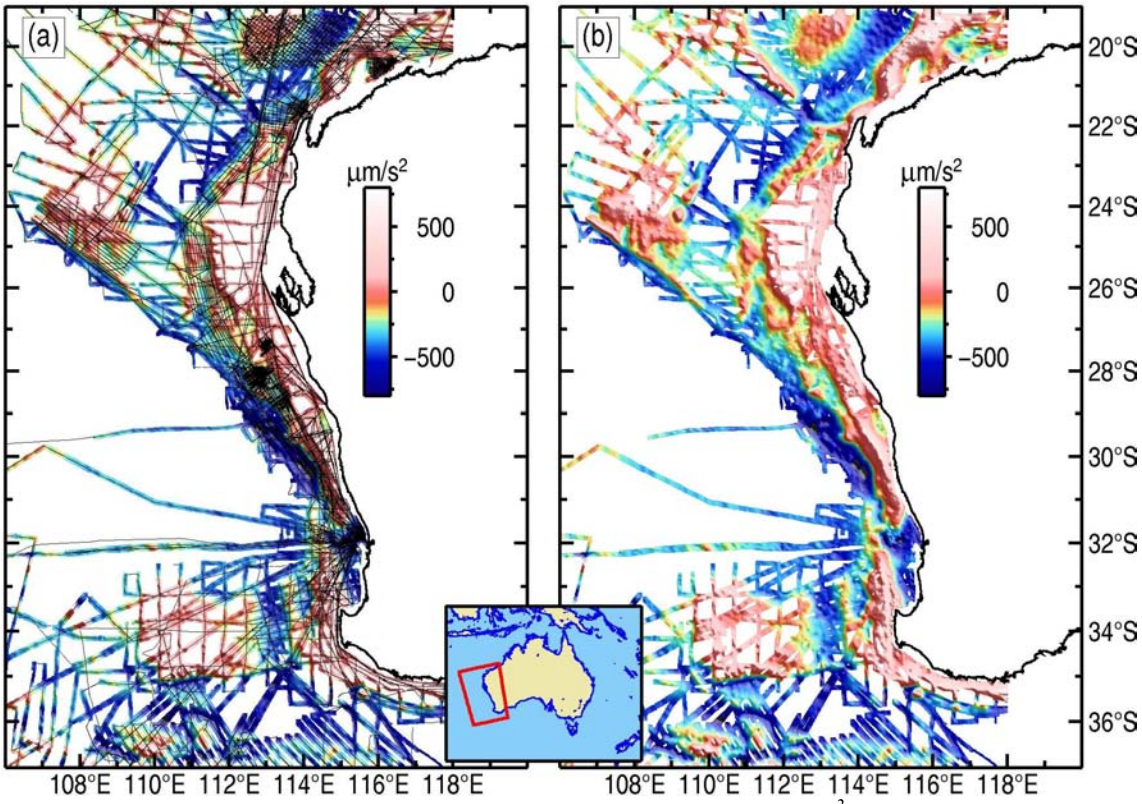

Figure 4.6: *Maps showing levelled gravity data (free-air anomalies in µm/s²). Grid cell size is 0.01°. The ship-tracks in (a) without colour either do not contain gravity data or were excluded from the levelling process due to their proximity to other tracks or due to spurious data.*

Table 10: Free-air anomaly data range and mis-tie statistics before and after levelling (values in $\mu m/s^2$). Mis-tie statistics include mis-ties between ship-track and satellite altimetry data.

	MINIMUM	MAXIMUM	MEAN	MEDIAN	SD
Before levelling	-2869	858	60.9	34.7	101.3
After levelling	-1643	2227	15.3	12.6	17.8

4.5 APPLICATION OF BOUGUER AND TERRAIN CORRECTIONS

4.5.1 Bouguer anomaly computation

In marine areas, the large density contrast at the seafloor (sea water versus sediment) means that the free-air anomaly generally retains a strong correlation with bathymetry (compare Figure 2.5 and Figure 4.6). The correlation between free-air gravity and bathymetry can be removed by applying the Bouguer correction (see Appendix A). This correction removes the gravity effect of the large density contrast at the seafloor by assuming that the seawater is replaced by rock with a density that minimises the correlation with bathymetry. The resulting Bouguer anomaly primarily reflects the crustal density distribution and Moho depth variations (cf. Appendix A).

Spherical cap Bouguer corrections were computed using the INTREPID Gravity Field Reduction tool (Argast et al., 2009). For simplicity, water depths used in the Bouguer correction were interpolated at each data point from the AUSBATH09 bathymetry grid described in Section 2.4, downsampled to a grid cell size of 0.01°. "Simple" Bouguer anomalies (i.e. Bouguer anomalies without terrain corrections) were computed for seafloor sediment densities of 1500, 1800 and 2400 kg/m^3 (Figure 4.7). For all densities, short-wavelength features remain in the Bouguer anomaly data and these features correlate with the deep canyons cut into the continental slope. This highlights the need to apply a terrain correction.

4.5.2 Terrain correction

Terrain corrections were computed using the INTREPID Gravity Field Reduction tool and the same AUSBATH09 grid (which includes onshore topography) that was used to compute the initial Bouguer corrections. Computations were made after projecting the bathymetry grid and gravity data files to UTM Zone 49°S eastings and northings (with a 1000 m cell size).

The INTREPID terrain correction methodology (Intrepid Geophysics, 2009b) divides the region surrounding individual gravity data points into a number of concentric rings (2 to 5) whose radius increases with distance from the measurement point. Each of these rings is divided into square prisms. The horizontal dimensions of the cells in the innermost ring are dictated by the resolution of the topography/bathymetry grid. The vertical extent of the prisms is governed by the mean topography or water depth within the cell. Cells in the innermost ring, to which gravity measurements are most sensitive, can have sloping tops (or bottoms) to more accurately represent topography or bathymetry. To speed up computations, the gravity effect of outer rings is computed using vertical rods to approximate increasingly large cells.

The terrain correction computations made here used flat-topped prisms in three concentric rings of radius 16, 32 and 64 km (the default radii). Tests showed that using a larger number of rings and sloping-top prisms did not greatly influence the resulting "complete" Bouguer anomalies. Densities used in the terrain correction were 1030 kg/m^3 for sea water, 1800 kg/m^3 for marine sediment and 2670 kg/m^3 for land areas. The density for marine sediments (1800 kg/m^3) was chosen because it tended to give the least correlation between simple Bouguer anomalies and bathymetry. Figure 4.8 shows the "complete" (i.e. terrain-corrected) Bouguer anomalies for the southwest margin dataset.

Figure 4.9 shows a comparison between simple and complete Bouguer anomalies for a portion of the dataset in the northern Perth Basin. This figure shows the degree to which anomaly features that

correlate with bathymetry have been removed. Whilst many of the anomalous features that correlate with deep canyons on the continental slope are reduced (cf. Figure 4.7), a bathymetry/gravity correlation still remains. This residual correlation is also evident if sediment densities of 1500 and 2400 kg/m^3 are used for the terrain correction (Figure 4.10). The persistent existence of this correlation is probably an indication that the single density value used for the terrain correction is not representative of the rocks exposed over the full depth of the canyons. As a result, geological interpretations in the vicinity of the continental slope need to take account of these residual, non-geological effects.

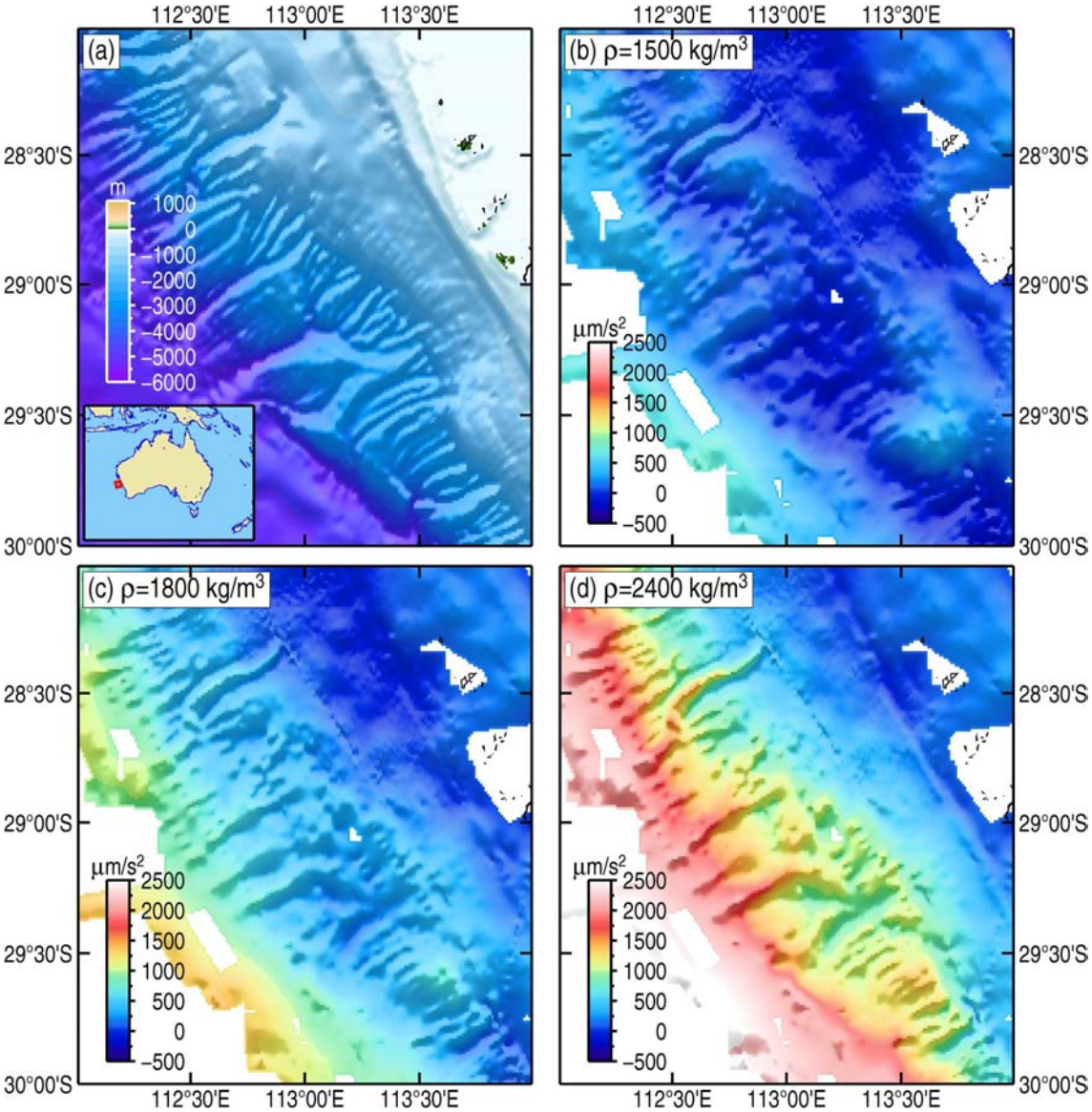

Figure 4.7: *Maps showing bathymetry and simple (no terrain correction) Bouguer anomalies for a portion of the northern Perth Basin with steep seafloor topography related to deep canyons (location shown in Figure 4.8).* ***(a)*** *AUSBATH09 bathymetry downsampled to a grid cell size of 0.01°. Simple Bouguer anomalies (in μm/s^2) are shown for assumed seafloor sediment densities of* ***(b)*** *1500 kg/m^3,* ***(c)*** *1800 kg/m^3 and* ***(d)*** *2400 kg/m^3.*

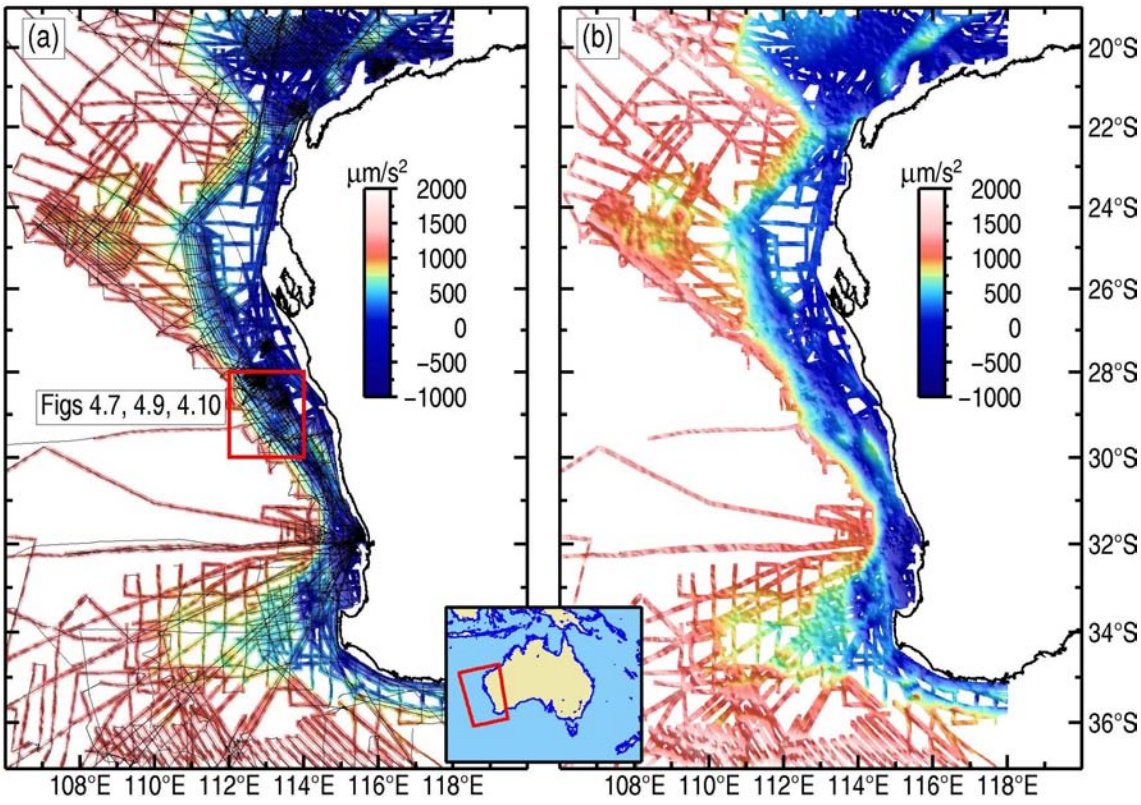

Figure 4.8: *Map showing complete (i.e. terrain corrected) Bouguer anomalies (in µm/s²) for the southwest margin of Australia. The box outlines the area shown in Figure 4.7, Figure 4.9 and Figure 4.10. Grid cell size is 0.01°. The ship-tracks in (a) without colour either do not contain gravity data or were excluded from the levelling process due to their proximity to other tracks or due to spurious data.*

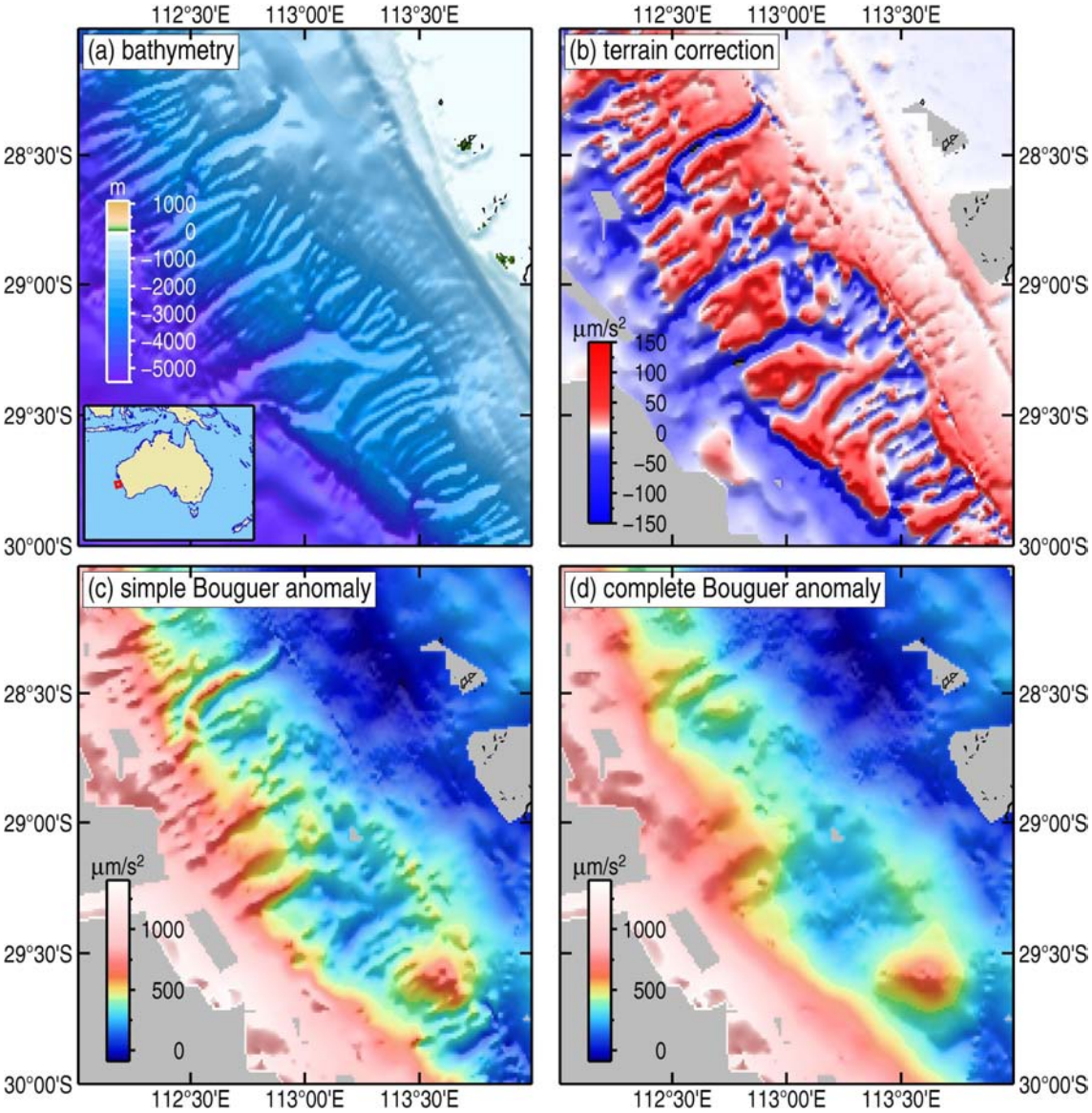

Figure 4.9: *Maps showing* ***(a)*** *AUSBATH09 bathymetry,* ***(b)*** *terrain corrections,* ***(c)*** *simple Bouguer anomalies and* ***(d)*** *complete Bouguer anomalies for a portion of the northern Perth Basin computed assuming a seafloor sediment density of 1800 kg/m^3 (location shown in Figure 4.8). The grid cell size in each image is 0.01°.*

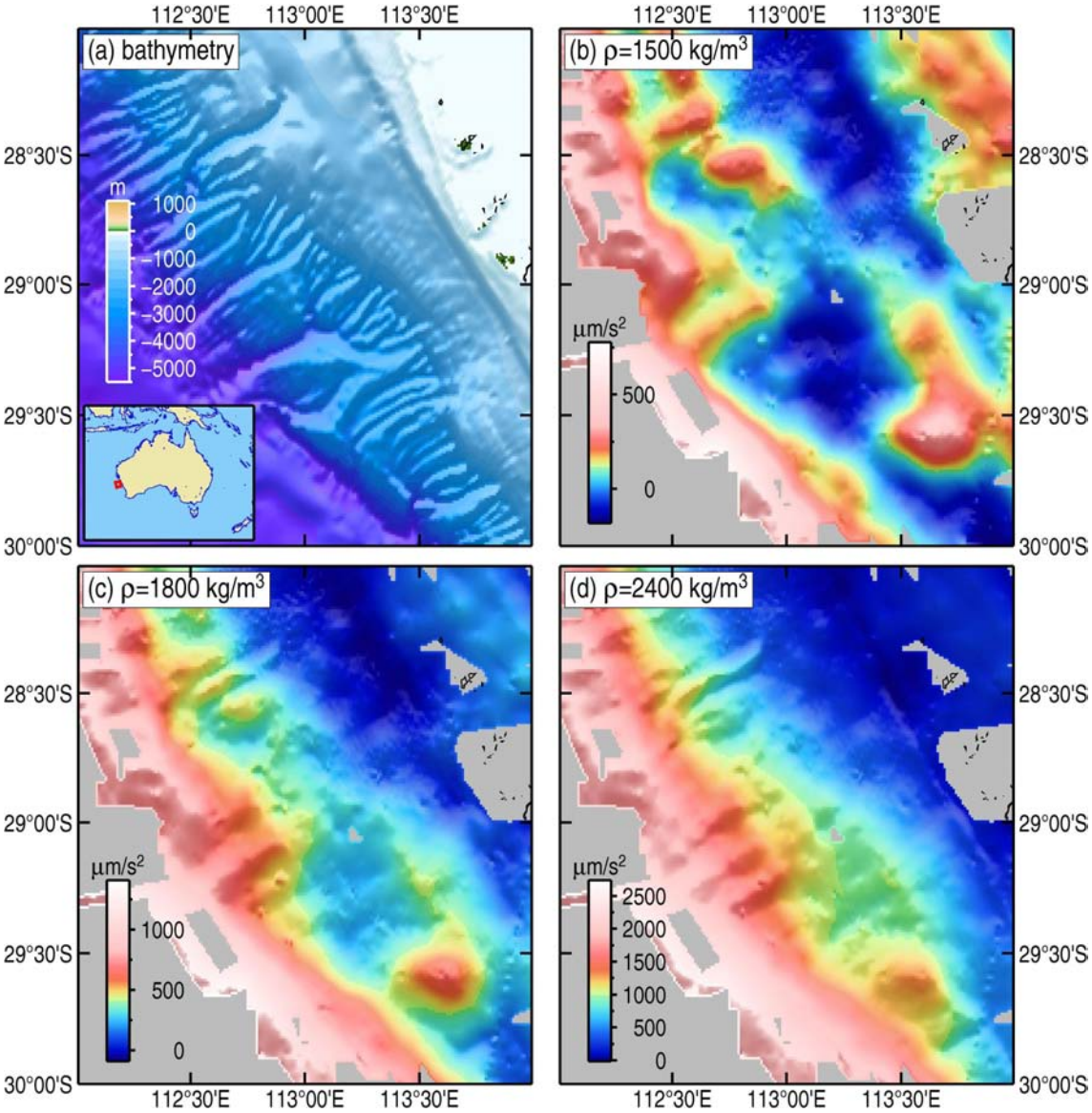

Figure 4.10: *Maps showing complete Bouguer anomalies for a portion of the northern Perth Basin (location shown in Figure 4.8) computed using different seafloor sediment densities.* ***(a)*** *AUSBATH09 bathymetry. Complete Bouguer anomalies (in μm/s^2) are shown for seafloor sediment densities of* ***(b)*** *1500 kg/m^3,* ***(c)*** *1800 kg/m^3 and* ***(d)*** *2400 kg/m^3. Note the residual correlation with the deep canyons cutting into the continental slope. The grid cell size in each image is 0.01°.*

5 Combining marine and land data

The newly levelled marine data described in Section 4 were combined with onshore data to provide a seamless onshore/offshore dataset. This is useful for regional scale studies, including the interpretation of basement structure and composition and for inferring the distribution of basement domains on the southwest margin of Australia (e.g. Hall et al., 2012; Hall, in prep.). The offshore and onshore magnetic data were combined by merging gridded data, whereas gravity data were combined as point data and then re-gridded together. These different approaches reflect the availability of pre-prepared high-resolution gridded magnetic data (Section 2.2.1) and the need to partially re-process onshore gravity data to ensure compatibility with the offshore data.

Table 11 summarises the different datasets that were combined to produce onshore/offshore gridded data for interpretation.

Table 11: List of the datasets used to produce the combined onshore/offshore gravity and magnetic datasets covering the southwest margin of Australia. Dataset format: L, line data; P, point data; G, grid data. The "SW Margin levelled" dataset includes data from the 2001 levelled data described by Petkovic et al. (2001) and the GA-310, GA-2476 and Moon AM02 surveys (Section 4).

DATASET (LEASE AREA)	YEAR	GRAVITY	MAGNETIC	SECTION
SW Margin levelled	1960–2009	L	L	4
Mag. Map Australia	5th Ed. 2010	--	G	2.2.1
Onshore gravity	2010 release	P	--	2.2.2
DNSC08GRA	2010	G	--	2.3
"East Abrolhos" (WA-325-P)	2003	--	G	2.1.2
"Beagle B92" (WA-228-P)	1992	--	G	2.1.2

5.1 MAGNETICS

Prior to merging with the gridded airborne data, the levelled ship-track magnetic data were gridded at a 0.01° cell size (~1 km), as were data from the "East Abrolhos" and "Beagle B92" surveys (Figure 5.1) that were not included in the 5th Edition Magnetic Anomaly Map of Australia (Section 2.1.2). For the region bound by 112–120°E and 19–37°S, the gridded magnetic data from the Magnetic Anomaly Map of Australia were downsampled to a grid cell size of 0.005° (~500 m). This downsampling made processing quicker whilst maintaining a resolution sufficient for the interpretation purposes outlined above.

The four separate magnetic datasets were merged using the INTREPID `GridMerge` tool (Intrepid Geophysics, 2009a). This tool applies a constant shift to align overlapping grids vertically, a surface adjustment to apply tilts to better align the separate grids and then merges the grids by applying a feathering process to generate a seamless join between grids. The vertical shift and surface adjustment can be applied with reference to a base grid that is not adjusted and a grid hierarchy can be defined during the feathering process to ensure that the highest-quality grids (i.e. aeromagnetic data) are prioritised over poorer quality data (i.e. ship-track data).

The merged magnetic grid for the southwest margin of Australia is shown in Figure 5.2. No base grid was assigned during vertical shifting and surface adjustment, but the East Abrolhos and Beagle B92 aeromagnetic surveys were assigned a high ranking for merging and feathering, whereas the levelled ship-track data were ranked the lowest. Third-order polynomials were used for the surface adjustment process. The cell size of the merged grid is 0.005° (i.e. the cell size in the final grid is the

same as for the highest-resolution grid; i.e. the downsampled 5th Edition Magnetic Anomaly Map of Australia).

Table 12: List of vertical shifts applied to each grid in the `GridMerge` process. Datasets are listed in the order of the ranking (from highest to lowest). Values are in nT.

DATASET/GA SURVEY (LEASE AREA)	VERTICAL SHIFT
"East Abrolhos" (WA-325-P)	0
"Beagle B92" (WA-228-P)	86.4
Mag. Map Australia	38.9
New levelled marine dataset	84.4

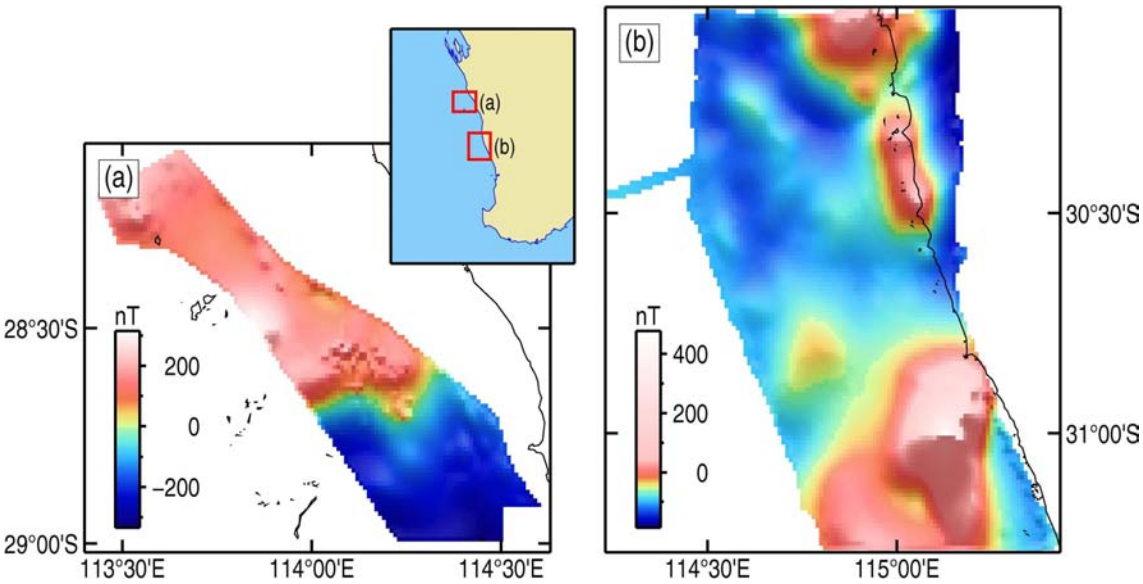

Figure 5.1: *Maps showing gridded aeromagnetic data from the* ***(a)*** *East Abrolhos and* ***(b)*** *Beagle B92 surveys. The grid cell size in each image is 0.01°.*

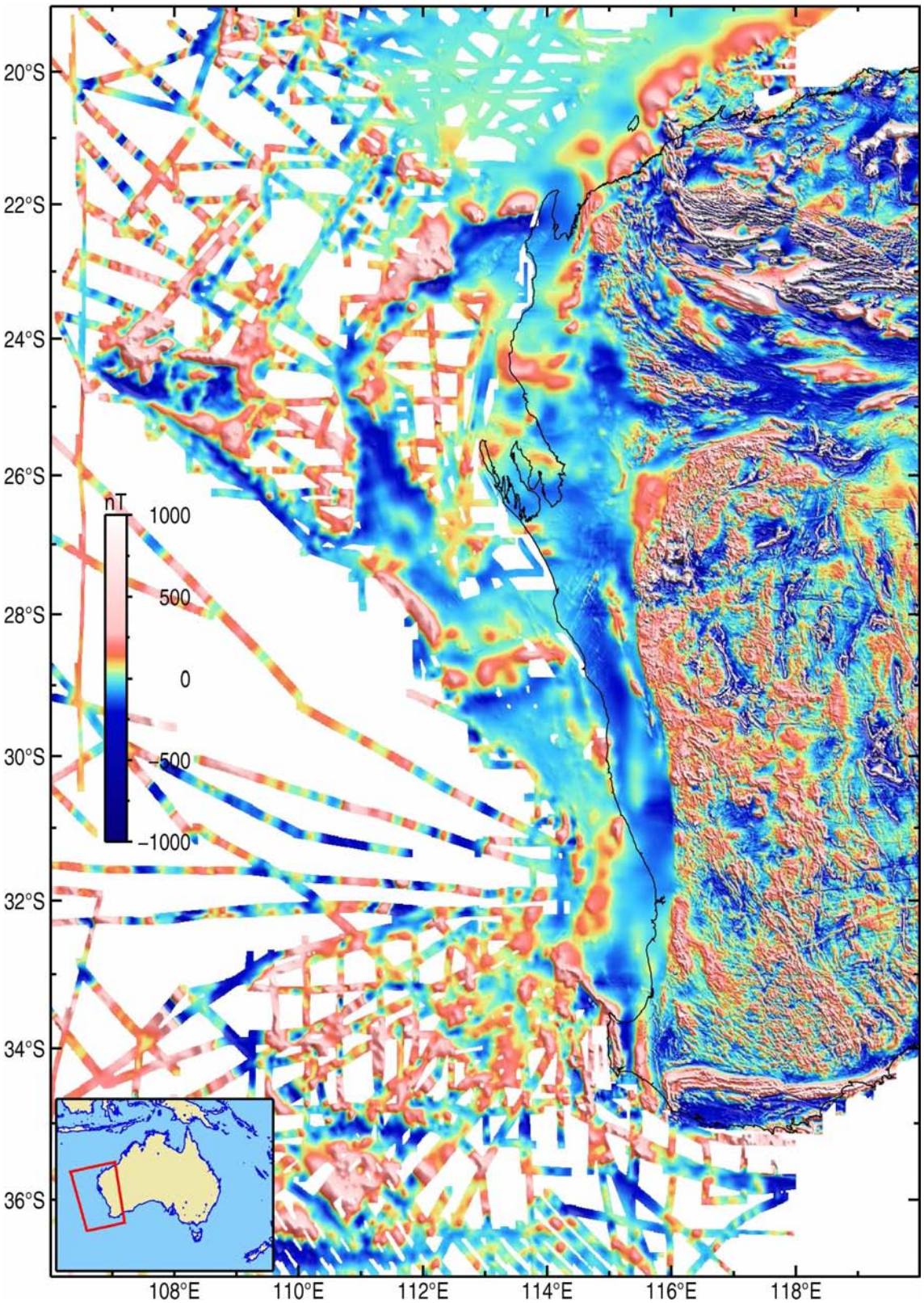

Figure 5.2: *Map showing the merged total magnetic intensity dataset that combines newly-levelled ship-track with aeromagnetic data. The grid cell size is 0.005°.*

5.2 GRAVITY

Initial attempts to combine land and marine (including satellite altimetry) data using the `gridmerge` tool proved unsatisfactory. As a result, point data were used to combine the onshore and offshore gravity data. Onshore point data from the 2010 release of the Australian National Gravity Database were obtained for the region 112–120°E and 19–37°S (Section 2.2.2), while the gridded DNSC08GRA satellite altimetry data (Section 2.3) were saved as point data.

A spherical Bouguer cap correction was computed for the onshore data using a standard correction density of 2670 kg/m^3 (e.g. Hinze, 2003) and heights relative to the geoid. Unlike the offshore ship-track data, the onshore gravity data were not terrain corrected. However, this discrepancy has little influence on interpretation as terrain corrections are generally less than 50 μm/s^2 for most of the onshore area considered here (cf. Kuhn et al., 2009). The onshore and ship-track gravity were then combined into a single dataset and gridded using a cell size of 0.01° (Figure 5.3).

The land and ship-track dataset was also combined with the DNSC08GRA gravity data described in Section 2.3. In order to generate Bouguer gravity values for the DNSC08GRA data, a bathymetry value was interpolated at each grid point from a low-pass filtered version of the AUSBATH09 bathymetry dataset. An observed gravity value was back-computed from the free-air gravity so that the INTREPID Gravity Field Reduction tool could be used to compute simple Bouguer anomalies. In order to give preference to land and ship gravity values, DNSC08GRA values within 0.03° of a land or ship measurement point were excluded before all data were combined into a single point dataset and gridded (Figure 5.4).

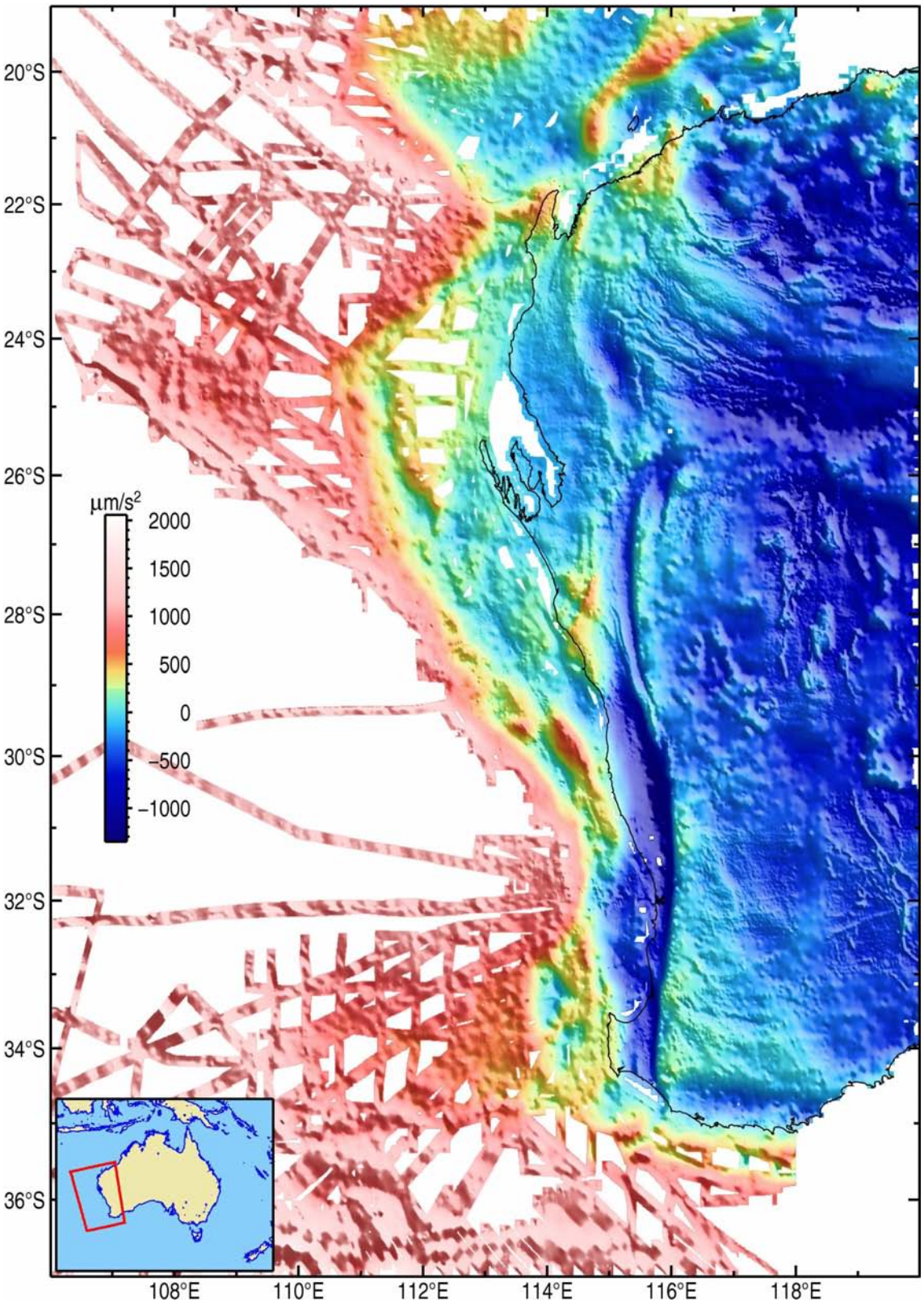

Figure 5.3: *Map showing Bouguer gravity anomalies after combining the newly-levelled ship-track gravity data with onshore data. The grid cell size is 0.01°.*

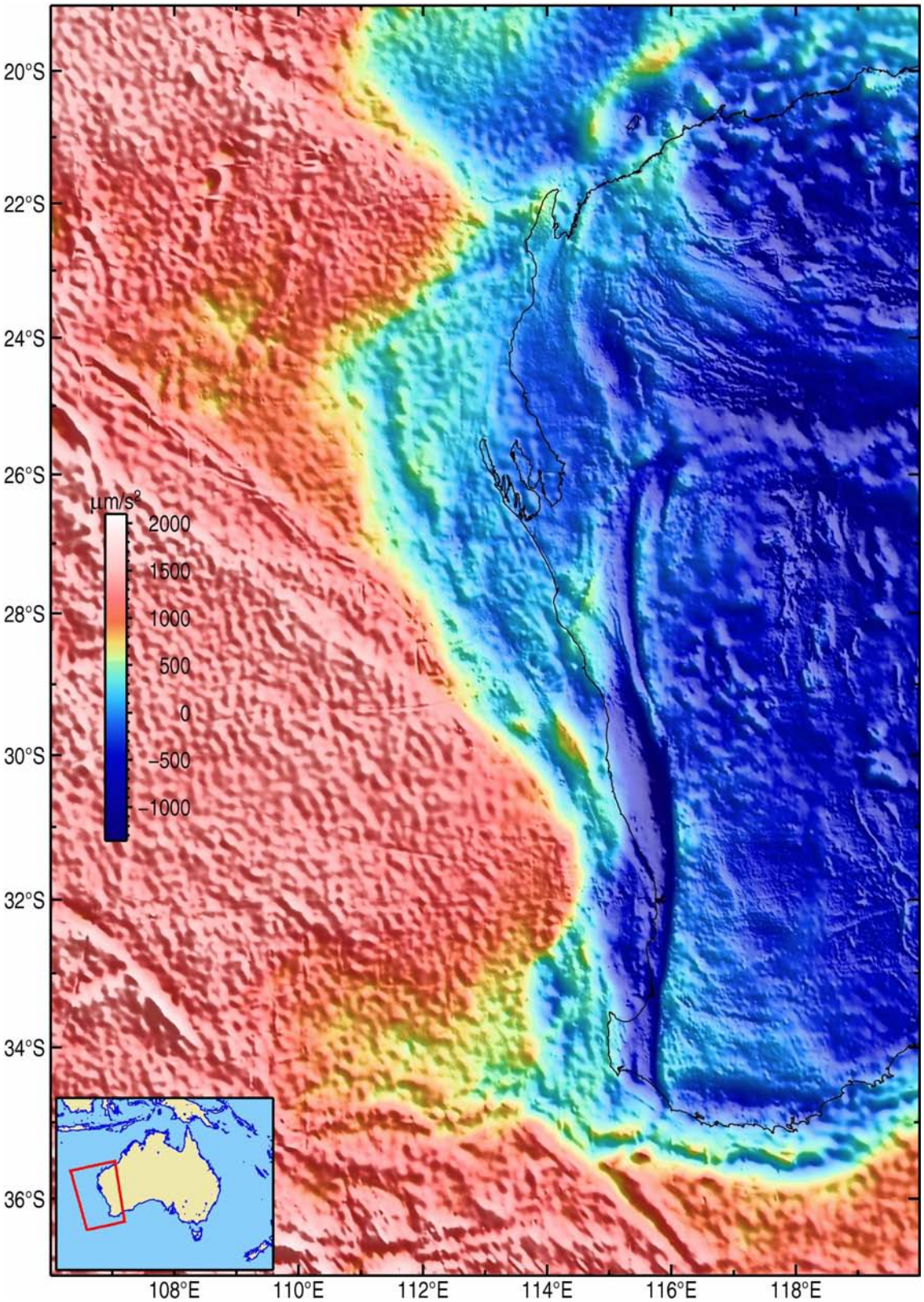

Figure 5.4: *Map showing Bouguer gravity anomalies after combining newly-levelled ship-track data, onshore data and DNSC08GRA satellite altimeter-derived data. The grid cell size is 0.01°.*

6 Derivative images for interpretation

This section displays and describes various derivative images that can be used to facilitate geological interpretation. These images are derived by enhancing various components of the gravity and magnetic signal to highlight anomalies that are likely to be associated with specific geological features (e.g. basins, faults and basement domains, etc.).

6.1 POLE-REDUCTION

The dipole nature of the Earth's magnetic field means that, unlike gravity anomalies that tend to be centred over mass anomalies, magnetic anomalies are generally displaced from their source body and form part of a skewed positive–negative coupled anomaly (e.g. Blakely, 1996, p330). This is the case whenever the inclination of the Earth's magnetic field is non-vertical, as it is everywhere but the magnetic poles. Dipole magnetic anomalies can be difficult to interpret, but the problems can be overcome by reducing the magnetic data to the pole. Pole reduction removes complications that inhibit interpretation by laterally shifting anomalies to be located over the associated source. After pole reduction, anomalies related to a symmetrical source take on the symmetrical form they would have if measured at a magnetic pole. It is important to note that pole reduction assumes only induced magnetisation.

Pole reduction requires a latitude and longitude value so that field orientation parameters (i.e. inclination and declination from the International Geomagnetic Reference Field) can be determined. However, for a large dataset with a wide latitude range, the orientation of the ambient magnetic field varies considerably and the assumption of a single inclination and declination for pole reduction is invalid. For example, for the latitude range of the southwest margin dataset (19–37°S), assuming a mid-range latitude for pole reduction means that discrepancies in inclination at the northern and southern extremities of the data will reach 10°. This leads to errors in the pole-reduced anomalies.

To overcome this, a variable-latitude pole reduction can be computed. The INTREPID implementation of variable-latitude pole reduction uses a Taylor series expansion to approximate the gradient of inclination and declination across the data grid. The variable-latitude pole-reduced magnetic data for the southwest margin of Australia are shown in Figure 6.1a. The difference between the standard and variable-latitude pole-reduced magnetic data is shown in Figure 6.1b.

6.2 REGIONAL–RESIDUAL FIELD SEPARATION

Long-wavelength regional trends in gravity data will tend to obscure anomalies of interest, in this case those that provide insight into the structural architecture of sedimentary basins and associated basement. Regional trends are particularly obvious in the Bouguer gravity field (Figure 5.3; see also Appendix A) because it still reflects crustal structure. The Bouguer anomaly is broadly negative onshore, reflecting thick continental crust, and broadly positive offshore, reflecting thin oceanic crust and the proximity to the surface of shallow, high-density mantle.

Many methods are used to remove regional trends (e.g. Mallick et al., 2011). These include spectrally-based filtering and upward continuation to define the regional field that is subsequently subtracted from the original field.

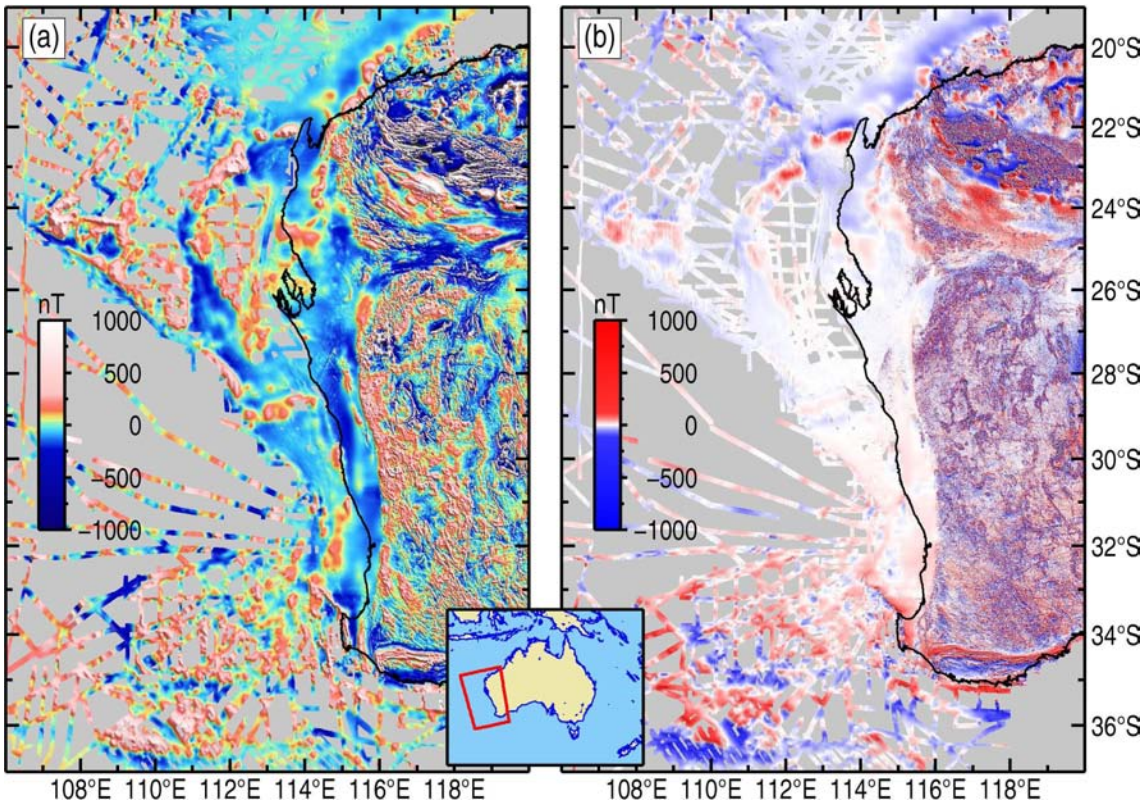

Figure 6.1: *Maps showing* ***(a)*** *variable-latitude reduced-to-pole magnetic anomalies and* ***(b)*** *the difference between standard and variable-latitude pole-reduced grids. The grid cell size is 0.01°*

6.2.1 Upward-continuation filters

Upward continuation is a process by which potential-field data are transformed to simulate their form when measured at a higher elevation (i.e. further from the anomaly sources) (e.g. Blakely, 1996, p313). By effectively shifting measurements to a higher level, the high-frequency (short wavelength) anomalies associated with upper-crustal structure are attenuated or removed. The upward continued field can then be used to separate the longer-wavelength components of the field, generally related to deeper crustal structure, from the anomalies related to shallower geological features that are of more direct interest (e.g. sedimentary basins, basement structure). Jacobsen (1987) argues that separation filters based on upward continuation are more readily comprehensible than band-pass filtering.

Upward continuation filtering has been applied with good effect to studies of the Bass Strait region between mainland Australia and Tasmania (e.g. Morse, 2010) and a similar approach is applied here. Figure 6.2a shows a residual gravity image computed by subtracting from the Bouguer gravity image (Figure 5.3) its upward continuation to 25 km (Figure 6.2b). This filter highlights upper-crustal density contrasts and is therefore useful for highlighting relative depth-to-basement variations where there is a strong density contrast between basement and sedimentary fill. For example, compared to the Bouguer image, this map highlights gravity highs associated with basement highs (e.g. Turtle Dove Ridge, Yallingup Shelf) and gravity lows associated with basin depocentres (e.g. the Dandaragan and Bunbury troughs of the onshore Perth Basin; the Eastern Mentelle Basin; and the Zeewyck and Abrolhos sub-basins of the offshore Perth Basin).

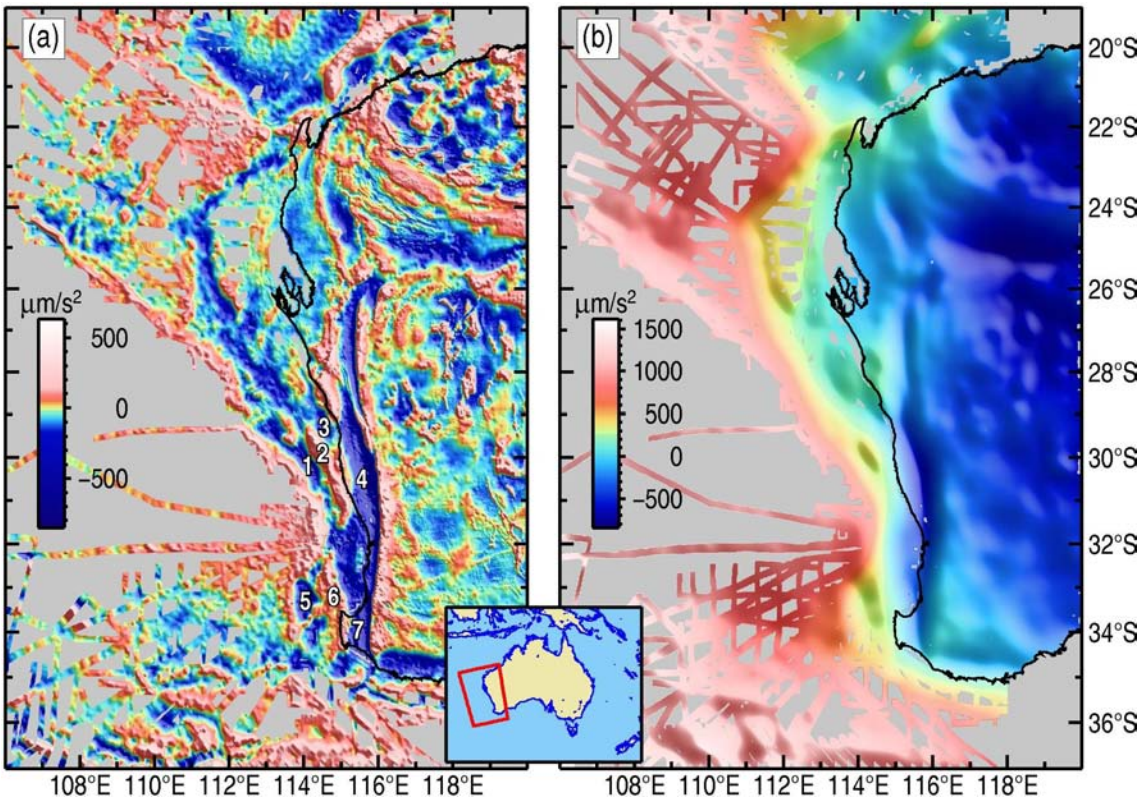

Figure 6.2: *Map showing* ***(a)*** *residual gravity computed by subtracting the 25 km upward continued field, shown in* ***(b)****, from the original Bouguer gravity (Figure 5.3). The grid cell size is 0.01°. The labelled features in (a) are: 1 – Zeewyck Sub-basin; 2 – Turtle Dove Ridge; 3 – Abrolhos Sub-basin; 4 – Dandaragan Trough; 5 – Eastern Mentelle Basin; 6 – Yallingup Shelf; 7 – Bunbury Trough.*

6.2.2 Spectral Filtering

Filtering based on spectral analysis utilises the power spectrum of gridded data to isolate and then remove or retain specific wavelength ranges within the data. To allow rapid computation, spectral filtering is conducted in the frequency domain using the Fast Fourier Transform. Spectral-domain filters include:

- Low-pass filter: retains long-wavelength signal beyond a certain cut-off wavelength, thereby suppressing noise and preserving anomaly features related to deeper features
- High-pass filter: retains short-wavelength signal, including noise, below a certain cut-off wavelength, thereby retaining anomaly features related to shallower geological features
- Band-pass filter: retains wavelengths within a specific range of wavelengths

Isolating the signal associated with specific wavelengths is useful because, in general, longer wavelengths relate to deeper structures, whereas shorter wavelengths tend to reflect shallower structures. However, given the inherent ambiguity in potential field data, this correlation does not always hold (e.g. a broad, shallow structure can also be associated with a long-wavelength anomaly).

Figure 6.3 shows band-pass filtered Bouguer gravity data preserving wavelengths in the range 8–100 km. This filter removes: 1) higher-frequency signal, thereby smoothing the anomalies to remove noise; and 2) longer-wavelength variations related to changes in crustal thickness between onshore and offshore areas. The resulting image tends to highlight the gravity signal of geological features such as basin depocentres and basement structures (cf. Hall, in prep.).

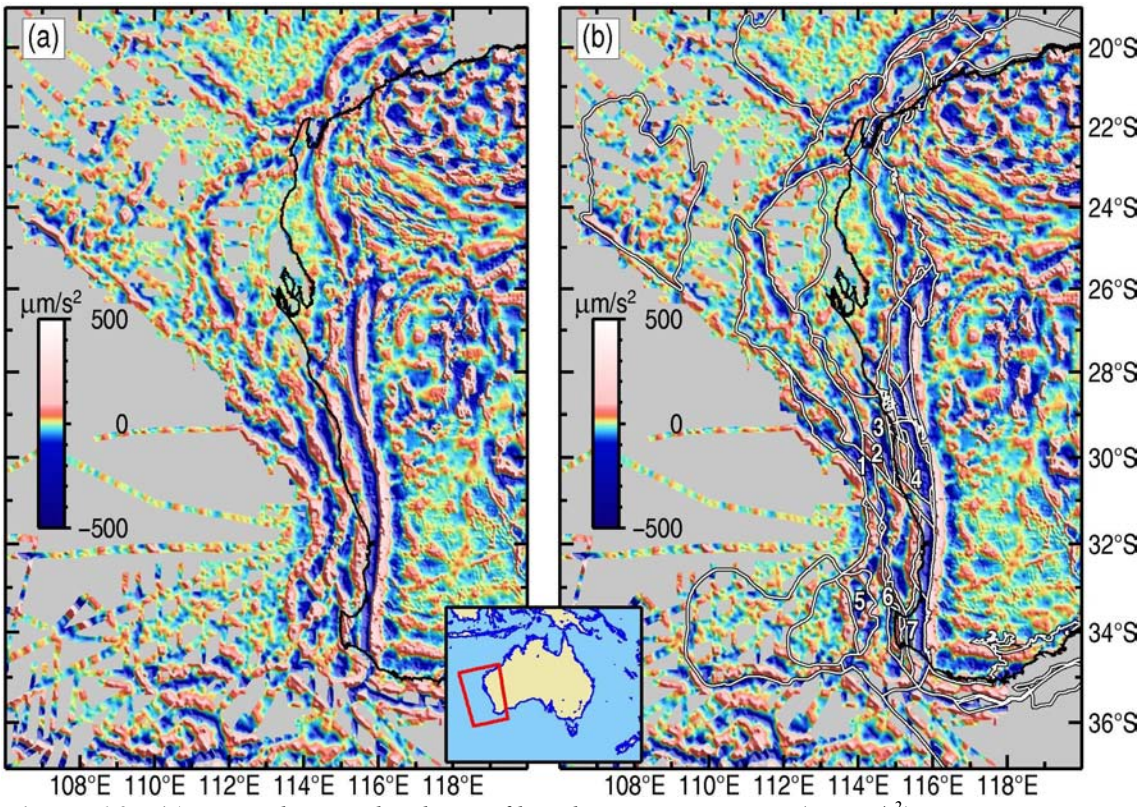

Figure 6.3: (a) *Map showing band-pass filtered Bouguer gravity (in µm/s²) preserving wavelengths in the range 8–100 km. The grid cell size is 0.01°.* ***(b)*** *As in (a) with structural elements from the Geoscience Australia Provinces Database (Figure 1.1). Labelled features are as in Figure 6.2a.*

6.3 GRADIENT-BASED FILTERS

6.3.1 Vertical derivative

The vertical derivative of gravity or magnetic data is a measure of the rate of change in the vertical direction. It tends to remove most of the regional trend and improves the resolution of shallower geological features (e.g. Blakely, 1996, p325; Swain and Kirby, 2011). It can, however, enhance noise. For noisy data, a fractional vertical derivative (e.g. 0.5, 1.5) can be computed so that less of the noise is enhanced (e.g. Cooper and Cowan, 2003).

In onshore areas, where data resolution is higher, the first vertical derivative of magnetic and Bouguer gravity data (Figure 6.4a and Figure 6.5a) enhances anomalies related to upper-crustal structure. In contrast however, the first vertical derivative filter tends to highlight noise in offshore areas. Most of this noise reflects the residual misfit that remains at line cross-overs after levelling. In offshore areas, the "half" vertical derivative (Figure 6.4b and Figure 6.5b) is not as noisy and is easier to interpret.

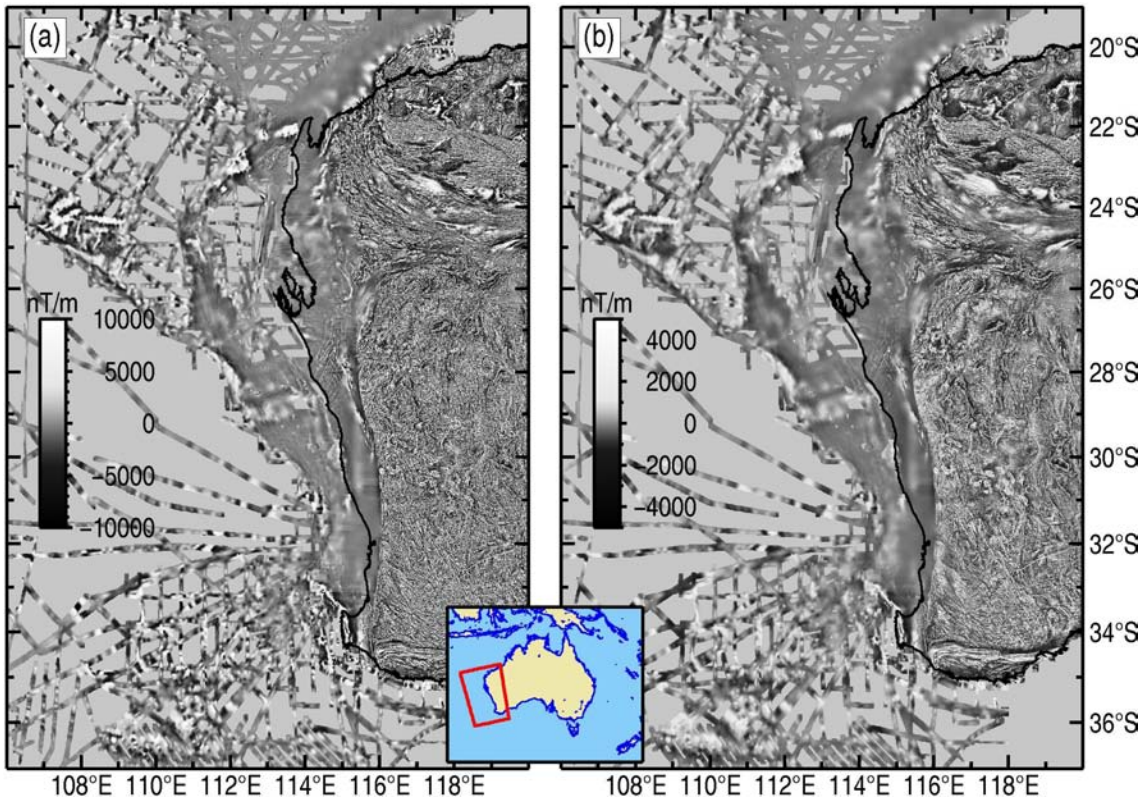

Figure 6.4: *Maps showing* ***(a)*** *first vertical derivative and* ***(b)*** *"half" vertical derivative of southwest margin magnetic data (grid cell size is 0.005°).*

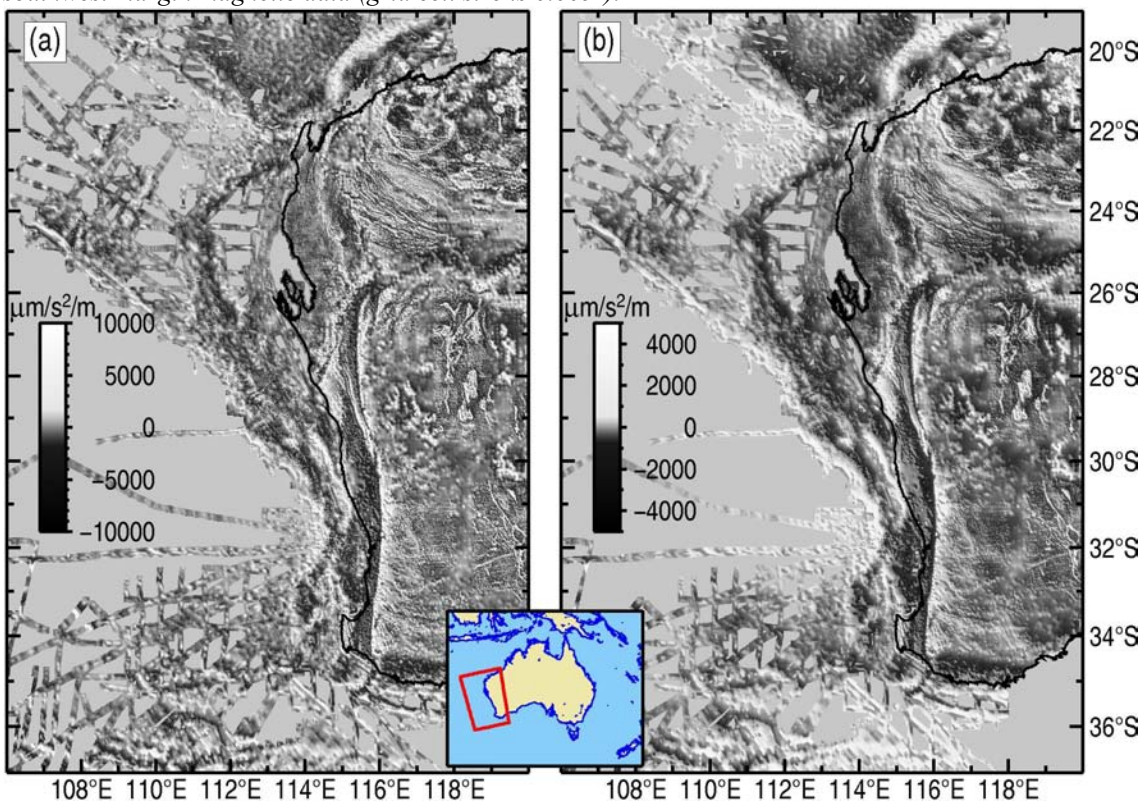

Figure 6.5: *Maps showing* ***(a)*** *first vertical derivative and* ***(b)*** *"half" vertical derivative of southwest margin gravity data (grid cell size is 0.01°).*

6.3.2 Analytic signal and tilt angle

Computation of the analytic signal has a similar goal to pole reduction (cf. Section 6.1) in that it helps to remove the dipole nature (skewness) of magnetic anomalies away from the magnetic poles and to locate the edges of source bodies. The form of the analytic signal depends on the location of the causative bodies but is independent of magnetisation direction. This characteristic of the analytic signal means that it is useful in identifying the existence of remanent magnetisation (e.g. Roest and Pilkington, 1993).

The amplitude of the analytic signal is given by the square root of the sum of the squares of the vertical and horizontal derivatives of the gravity or magnetic field, $\partial f/\partial x$, $\partial f/\partial y$ and $\partial f/\partial z$ (Roest et al., 1992):

$$AS = \sqrt{\left(\frac{\partial f}{\partial x}\right)^2 + \left(\frac{\partial f}{\partial y}\right)^2 + \left(\frac{\partial f}{\partial z}\right)^2}\ .$$

The so-called tilt angle (Miller and Singh, 1994) gives a measure of the phase of the analytic signal and is defined by:

$$TA = \tan^{-1}\left(\frac{\partial f}{\partial z} \Big/ \frac{\partial f}{\partial h}\right)$$

where

$$\frac{\partial f}{\partial h} = \sqrt{\left(\frac{\partial f}{\partial x}\right)^2 + \left(\frac{\partial f}{\partial y}\right)^2}$$

is the total horizontal derivative.

The tilt angle has the property that it is positive over anomaly sources and negative elsewhere and, because it is the ratio of vertical to horizontal derivative, it tends to balance the signature of high and low amplitude anomalies.

Analytic signal and tilt angle for the southwest margin dataset are shown in Figure 6.6.

Once the tilt angle has been computed, polygons can be defined from the positive parts of the tilt angle. These polygons then approximate the outline of source bodies, regardless of their magnetisation direction, and thus serve as a useful aid to geological interpretation and structural mapping (Morse, 2010). Source polygons for the southwest margin magnetic dataset are shown in Figure 6.7. To reduce the effects of noise, the magnetic data were upward continued to 5 km prior to computation of the tilt angle.

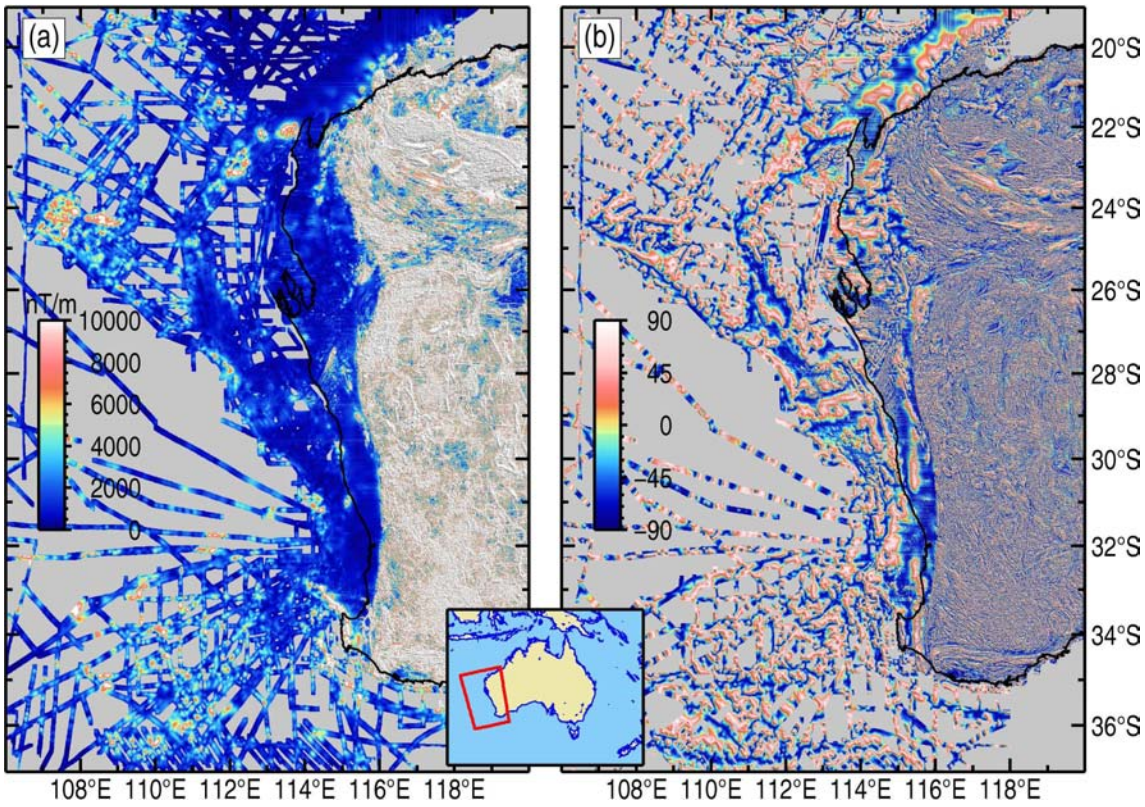

Figure 6.6: *Maps showing* ***(a)*** *analytic signal and* ***(b)*** *tilt angle of southwest margin magnetic data (grid cell size 0.005°).*

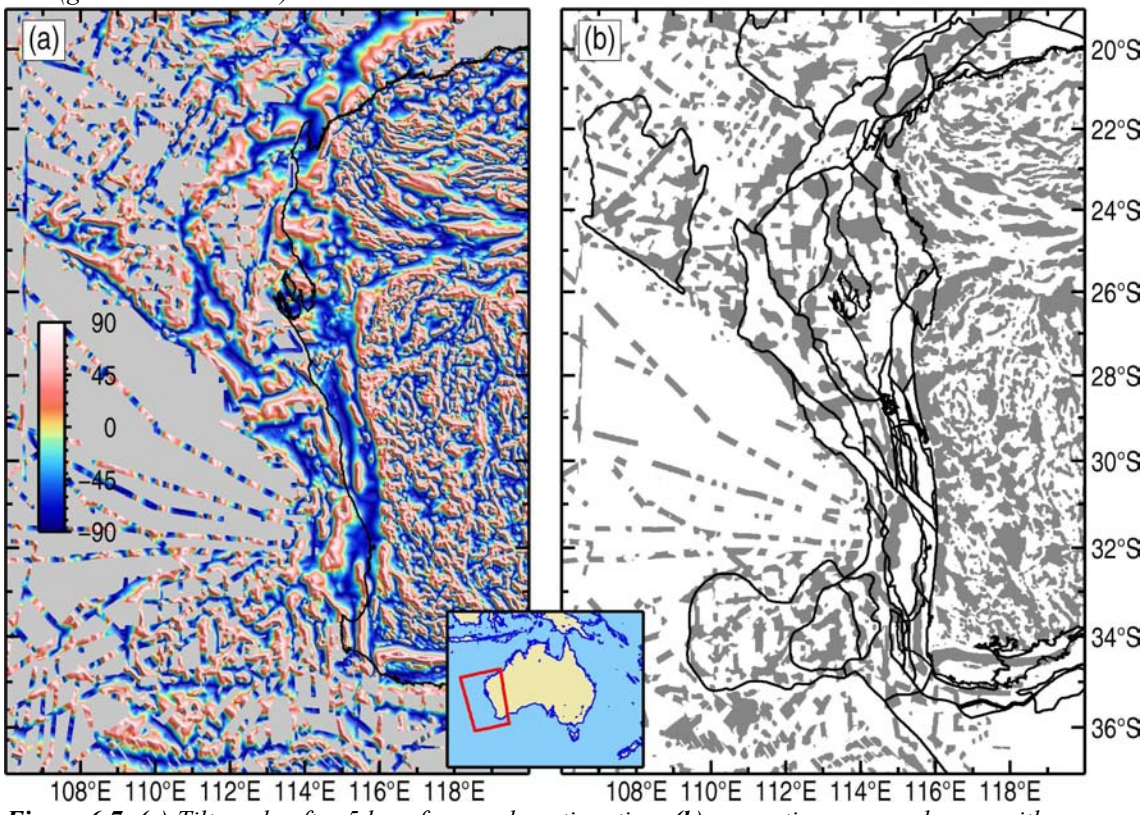

Figure 6.7: (a) *Tilt angle after 5 km of upward continuation;* ***(b)*** *magnetic source polygons with the main geological elements of the southwest margin (Figure 1.1). The grid cell size is 0.01°*

6.4 COMPARATIVE PROFILES AND QUALITATIVE INTERPRETATION

Figure 6.8 and Figure 6.9 show data from a profile across the northern Perth Basin to highlight the relationship between different anomaly types and the various filters applied to the data. The profile coincides with seismic reflection lines GA-310/29 and PM99-56MR (cf. figure 5 in Jones et al., 2011b).

Figure 6.8a and Figure 6.9a show a simplified geological cross-section that incorporates water, sediment and basement. Top basement is taken from an unpublished interpretation of the maximum depth to which sediments can be inferred from the seismic data ("base resolvable section"; C. Nicholson and G. Bernardel, *pers. comm.*, 2011). The cross section shows the two main sediment depocentres intersected along the profile (Zeewyck and Abrolhos sub-basins). These sub-basins are separated by a basement high (Turtle Dove Ridge). The interpretation of this profile is addressed further by Johnston and Petkovic (in prep.) and Petkovic (in prep.) using two-dimensional forward modelling of magnetic and gravity data.

Figure 6.8b and Figure 6.8c highlight the difference between the total magnetic intensity and the pole-reduced magnetic data, although the differences on this profile are subtle. The Zeewyck and Abrolhos sub-basins are associated with subdued magnetic anomalies and the Turtle Dove Ridge correlates with a relative magnetic high. The analytic signal profile is noisy (Figure 6.8d), but highlights magnetic contacts on the flanks of the Turtle Dove Ridge. Whilst the tilt angle is also affected by noise (Figure 6.8e), prominent peaks are evident at several locations. These peaks theoretically correlate with magnetised source bodies (Section 6.3.2) and, therefore, suggest that a dual source contributes to the high associated with the Turtle Dove Ridge. Less significant sources are evident in and adjacent to the Zeewyck Sub-basin and a prominent source lies to the east of the Abrolhos Sub-basin. The source bodies that would be inferred on the basis of the tilt angle are consistent with those inferred from two-dimensional forward models along the same profile (cf. figure 4 in Johnston and Petkovic, 2012). The vertical derivatives (Figure 6.8f and g) suggest the existence of similar magnetic sources, though several are less obvious than in the tilt angle profile.

The free-air anomaly profile (Figure 6.9b) has a strong correlation with water depth and is most negative at the southwestern end of the profile where water depths reach almost 5 km. The Bouguer anomaly profile (Figure 6.9c) shows relative lows over the Zeewyck and Abrolhos sub-basins and suggests that the Turtle Dove Ridge might be a wider feature than interpreted from the seismic reflection data. The lows associated with the sub-basins are more prominent when a long-wavelength regional trend is removed either by subtracting the 25 km upward continuation (dashed line in Figure 6.9c) or band-pass filtering (Figure 6.9e). The first and half vertical derivatives (Figure 6.9f and g) show similar correlations with the interpreted geology, although the first vertical derivative is affected by noise.

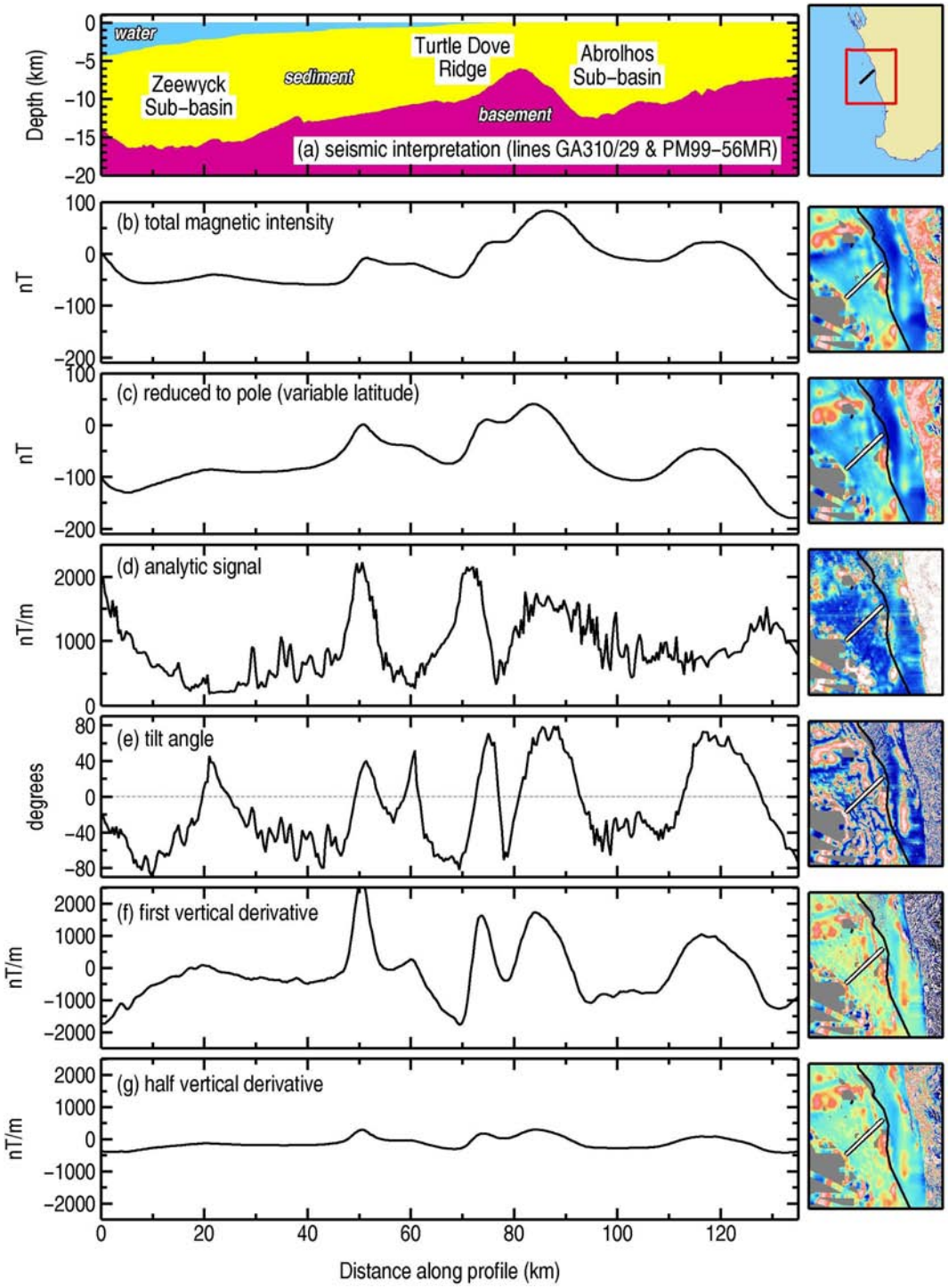

Figure 6.8: *Profiles along seismic reflection lines GA-310/29 and PM99-56MR showing raw and filtered magnetic data across the Zeewyck Sub-basin, Turtle Dove Ridge and Abrolhos Sub-basin.* ***(a)*** *Geological cross-section based on unpublished seismic interpretation of "base resolvable section";* ***(b)*** *total magnetic intensity;* ***(c)*** *variable-latitude pole reduced magnetic data;* ***(d)*** *analytic signal (note the enhancement of noise);* ***(e)*** *tilt angle, the positive parts of which represent the location of source bodies;* ***(f)*** *first vertical derivative; and* ***(g)*** *half vertical derivative. Note that all profiles are interpolated from gridded data with a cell-size of 0.005°.*

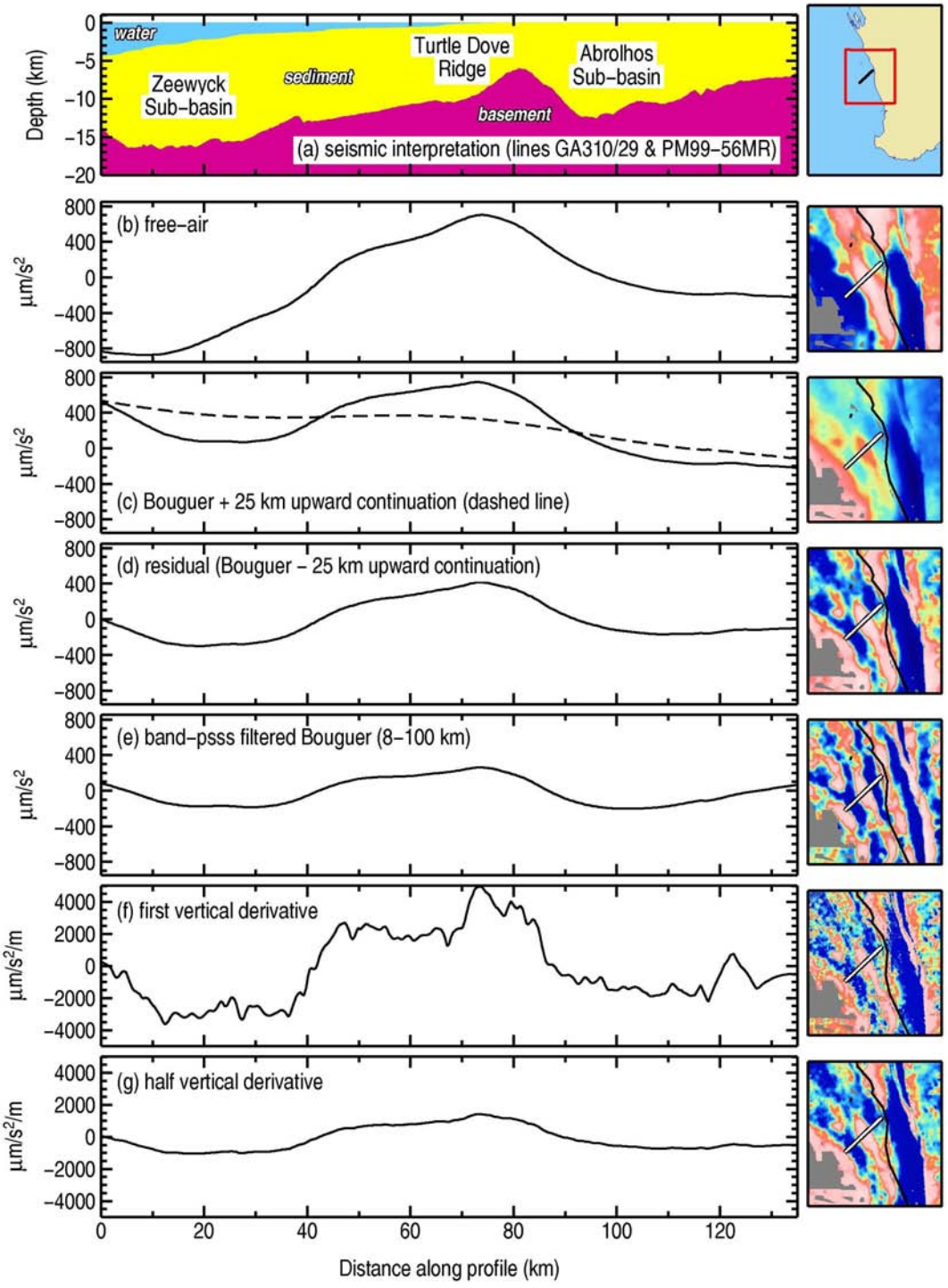

Figure 6.9: *Profiles along seismic reflection lines GA-310/29 and PM99-56MR showing raw and filtered gravity data across the Zeewyck Sub-basin, Turtle Dove Ridge and Abrolhos Sub-basin.* ***(a)*** *Geological cross-section based on unpublished seismic interpretation of "base resolvable section";* ***(b)*** *free-air anomaly;* ***(c)*** *Bouguer anomaly and its 25 km upward continuation (i.e. regional field);* ***(d)*** *residual Bouguer anomaly computed by subtracting its 25 km upward continuation;* ***(e)*** *band-pass filtered Bouguer gravity preserving wavelengths in the range 8–100 km;* ***(f)*** *first vertical derivative; and* ***(g)*** *half vertical derivative. Note that all profiles are interpolated from gridded data with a cell-size of 0.01°.*

6.5 MULTI-SCALE EDGE DETECTION

Multi-scale edge detection is a method used to automatically map maxima in the total horizontal derivative of gravity and magnetic anomalies at various levels of upward continuation (Archibald et al., 1999; Hornby et al., 1999). The horizontal gradient maxima are mapped as curvilinear features ("worms") that delineate the edges of source bodies (e.g. Blakely and Simpson, 1986). These features resemble the lines that a geoscientist would manually draw during interpretation of a gravity or magnetic image. By computing edges at various levels of upward continuation, both small-scale (high frequency, short wavelength) and large-scale (low frequency, long wavelength) edges can be inferred. Figure 6.10 and Figure 6.11 show edge features at various scales (i.e. levels of upward continuation) for the southwest margin gravity and magnetic datasets.

The mapped multi-scale edges can be used to facilitate the interpretation of key structural trends within any given region (Milligan et al., 2003). Straight lines can be fit to edge features that are close to linear and then the strike of these straight-line segments can be used to help quantify dominant geological trends within any particular area. The application of these edge lineaments to structural analysis of the southwest margin of Australia is discussed in Hall (in prep.). Multi-scale edge lineaments derived from the southwest margin gravity and magnetic datasets are shown in Figure 6.12 and Figure 6.13, respectively.

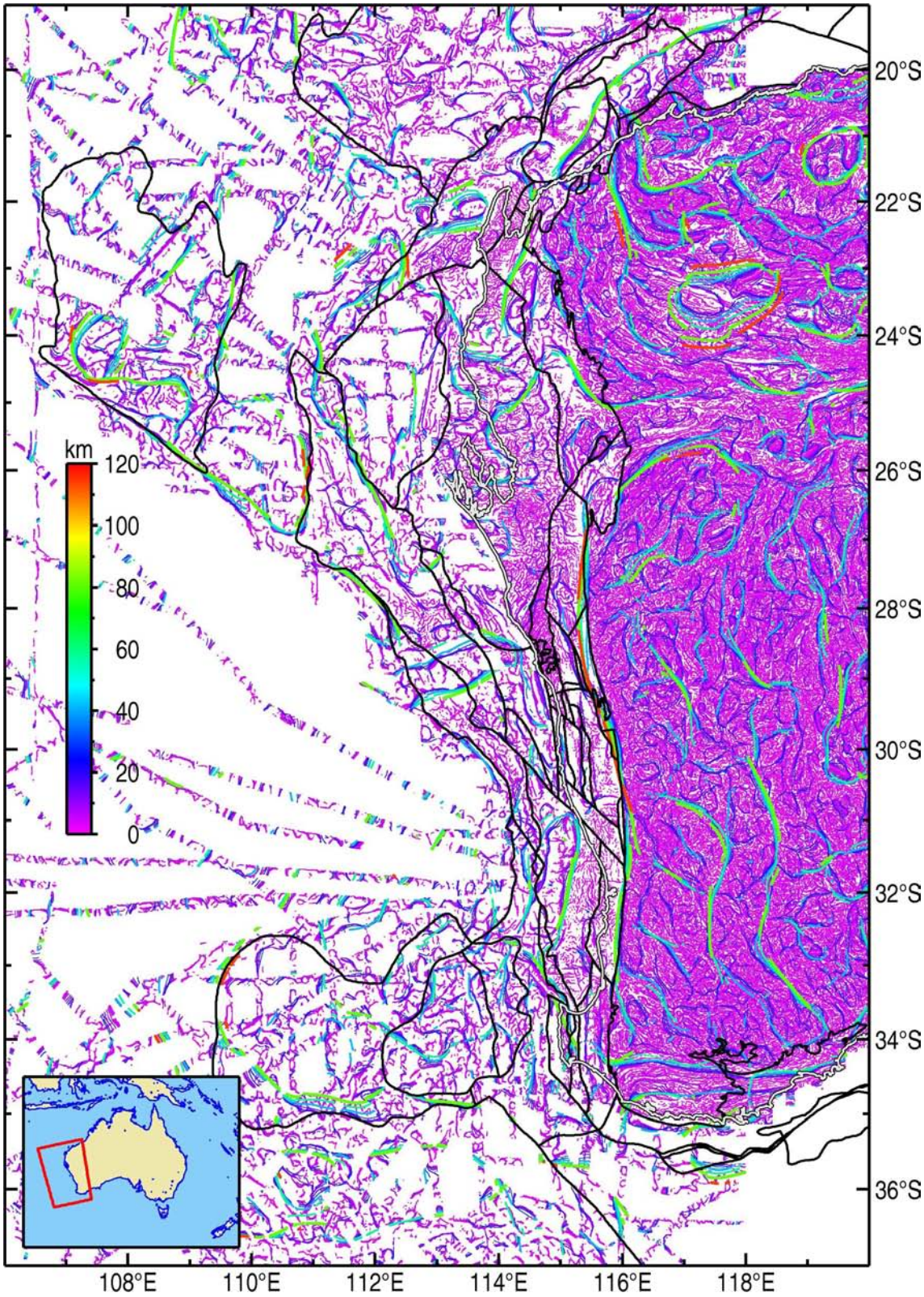

Figure 6.10: *Multi-scale edge features ("worms") in variable-latitude reduced-to-pole magnetic data coloured by upward continuation level (0.7, 1.0, 1.5, 2.0, 2.8, 4.0, 5.5, 7.7, 10.8, 15.1, 21.1, 29.7, 41.5, 58.1, 81.4, 114.0 and 159.5 km). Black lines show major geological elements of the southwest margin of Australia (cf. Figure 1.1).*

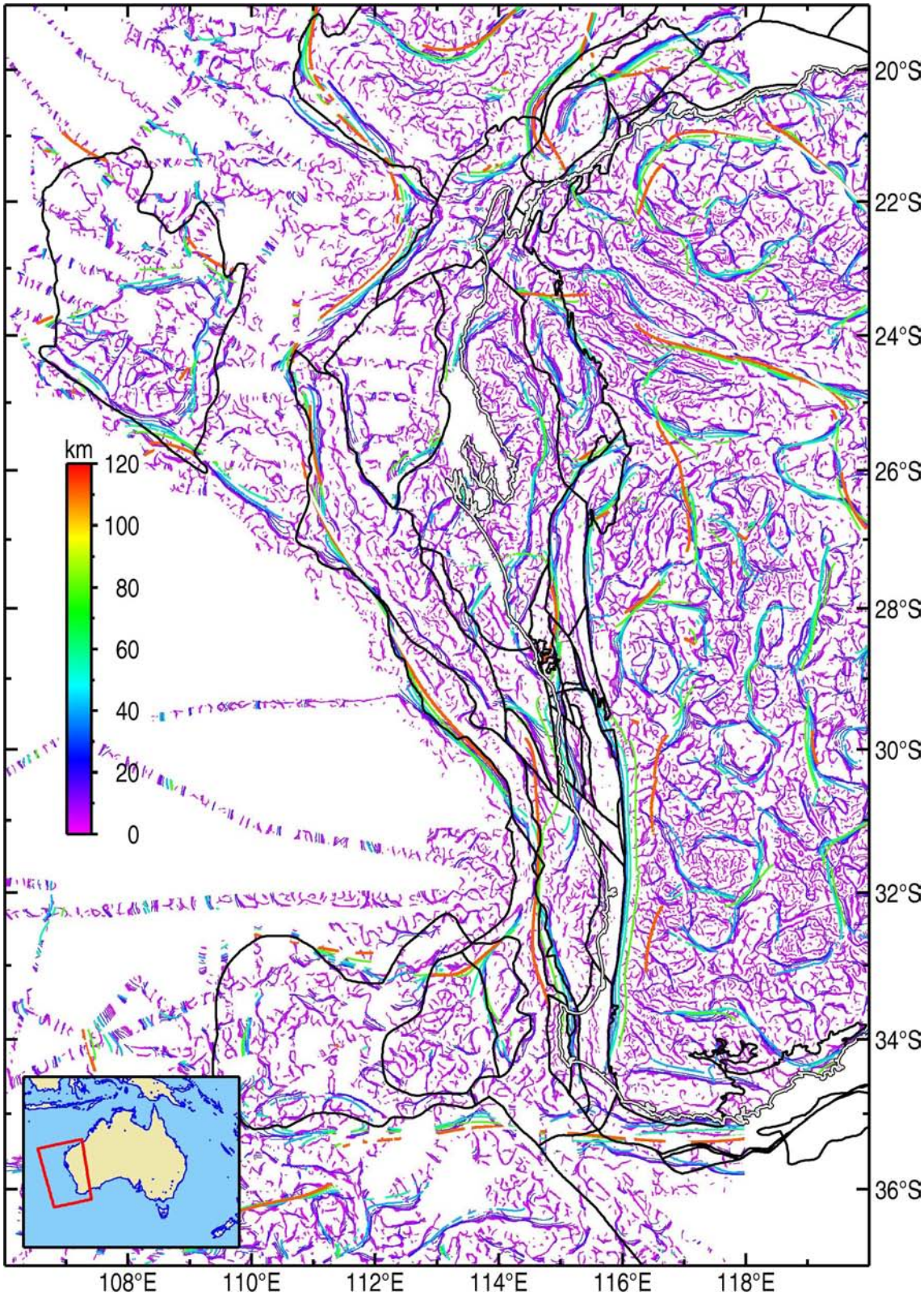

Figure 6.11: *Multi-scale edge features ("worms") in Bouguer gravity data coloured by upward continuation level (1.4, 2.0, 2.7, 3.8, 5.4, 7.5, 10.5, 14.8, 20.7, 29.0, 40.5, 56.7, 79.4, 111.2 and 155.6 km). Black lines show major geological elements of the southwest margin of Australia (cf. Figure 1.1).*

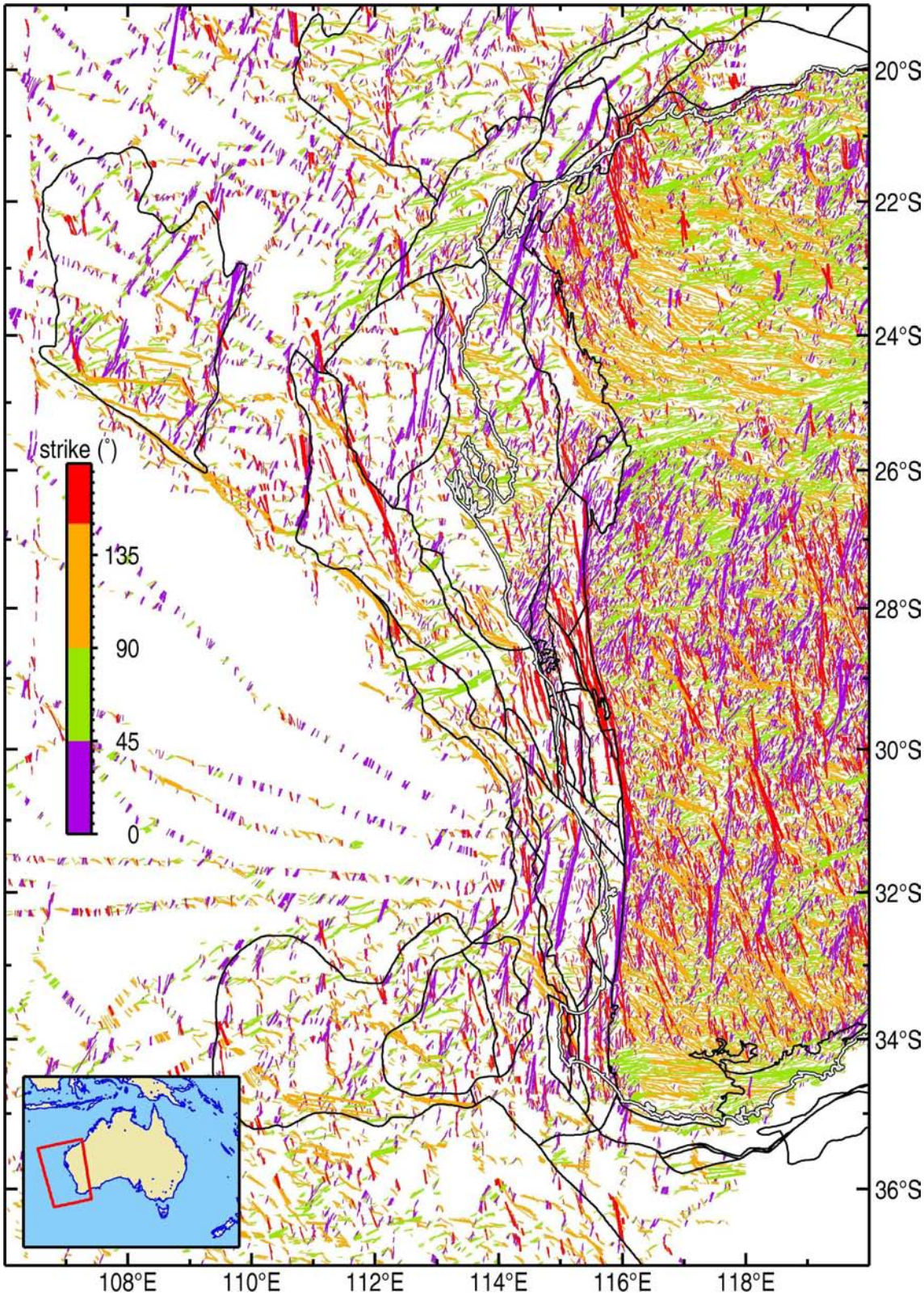

Figure 6.12: *Magnetic lineaments, coloured by strike direction, derived from multi-scale edges shown in Figure 6.10. Black lines show major geological elements of the southwest margin of Australia (cf. Figure 1.1).*

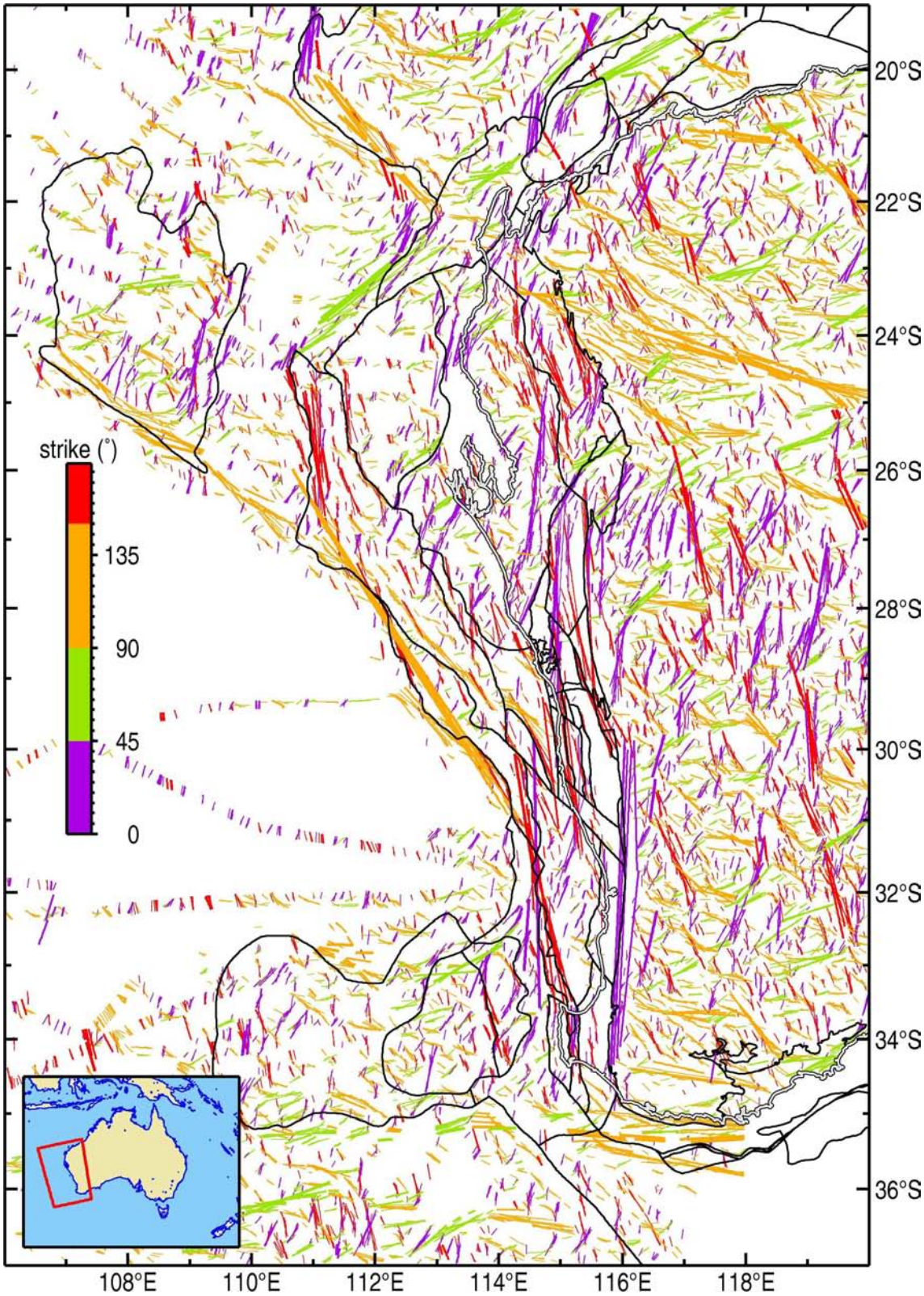

Figure 6.13: *Gravity lineaments, coloured by strike direction, derived from multi-scale edges shown in Figure 6.11. Black lines show major geological elements of the southwest margin of Australia (cf. Figure 1.1).*

7 Data availability

Several of the basic datasets described here (i.e. total magnetic intensity, reduced-to-pole magnetics, free-air, Bouguer and residual Bouguer gravity) are available for download from the Geophysical Archive Data Delivery Systems (GADDS; http://www.geoscience.gov.au/gadds/). Table 13 lists the files that can be downloaded. Additional derivative datasets can be computed from the downloadable data or requested from the author. A document summarising the processing steps detailed in this record is also provided with the downloaded data (see Appendix B).

Table 13: Southwest margin potential-field data available for direct download from the Geophysical Archive Data Delivery System (GADDS; http://www.geoscience.gov.au/gadds/). Data format codes are as follows: A, ascii columns; I, INTREPID database; E, ER MAPPER grid.

FILE	DESCRIPTION	FORMAT
mag_SWM_Lev_20101201.dat	Magnetic line data	A
mag_SWM_Lev_20101201..DIR	Magnetic line data	I
mag_SWM_Merge_20110610.ers	Gridded magnetic anomalies	E
mag_SWM_Merge_VRTP_20110610.ers	Gridded pole-reduced (variable latitude) magnetic anomalies	E
grv_SWM_Lev_20110217.dat	Gravity line data	A
grv_SWM_Lev_20110217..DIR	Gravity line data	I
grv_SWM_ShipLand_FA_20110419.ers	Gridded free-air anomalies	E
grv_SWM_BA_ShipLand_20110418.ers	Gridded complete Bouguer anomalies	E
grv_SWM_ShipLand_resBA-UC25_20110419.ers	Gridded residual Bouguer anomalies after subtracting 25 km upward continuation.	E

8 Summary

This record describes the compilation and levelling of ship-track gravity and magnetic data that cover the southwest margin of Australia. When combined with existing onshore data, the new datasets provide a useful aid to interpreting the geology of the southwest margin. The data can be used to quantify structural trends within and adjacent to these basins (Hackney et al., 2012), to estimate the depth-to-basement below the basins (Johnston and Petkovic, 2012; Johnston and Petkovic, in prep.; Petkovic, in prep.) and to help delineate distinct basement geological domains characterised by similar strength, structure and composition (Hall et al., 2012). When combined with seismic, well and geological data, the gravity and magnetic data contribute to assessments of the petroleum prospectivity of the frontier Mentelle, Perth and Southern Carnarvon basins. The data are also an integral part of predictive basin analysis that allows interpretation to be extended to areas where seismic, well and geological data are limited or absent (Hall et al., 2012; Hall, in prep.).

Acknowledgements

I thank Michael Morse for assistance with preparing and reformatting GA-310 and GA-2476 data, Stephen Johnston for help in locating older ship-track data, and Peter Milligan and Lisa Hall for review. This record is published with the permission of the Chief Executive Officer, Geoscience Australia.

References

Amante, C. and Eakins, B.W., 2009. ETOPO1 1 Arc-Minute Global Relief Model: Procedures, Data Sources and Analysis. NOAA Technical Memorandum NESDIS NGDC-24, 19pp.

Andersen, O.B. and Knudsen, P., 2000. The role of satellite altimetry in gravity field modelling in coastal areas. *Physics and Chemistry of the Earth*, **25**(1), 17–24

Andersen, O.B., Knudsen, P. and Berry, P., 2010a. The DNSC08GRA global marine gravity field from double retracked satellite altimetry. *Journal of Geodesy*, **84**(3), 191–199, doi:10.1007/s00190-009-0355-9.

Andersen, O.B., Knudsen, P., Berry, P.A.M., Kenyon, S. and Trimmer, R., 2010b. Recent developments in high-resolution global altimetric gravity field modeling. *The Leading Edge*, **29**, 540–545, doi:10.1190/1.3422451.

Anderson, H., Jones, N. and Ameglio, L., 2006. Reducing Seismic Risk From The Air: Utilising airborne geophysics to assist petroleum exploration. In: C.H. Mehta (Editor), Proceedings of the 6th Conference & Exposition on Petroleum Geophysics, January 9–11, Kolkata, India. Society of Petroleum Geophysicists, India.

Archibald, N., Gow, P. and Boschetti, F., 1999. Multiscale edge analysis of potential field data. *Exploration Geophysics*, **30**(2), 38–44, doi:10.1071/EG999038.

Argast, D., Bacchin, M. and Tracey, R., 2009. An extension of the closed-form solution for the gravity curvature (Bullard B) correction in the marine and airborne cases. *ASEG Extended Abstracts*, **2009**(1), 6pp, doi:10.1071/ASEG2009ab129.

ARK, 2009. Report on the processing of marine gravity and magnetic data acquired offshore southwest Western Australia. ARK Geophysics Ltd. Project No. AUS08029E, 35pp.

Austin Exploration, 2003. Final Marine Gravity and Magnetic Data Processing Report, Offshore Western Australia, North Perth Basin (WA-326-P / WA-328-P). Austin Exploration Inc. Job Number: AEX #400, 25pp.

Austin Exploration, 2009. Final acquisition report: Marine gravity and magnetic data acquisition, Southwest Margin seismic survey 2008/2009. Austin Exploration Inc. Job Number: AEX #530, 16pp.

Blakely, R.J. and Simpson, R.W., 1986. Approximating edges of source bodies from magnetic or gravity anomalies. *Geophysics*, **51**(7), 1494–1498, doi:10.1190/1.1442197.

Blakely, R.J., 1996. Potential theory in gravity and magnetic applications. Cambridge University Press, 441 pp.

Borissova, I., Bradshaw, B.E., Nicholson, C., Struckmeyer, H.I.M. and Payne, D., 2010. New exploration opportunities on the southwest Australian margin: deepwater frontier Mentelle Basin. *APPEA Journal*, **50**, 1–13

Borissova, I. and Nelson, G., 2011. Petroleum potential of offshore southern Carnarvon Basin—insights from the new Geoscience Australia data. *APPEA Journal and Conference Proceedings, Extended Abstracts*, **51**, 4pp.

Buswell, A.J., Powell, W.D. and Scholefield, T., 2004. The northern Perth Basin - from marginally prospective for gas to highly prospective for both oil and gas. *APPEA Journal*, **44**(1), 181–199

Cooper, G. and Cowan, G., 2003. The application of fractional calculus to potential field data. *Exploration Geophysics*, **34**, 51–56, doi:10.1071/EG03051.

Daniell, J., Jorgensen, D.C., Anderson, T., Borissova, I., Burq, S., Heap, A.D., Hughes, M., Mantle, D., Nelson, G., Nichol, S., Nicholson, C., Payne, D., Przeslawski, R., Radke, L., Siwabessy, J., Smith, C. and Shipboard Party, 2009. Frontier Basins of the West Australian Continental Margin: Post-survey Report of Marine Reconnaissance and Geological Sampling Survey GA2476. Geoscience Australia Record 2009/38, 229pp.

Deng, X. and Featherstone, W.E., 2006. A coastal retracking system for satellite radar altimeter waveforms: Application to ERS-2 around Australia. *Journal of Geophysical Research*, **111**, C06012, doi:10.1029/2005JC003039.

DFA, 1999. Reprocessing of southern margins marine gravity, magnetic and bathymetry data. Desmond Fitzgerald and Associates, Pty. Ltd. Unpublished Report, 16pp.

DFA, 2001. Reprocessing of south and southeast Australia marine gravity and magnetic data. Desmond Fitzgerald and Associates, Pty. Ltd. Unpublished Report, 32pp.

Foster, C., Goleby, B., Borissova, I. and Heap, A., 2009. Southwest margin surveys completed: Surveys investigate basin structure, hydrocarbon potential and marine habitat. *AusGeo News*, **94**, http://www.ga.gov.au/ausgeonews/ausgeonews200906/.

Geoscience Australia, 2011. Energy Security Program Achievements—Towards Future Energy Discovery. https://www.ga.gov.au/products/servlet/controller?event=GEOCAT_DETAILS&catno=71823.

Götze, H.-J., 2011. International Gravity Formula. *In*: H.K. Gupta (Editor), *Encyclopedia of Solid Earth Geophysics*. Encyclopedia of Earth Science Series, Springer, Dordrecht, pp. 511–512.

Hackney, R., 2011. Gravity, Data to Anomalies. *In*: H.K. Gupta (Editor), *Encyclopedia of Solid Earth Geophysics*. Encyclopedia of Earth Science Series, Springer, Dordrecht, pp. 524–533.

Hackney, R.I., 2010. Potential-field Data Covering the Capel and Faust Basins, Australia's Remote Offshore Eastern Frontier. Geoscience Australia Record 2010/34, 40pp.

Hackney, R.I., Hall, L. and Köther, N., 2012. Potential-field data for structural interpretation in the northern Perth Basin, Australia. *ASEG Extended Abstracts*, **2012**(1), 4pp, doi:10.1071/ASEG2012ab167.

Hall, L., Hackney, R. and Johnston, S., 2012. Understanding Australia's Southwest Margin: Basement Architecture as a Framework for Predictive Basin Analysis. *AusGeo News*, **105**, http://www.ga.gov.au/ausgeonews/ausgeonews201203/southwest.jsp.

Hall, L., in prep. Basement Terranes, Structure and Composition of Australia's Southwest Margin. Geoscience Australia Record.

Hinze, W.J., 2003. Bouguer reduction density, why 2.67? *Geophysics*, **68**(5), 1559–1560, doi: 10.1190/1.1620629.

Hornby, P., Boschetti, F. and Horowitz, F.G., 1999. Analysis of potential field data in the wavelet domain. *Geophysical Journal International*, **137**(1), 175–196

Hwang, C., Guo, J., Deng, X., Hsu, H.Y. and Liu, Y., 2006. Coastal gravity anomalies from retracked Geosat/GM altimetry: improvement, limitation and the role of airborne gravity data. *Journal of Geodesy*, **80**(4), 204–216, doi:10.1007/s00190-006-0052-x.

Intrepid Geophysics, 2004. Processing of Moon 2D Gravity and Magnetic Data. Intrepid Geophsyics unpublished report, 23pp.

Intrepid Geophysics, 2009a. GridMerge—merging multiple grids (T24). Intrepid Geophysics User Manual, 42pp.

Intrepid Geophysics, 2009b. Gravity corrections (T54). Intrepid Geophysics User Manual, 46pp.

Jacobsen, B.H., 1987. A case for upward continuation as a standard separation filter for potential-field maps. *Geophysics*, **52**(8), 1138–1148, doi:10.1190/1.1442378.

Johnston, S. and Petkovic, P., 2012. Depth to magnetic sources in the offshore northern Perth Basin. *ASEG Extended Abstracts*, **2012**(1), 4pp, doi:10.1071/ASEG2012ab274.

Johnston, S.W. and Petkovic, P., in prep. Northern Perth Basin 2D and 3D models of depth to magnetic basement. Geoscience Australia Record.

Jones, A., Jorgensen, D.C., Hackney, R.I. and Nicholson, C., 2011a. Hydrocarbon potential of the offshore northern Perth Basin: new data and knowledge deliver opportunities for petroleum explorers. *AusGeo News*, **103**, http://www.ga.gov.au/ausgeonews/ausgeonews201109/.

Jones, A.T., Kennard, J.M., Nicholson, C.J., Bernardel, G., Mantle, D., Grosjean, E., Boreham, C.J., Jorgensen, D.C. and Robertson, D., 2011b. New exploration opportunities in the offshore northern Perth Basin. *APPEA Journal*, **51**, 45–78.

Kuhn, M., Featherstone, W.E. and Kirby, J.F., 2009. Complete spherical Bouguer gravity anomalies over Australia. *Australian Journal of Earth Sciences*, **56**(2), 213–223, doi:10.1080/08120090802547041.

Louis, G., Lequentrec-Lalancette, M.F., Royer, J.Y., Rouxel, D., Géli, L., Maïa, M. and Faillot, M., 2010. Ocean Gravity Models From Future Satellite Missions. *EOS, Transactions, American Geophysical Union*, **91**(3), 21–22, doi:10.1029/2010EO030001.

Macmillan, S. and Maus, S., 2005. International Geomagnetic Reference Field—the tenth generation. *Earth Planets Space*, **57**, 1135–1140.

Mallick, K., Vasanthi, A. and Sharma, K.K., 2011. Gravity Data, Regional - Residual Separation. *In*: H.K. Gupta (Editor), *Encyclopedia of Solid Earth Geophysics*. Encyclopedia of Earth Sciences Series, Springer Netherlands, pp. 466–471.

Maus, S., Yin, F., Lühr, H., Manoj, C., Rother, M., Rauberg, J., Michaelis, I., Stolle, C. and Müller, R.D., 2008. Resolution of direction of oceanic magnetic lineations by the sixth-generation lithospheric magnetic field model from CHAMP satellite magnetic measurements. *Geochem. Geophys. Geosyst*, **9**, Q07021, doi:10.1029/2008GC001949.

Maus, S., Barckhausen, U., Berkenbosch, H., Bournas, N., Brozena, J., Childers, V., Dostaler, F., Fairhead, J.D., Finn, C. and von Frese, R.R.B., 2009. EMAG2: A 2–arc min resolution Earth Magnetic Anomaly Grid compiled from satellite, airborne, and marine magnetic measurements. *Geochemistry Geophysics Geosystems*, **10**(8), Q08005, doi:10.1029/2009GC002471.

Miller, H.G. and Singh, V., 1994. Potential field tilt—a new concept for location of potential field sources. *Journal of Applied Geophysics*, **32**(2–3), 213–217, doi:10.1016/0926-9851(94)90022-1.

Milligan, P., Lyons, P. and Direen, N.G., 2003. Spatial and directional analysis of potential field gradients: new methods to help solve and display three-dimensional crustal architecture. *ASEG Extended Abstracts*, **2003**(2), 4pp, doi:10.1071/ASEG2003ab108.

Milligan, P.R., Franklin, R., Minty, B.R.S., Richardson, L.M. and Percival, P.J., 2010. Magnetic Anomaly Map of Australia (Fifth Edition), 1:15 000 000 scale. Geoscience Australia, Canberra, https://www.ga.gov.au/products/servlet/controller?event=GEOCAT_DETAILS&catno=70282.

Mishra, D.C. and Tiwari, V.M., 2011. Gravity Method, Surface. *In*: H.K. Gupta (Editor), *Encyclopedia of Solid Earth Geophysics*. Encyclopedia of Earth Science Series, Springer, Dordrecht, pp. 513–518.

Morse, M., 2010. Potential field methods prove effective for continental margin studies. *AusGeo News*, **98**

Mory, A.J. and Iasky, R.P., 1996. Stratigraphy and structure of the onshore northern Perth Basin. Geological Survey of Western Australia Report 46, 781–789pp.

Nelson, G., Hughes, M., Przeslawski, R., Nichol, S., Lewis, B. and Rawsthorn, K., 2009. Revealing the Wallaby Plateau: Recent survey delivers geophysical, geological and biophysical data. *AusGeo News*, **94**, http://www.ga.gov.au/ausgeonews/ausgeonews200906/wallaby.jsp.

Nicholson, C.J., Borissova, I., Krassay, A.A., Boreham, C.J., Monteil, E., Neumann, V., di Primio, R. and Bradshaw, B.E., 2008. New exploration opportunities in the southern Vlaming Sub-basin. *APPEA Journal*, **48**, 371–379

Norvick, M.S., 2004. Tectonic and stratigraphic history of the Perth Basin. Geoscience Australia Record 2004/16, 30pp.

Payne, D., Mantle, D., Borissova, I., Nicholson, C. and Jorgensen, D.C., 2009. The geology and deep marine terrains of Australia's western margin: Preliminary results from major marine reconnaissance survey. *AusGeo News*, **94**, http://www.ga.gov.au/ausgeonews/ausgeonews200906/marine.jsp.

Percival, P.J., 2010. Index of airborne geophysical surveys: 11th edition. Geoscience Australia Record 2010/13, 308pp.

Petkovic, P., Fitzgerald, D., Brett, J., Morse, M. and Buchanan, C., 2001. Potential Field and Bathymetry Grids of Australia's Margins. *ASEG Extended Abstracts*, **2001**(1), 4pp, doi:10.1071/ASEG2001ab109.

Petkovic, P., in prep. Northern Perth Basin 2D gravity models. Geoscience Australia Record

Preview, 2011. Geophysics in the Surveys: News. *Preview*, **150**(February), 20–22

Prince, R.A. and Forsyth, D.W., 1984. A simple objective method for minimizing crossover errors in marine gravity data. *Geophysics*, **49**(7), 1070–1083, doi: 10.1190/1.1441722.

Quaife, R., Rosser, J. and Pagnozzi, S., 1994. The structural architecture and stratigraphy of the offshore northern Perth Basin. In: P.G. Purcell and R.R. Purcell (Editors), The Sedimentary Basins of Western Australia, Proceedings of the Petroleum Exploration Society of Australia Symposium, Perth, pp. 811–822.

Roest, W.R., Verhoef, J. and Pilkington, M., 1992. Magnetic interpretation using the 3-D analytic signal. *Geophysics*, **57**(1), 116–125, doi:10.1190/1.1443174.

Roest, W.R. and Pilkington, M., 1993. Identifying remanent magnetization effects in magnetic data. *Geophysics*, **58**(5), 653–659, doi:10.1190/1.1443449.

Sandwell, D.T. and Smith, W.H.F., 1997. Marine gravity anomaly from Geosat and ERS 1 satellite altimetry. *Journal of Geophysical Research*, **102**(B5), 10039–10054, doi:10.1029/96JB03223.

Sandwell, D.T. and Smith, W.H.F., 2009. Global marine gravity from retracked Geosat and ERS-1 altimetry: Ridge segmentation versus spreading rate. *Journal of Geophysical Research*, **114**, B01411, doi:10.1029/2008JB006008.

Swain, C.J. and Kirby, J.F., 2011. Gravity Data, Advanced Processing. *In*: H.K. Gupta (Editor), *Encyclopedia of Solid Earth Geophysics*. Encyclopedia of Earth Sciences Series, Springer Netherlands, pp. 461–466.

Tracey, R. and Nakamura, A., 2010. Complete Bouguer anomalies for the Australian National Gravity Database. *ASEG Extended Abstracts*, **2010**(1), 3pp, doi:10.1071/ASEG2010ab016.

Wessel, P. and Watts, A.B., 1988. On the Accuracy of Marine Gravity Measurements. *J. Geophys. Res.*, **93**(B1), 393–413, doi:10.1029/JB093iB01p00393.

Whiteway, T.G., 2009. Australian Bathymetry and Topography Grid, June 2009. Geoscience Australia Record 2009/21, 46pp.

Wynne, P. and Bacchin, M., 2009. Index of gravity surveys (Second Edition). Geoscience Australia Record 2009/07, 1849pp.

Appendix A: Illustration of geological contributions to different gravity anomalies

Figure A1 illustrates observed (absolute) gravity and different types of gravity anomalies in a marine area. A similar illustration for land areas can be found in Blakely (1996, p138–141). The schematic crustal model shown in Figure A1a represents submerged, extended continental crust (maroon) in local (Airy) isostatic equilibrium in which an underwater sedimentary basin (yellow) is compensated for by shallow mantle (pink). There is an arbitrary bathymetric high at the centre of the basin.

The observed gravity associated with this crustal model is large and positive because it reflects the mass of the entire Earth. In detail, there are "edge-effects" at the margins of the basin (negative on the basin side, positive on the basement side) and a prominent axial high associated with the bathymetric high. Though not represented in this example, observed gravity would also have a strong latitude-dependant gradient (increasing with increasing latitude).

In ocean areas, the free-air anomaly (Figure A1b) is computed by subtracting from the observed gravity a predicted value of gravity for each measurement point (Equation (1)). The predicted gravity value represents the Earth's "normal gravity" (i.e. the gravity effect of the GRS80 reference ellipsoid, computed using Equation (2)). The free-air anomaly therefore accounts for the gravity effect of "normal" crust and mantle; in Figure A1b colouring is removed for the parts of the model that are accounted for by subtracting normal gravity. The free-air anomaly associated with the schematic crustal model varies around zero. It is characterised by edge effects near the margins of the basin and an axial high related to the bathymetric high in the centre of the basin.

The axial gravity high in the centre of the basin results from the large density contrast between water (blue) and the basin sediments (or basement in areas adjacent to the basin). The Bouguer correction adjusts for this large density contrast by replacing the water layer with a layer of rock whose density is equivalent to the near-surface sediments. After application of the Bouguer correction, the gravity high associated with the bathymetric high is removed, but the edge effect anomalies at the margin of the basin remain.

The edge-effect anomaly is a combination of the gravity effect arising from: (1) the near-surface lateral density contrast between sediment and basement; and (2) the deeper density contrast between mantle and crust. The gravity effect of the shallower mantle under the basin, the "regional" field, is shown by the pink dashed line in Figure A1c. If this regional field is subtracted from the Bouguer gravity anomaly, the resulting residual anomaly reflects the mass deficit of the sedimentary basin (Figure A1d).

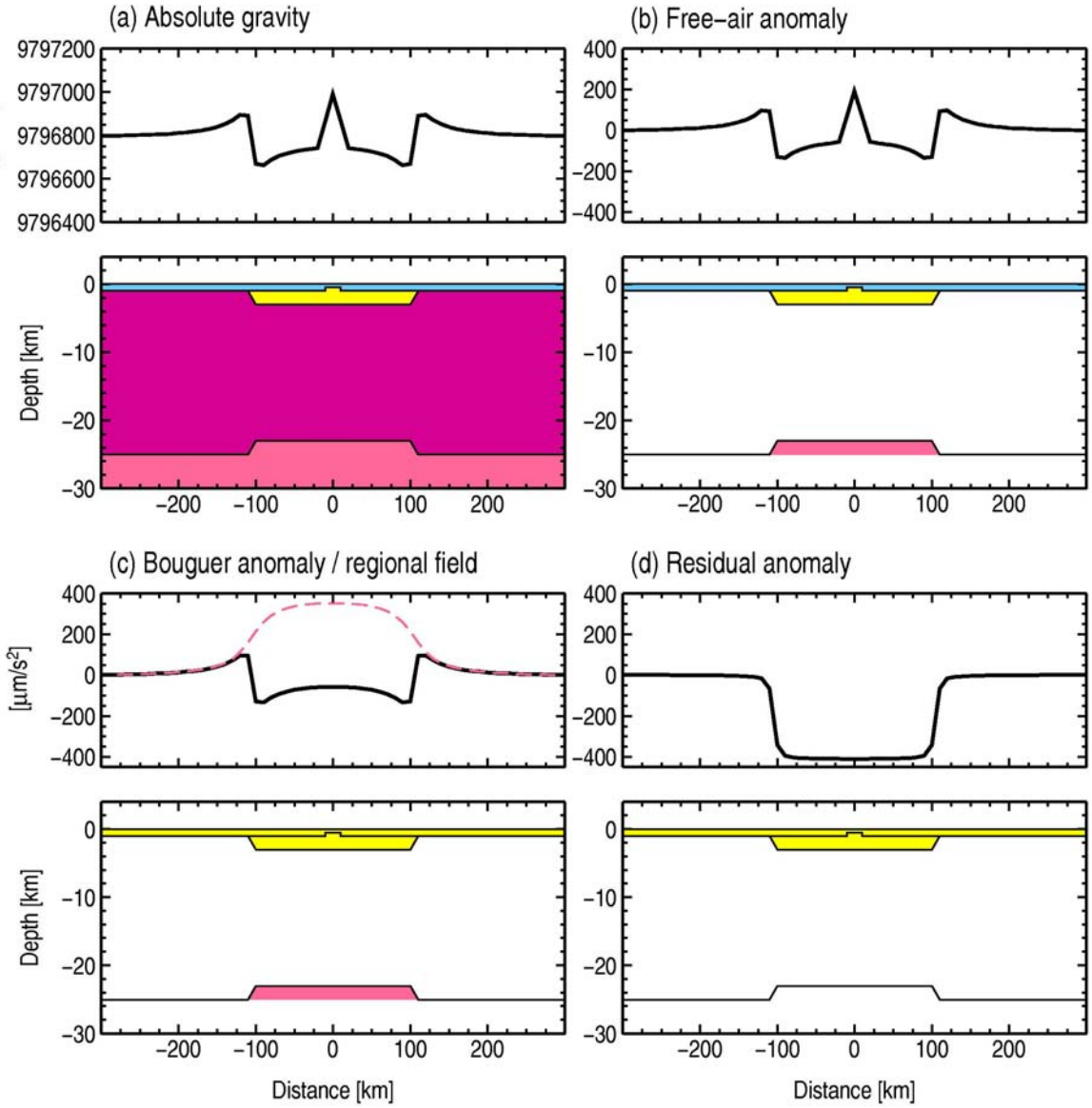

Figure A1: *Schematic crustal model and associated gravity effects illustrating the various types of gravity anomaly and the contributions of different parts of the crust and mantle to each anomaly. In all sections, the coloured parts of the model contribute to the associated gravity effect. (a) Observed (absolute) gravity for an isostatically-balanced model of submerged, extended continental crust comprising water layer (blue), basin sediments (yellow), crust (maroon) and mantle (pink). (b) Free-air anomaly profile for which the gravity effect of the bulk of the crust and mantle has been accounted for by subtracting normal gravity. (c) Bouguer anomaly profile in which the gravity effect of the density contrast between water and crust has been corrected for. The gravity effect of the shallower mantle (pink), shown by the dashed pink line, defines the "regional" field. (d) Residual anomaly computed by subtracting the regional field from the Bouguer anomaly. The only remaining contribution to the gravity profile is the low-density basin-fill sediment (yellow).*

Appendix B: GADDS Data Description

This Appendix provides a direct copy of the data description file that is provided when data are downloaded from the Geophysical Archive Data Delivery System. Only the table and figure numbers have been changed to maintain consistency within this record.

Levelled Gravity and Magnetic Data Covering the Southwest Margin of Australia

Metadata AnzlicID: ANZCW0703014975

This document describes levelled ship-track gravity and magnetic data, as downloaded from the Geophysical Archive Data Delivery System (GADDS). These data cover the southwest margin of Australia in the region enclosing 106–120°E and 19–37°S. Information is also included in `.txt` files that are downloaded with the data.

BACKGROUND

As part of the Australian Government's Offshore Energy Security Program (2006–2011), Geoscience Australia obtained pre-competitive geoscience data to aid assessments of the petroleum prospectivity and seabed environments off southwestern Australia. In late 2008 and early 2009, two marine surveys (GA-310 and GA-2476) acquired new seismic reflection, swath bathymetry and potential-field (gravity and magnetic) data over the Mentelle, Perth and Southern Carnarvon basins, as well as the Wallaby Plateau (Foster et al., 2009). These new data add to pre-existing data and enhance opportunities for improving the understanding of basin provinces off the southwest margin of Australia (e.g. Jones et al., 2011a).

DATA SOURCES

The data used in the combined gravity and magnetic datasets are listed in Table B1.

Table B1: List of the various datasets used to produce the combined gravity and magnetic datasets covering the southwest margin of Australia. The table indicates the dataset format: L, line data; P, point data; G, grid data.

DATASET/GA SURVEY (LEASE AREA)	YEAR	GRAVITY	MAGNETIC
Petkovic et al. (2001)	1960 – 2001	L	L
Mag. Map Australia	5th Ed. 2010	--	G
Onshore gravity	2010 release	P	--
GA-310	2008/09	L	L
GA-2476	2008/09	L	L
"Moon AM02" (WA-326-P/328-P)	2002/03	L	L
"East Abrolhos" (WA-325-P)	2003	--	G
"Beagle B92" (WA-228-P)	1992	--	G

LEVELLED MARINE DATA

The ship-track data (Table B1) were levelled using tools within the INTREPID software package (`splitline` and `marinelevel`) and a workflow previously used by Geoscience Australia (Petkovic et al., 2001; Hackney, 2010).

The marine free-air gravity data were prepared and levelled as follows:

- Where necessary, re-computation of free-air anomalies from observed gravity to ensure consistent use of normal gravity formula (i.e. using INTREPID WGS84 gravity "datum")
- Split tracks into relatively straight-line segments (to facilitate the computation of a single cross-over value for each line pair). Parameters were varied depending on sample interval (10–60 seconds, ~25–150 m)
- Line filtering for some surveys to smooth noisy data
- Editing to remove lines with bad data or lines that lay close to other lines
- Loop levelling using a reference surface based on regional gravity data derived from satellite radar altimeter measurements (DNSC08GRA dataset, Andersen et al., 2010a)
- Computation of complete Bouguer anomalies using a spherical-cap correction and a correction density of 770 kg/m^3 (i.e. assuming density just below the seafloor to be 1800 kg/m^3). Terrain corrections were computed using INTREPID tools and AUSBATH09 bathymetry (Whiteway, 2009).

The marine magnetic data were prepared and levelled as follows:

- Split tracks into relatively straight-line segments (to facilitate the computation of a single cross-over value for each line pair). Parameters were varied depending on sample interval (10–60 seconds, ~25–150 m)
- Line filtering of noisy data
- Editing to remove lines with bad data or lines that lay close to other lines
- Loop levelling

Tables B2 and B3 describe the data fields included in the gravity and magnetic files downloaded from GADDS.

GRIDDED ONSHORE/OFFSHORE DATA

The levelled marine gravity data were combined with onshore data as follows:

- Onshore point data were extracted from GADDS for the region 112–120°E and 19–37°S (downloaded 18 April 2011);
- The INTREPID gravity "datum" for onshore data was set to WGS84 (for consistency with offshore data). Note that the actual INTREPID gravity "datum" for the onshore data should be "GA07", which is tied to GDA94 (GRS80). However, for the purposes of this work, differences between WGS84 and GDA94 coordinates are insignificant;
- A spherical Bouguer cap correction was computed for the onshore data using a correction density of 2670 kg/m^3 and heights relative to the geoid. The onshore data were not terrain corrected;
- Onshore and offshore point data were combined in an INTREPID database and gridded using minimum curvature at 0.01° cell size (~1 km).

The combined Bouguer gravity grid available from GADDS is shown in Figure B1. This grid is suitable for further filtering and computation of residual fields. A free-air grid and a residual Bouguer anomaly grid are also available from GADDS.

The levelled marine magnetic data were combined with onshore data as follows:

- Magnetic data from the 5th Edition of the Magnetic Anomaly Map of Australia (Milligan et al., 2010) were downloaded from GADDS for the region 112–120°E and 19–37°S and downsampled to a cell size of 0.005°;
- Levelled ship-track magnetic data were gridded at 0.01° cell size and, using the INTREPID `gridmerge` tool, merged with: a) the downsampled grid of airborne data from the 5th Edition of the Magnetic Anomaly Map of Australia; and b) two airborne surveys not included in the 5th Edition Magnetic Anomaly Map of Australia – the "East Abrolhos" (Anderson et al., 2006) and "Beagle B92" surveys (see Table B1).

The merged magnetic anomaly grid available from GADDS is shown in Figure B2. A variable latitude reduced-to-pole grid is also available.

FURTHER INFORMATION

Contact Ron Hackney at Geoscience Australia
Email: ron.hackney@ga.gov.au
Tel: +61 2 6249 5861

Table B2: Description of data fields contained in line-levelled gravity data files downloaded from the Geophysical Archive Data Delivery System. Longitude and latitude fields are tied to the WGS84 ellipsoid and gravity quantities are in $\mu m/s^2$. Note that the INTREPID X and Y aliases can be assigned to the different coordinate sets depending on whether levelled and edited gravity data are to be dealt with. Null fields are assigned a value of 9999.

FIELD NAME	INTREPID ALIAS	DESCRIPTION
SURVEY	FlightNumber	Geoscience Australia survey identifier
SPLITLINE	LineNumber	Line number resulting from the INTREPID `splitline` process (10 000 x SURVEY + sequential number). Note that these line numbers do not coincide with line numbers associated with Geoscience Australia seismic line names
LONGITUDE	X	WGS84 geodetic longitude
LATITUDE	Y	WGS84 geodetic latitude
LongGrav	X	Coordinates tied to WGS84 for lines or portions of lines retained for line levelling (i.e. lines or portions of lines with bad data are excluded by nulling the coordinates)
LatGrav	Y	
AUSBATH09		Water depth interpolated from the Australian Bathymetry and Topography Grid (Whiteway, 2009)
ObsGravRev		Observed gravity reverse-computed from FreeAir4Lev
FreeAir4Lev		Free-air gravity prior to levelling
FreeAirLevLoopR		Loop levelled free-air gravity data with reference to DNSC08GRA satellite altimeter derived gravity data (Andersen et al., 2010a)
SBA1800		Simple Bouguer gravity anomaly computed using a spherical cap correction and a correction density of 770 kg/m^3 (i.e. difference between sediment and water density = 1800-1030 kg/m^3)
TC1800		Terrain corrections computed from an AUSBATH09 1 arc minute grid to a distance of 64 km (in three concentric rings) using a density of 1800 kg/m^3
CBA1800		Complete Bouguer gravity anomalies (i.e. terrain corrected) computed using TC1800 WARNING: Grids/images derived from the CBA1800 data field will contain artefacts related to the inability to completely correct the terrain effects associated with deep canyons on the shelf edge - e.g. in the Perth Basin, these artefacts generally trend WSW-ENE and should not be interpreted geologically!

Table B3: Description of data fields contained in line-levelled magnetic data files downloaded from the Geophysical Archive Data Delivery System. Longitude and latitude fields are tied to the WGS84 ellipsoid and magnetic quantities are in nT. Note that the INTREPID X and Y aliases can be assigned to the different coordinate sets depending on whether levelled and edited magnetic data are to be dealt with. Null fields are assigned a value of 9999.

FIELD NAME	INTREPID ALIAS	DESCRIPTION
SURVEY	FlightNumber	Geoscience Australia survey number
SPLITLINE	LineNumber	Line number resulting from the INTREPID `splitline` process (10 000 x SURVEY + sequential number). Note that these line numbers do not coincide with line numbers associated with Geoscience Australia seismic lines
LONGITUDE	X	WGS84 geodetic longitude/latitude for ALL lines (i.e. with and without magnetic data and before data editing)
LATITUDE	Y	
LongMag	X	Coordinates tied to WGS84 for lines or portions of lines retained for line levelling (i.e. lines or portions of lines with bad data are excluded by nulling the coordinates)
LatMag	Y	
EASTING	X	UTM Zone 49S projected coordinates tied to WGS84 (derived from LongMag/LatMag)
NORTHING	Y	
MagAnom4Lev		Unlevelled magnetic data after editing to remove bad data and after low-pass line filtering to smooth out noise
MagAnomLevLoop		Loop levelled magnetic data

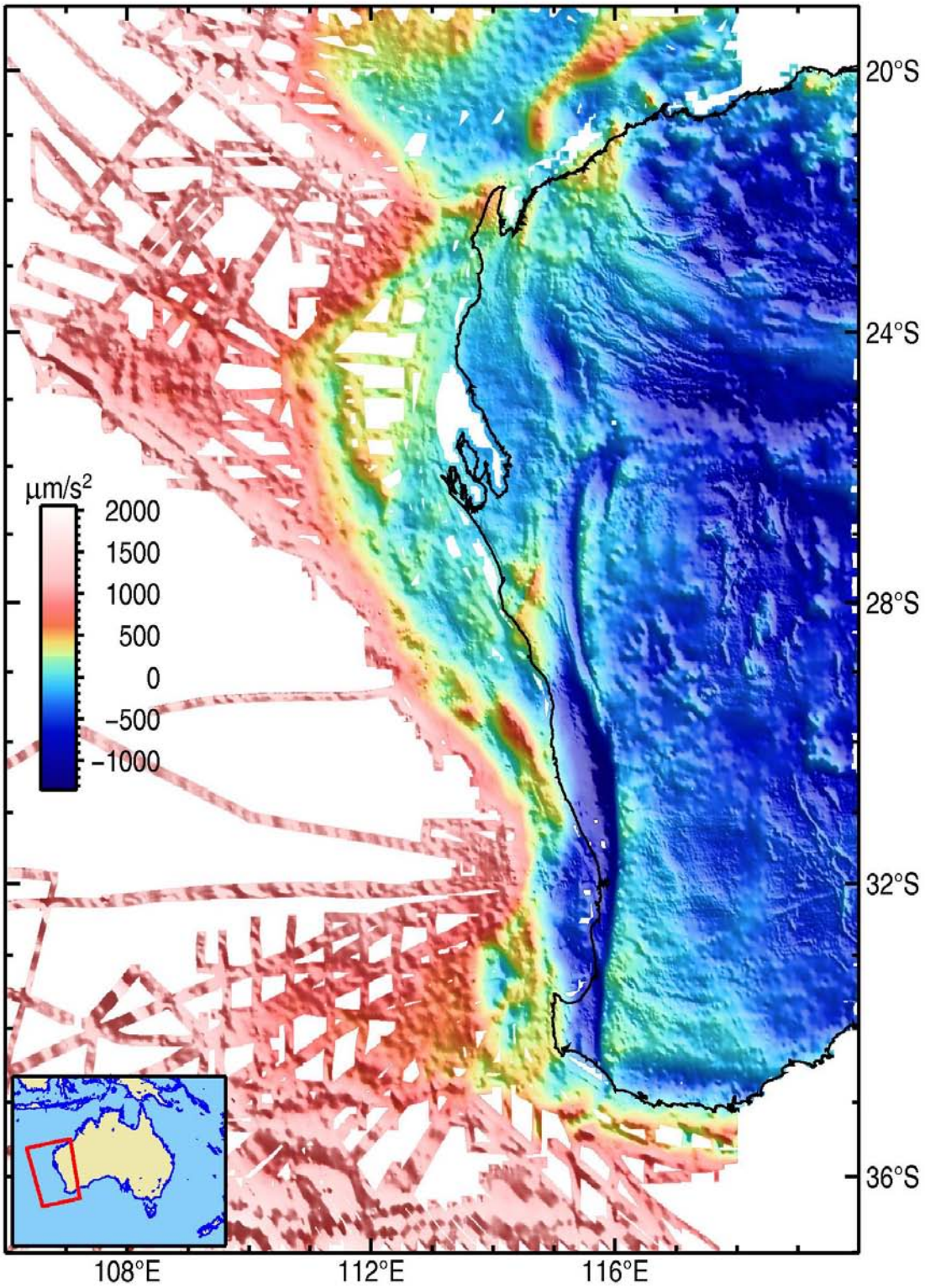

Figure B1: *Bouguer gravity image (cell size 0.01°) for the southwest margin of Australia combining levelled ship-track data and onshore point data.*

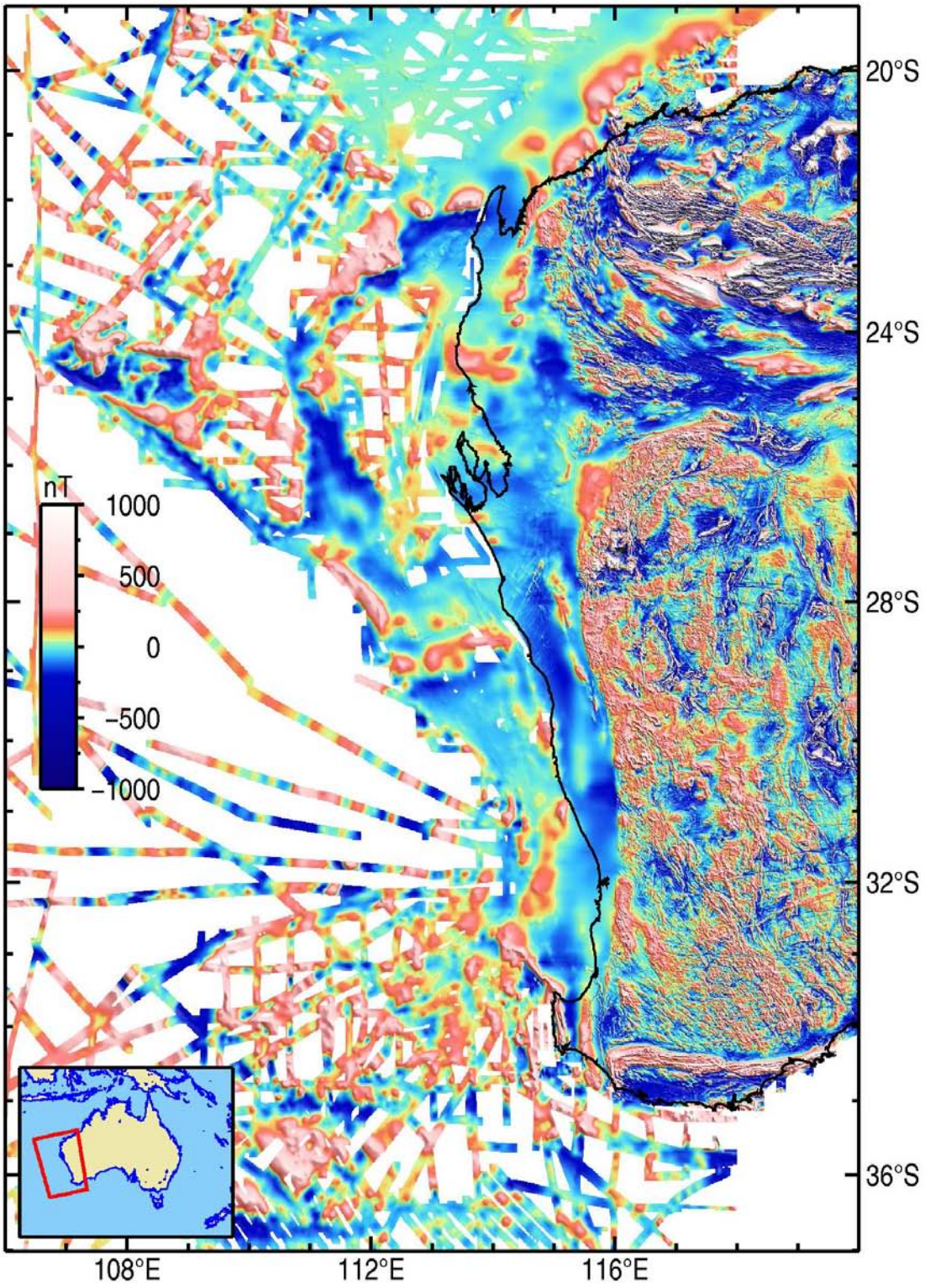

Figure B2: *Total magnetic intensity merged image (cell size 0.005°) for the southwest margin of Australia combining levelled ship-track data and airborne data from the 5th Edition of the Magnetic Anomaly Map of Australia (Milligan et al., 2010).*